PhD Dissertation

Insight into the role of skin microbiome in UV-induced immune modulation and its potential link to pathogenesis of polymorphic light eruption.

Submitted by

VijayKumar PATRA, MSc, B.E

For the Academic Degree of

Doctor of Philosophy

(PhD)

At the

Department of Dermatology

Medical University of Graz

Under the supervision of

Univ.-Prof. Dr. Peter WOLF

2018

Statutory Declaration

I hereby declare that this thesis is my own original work and that I have fully acknowledged by name all of those individuals and organizations that have contributed to the research for this thesis. Due acknowledgment has been made in the text to all other material used. Throughout this thesis and in all related publications I followed the "Standards of Good Scientific Practice and Ombuds Committee at the Medical University of Graz''.

Graz,

Disclosures

Parts of this thesis have been published in:

- Patra V, Byrne SN, and Wolf P. **The Skin Microbiome: Is It Affected by UV-induced Immune Suppression?** *Front. Microbiol* 2016 Aug 10; 7:1235 [Hypothesis and Theory] (1)

- Patra V, Laoubi L, Nicolas J-F, Vocanson M and Wolf P (2018) **A Perspective on the Interplay of Ultraviolet-Radiation, Skin Microbiome, and Skin Resident Memory TCRαβ+ Cells**. *Front. Med*. 5:166 [Perspective] (2)

- Patra V and Wolf P. **Microbial elements as the initial triggers in the pathogenesis of polymorphic light eruption?** Exp Dermatol 2016 Dec;25(12):999-1001 [Hypothesis]

- Patra V, Mayer G, Gruber-Wackernagel A, Horn M, Lembo S, Wolf P. **Unique profile of antimicrobial peptide expression in polymorphic light eruption lesions compared to healthy skin, atopic dermatitis, and psoriasis**. Photodermatol Photoimmunol Photomed. 2018 Mar;34(2):137-144 [Original article]

Parts of the thesis are also part of a prepared manuscript

- Patra V, Wagner K, Arulampalam V and Wolf P. **Skin microbiome modulates the effect of UV on cellular response and immune function** [Original article]

All co-authors who contributed to the research in this thesis agreed to the use of their data. These co-authors have actively contributed to the results reported in this thesis and agreed to the use of their data:

16s rRNA sequencing and microarray was done at Core facility for Molecular Biology, Center for Medical Research, Medical University of Graz, Austria (paid service)

Liquid chromatography (LC)/MS was done at Core facility for Lipidomics, Center for Medical Research, Medical University of Graz, Austria (paid service)

Léo Laoubi, Centre International de Recherche en Infectiologie, Institut National de la Santé et de la Recherche Médicale, U1111, Lyon, France (FACS)

Bettina Halwachs-Wenzl, Theodor Escherich Laboratory for Medical Microbiome Research, Institute of Pathology, Medical University of Graz, Graz, Austria (microbiome analysis)

Meghana Somlapura, Molecular Pathology Laboratory, Medical University of Graz, Graz, Austria (animal experiments support: cis-UCA, microbiome analysis)

Velmurugesan Arulampalam, Core Facility for Germfree Research (CFGR), Karolinska Institutet, Stockholm, Sweden (material and administrative support for GF animals)

Karin Wagner, Center for Medical Research, Medical University of Graz, Graz, Austria (microarray data analysis)

Alexandra Gruber-Wackernagel, Department of Dermatology and Venereology, Medical University of Graz, Graz, Austria (material support: skin samples)

Michael Horn, Department of Dermatology and Venereology, Medical University of Graz, Graz, Austria (material support: skin samples)

Gerlinde Mayer, Department of Dermatology and Venereology, Medical University of Graz, Graz, Austria (technical support)

Prof. Peter Wolf, Department of Dermatology and Venereology, Medical University of Graz, Graz, Austria

Acknowledgments

This thesis is the end of my journey in obtaining my Ph.D. I have not traveled in a vacuum in this journey. This thesis has been kept on track and been seen through to completion with the support and encouragement of numerous people and institutions. At the end of my thesis, I would like to thank all those people who made this thesis possible and contributed towards it in many ways to success of this study and gave me an unforgettable experience.

There are no proper words to convey my deep gratitude and respect for my thesis and research advisor, Prof. Peter Wolf. He has inspired me to become an independent researcher and provided me constant support, guidance and encouragement. Throughout my research and thesis-writing period, he provided sound advice, good teaching, good company, and lots of good ideas. I could not have imagined having a better advisor and mentor for my Ph.D. study. I am very thankful for giving me freedom to pursue my ideas and supporting them.

I thank my thesis committee members, Dr. Gregor Gorkiewicz and Prof. Herbert Strobl for their valuable input and support.

I am also extremely grateful for Dr. Marc Vocanson for his enormous help during my research stay in Lyon. I am very thankful for training me and making me a part of exciting projects in his lab. Special thanks to Dr. Velmurugesan Arulampalam for hosting me in your facility and helping me with the germ-free animal work.

Special thanks to everybody from the DK-MOLIN for making this PhD thesis possible. I would like to express my thanks to the core-facilities of Molecular biology and Lipidomics for your support during my work.

I am deeply grateful for the members of my lab, Nina, Eleonora, Pablo, Nitesh, Theresa and Saptaswa. Thanks for all the support you guys have provided me. I have learnt a lot of things being with you guys, keep rocking wherever you are! Thank you, Gerlinde and Isabella for your constant support and help. This work couldn't be completed without you guys. I thank all my friends, especially Andras, Andrea,

Nanditha, Ridhima for making my first years in Graz a really fun and exciting and helping me through everything. I also thank all my friends and colleagues from DK-MOLIN for all the fun we shared during this Ph.D. Pablo, thank you for all your help and support and our constant discussions from science to anything. Theresa, Claudia and Alex (tequila mockingbirds), thank you for all the help. I forget about all the difficulties of work when I am with you guys, thanks for all the discussions, recipes, nags about healthy food (thank you for making me eat less chips), fun and jokes.

I am greatly indebted (literally!) to Meghana, thank you for starting the journey with me in pursuit of Ph.D. Thank you for helping me get through the difficult times, and for all the emotional support, comraderie, entertainment, and caring and experiences. I will always remember and cherish them.

Most importantly, I wish to thank my parents, they supported me, taught me, and loved me and having patience. To them I dedicate this thesis.

Lastly, Thank you Charlene, for all the love, support and care. I am grateful for your constant words of encouragement and your patience (look I "finally" finished my thesis) and keeping me sane. Thank you for showing me that there is also a beautiful life apart from work.

This study has been funded by the Medical University of Graz through the PhD Program Molecular Fundamentals of Inflammation (DK-MOLIN) via the Austrian Science Fund (FWF, project number W1241).

Learning is a treasure that will follow its owner everywhere.

-Chinese Proverb

Table of contents

Abbreviations and Definitions
List of figures
List of tables
Abstract
Zusammenfassung

Part 1 of thesis: Role of skin microbiome in UV-induced immune modulation 1

1. Introduction to ultraviolet radiation 2
1.1.1 UV-A 3
1.1.2 UV-B 3
1.1.3 UV-C 3

1.2 Photoimmunology 4
1.2.1 UV-induced immune suppression 4
1.2.2 Mechanisms of UV-induced immune suppression 6
1.2.3 Molecular mechanisms of UV-induced cellular apoptosis 7
1.2.3.1 Modulation of immune responses by UVR through cellular apoptosis 8
1.2.4 UV-Induced innate responses 9
1.2.4.1 Antimicrobial peptides 9
1.2.4.2 Toll-like receptors 9
1.2.4.3 Cytokines 12
1.2.4.4 Langerhans cells (LCs 13
1.2.4.5 Mast cells 13
1.2.4.6 Neutrophils 14
1.2.4.7 Monocyte/Macrophage 15
1.2.5 UV-induced adaptive immune response 17
1.2.6 Contact hypersensitivity assay 18
1.2.6.1 Sensitization phase 18
1.2.6.2 Elicitation phase 21

1.3 Skin microbiome 23
1.3.1 Skin microbiome and immunity dialog 25

1.4 Hypothesis and Aims 28

1.5 Material and methods 29
1.5.1 Animals 29
1.5.2 Skin disinfection 29
1.5.3 UV-B source and irradiation 29

1.5.4 Skin sampling for microbiome analysis 30
1.5.5 Skin sampling for urocanic acid quantification 30
1.5.6 Liquid chromatography (LC)/MS for analysis of *cis* and *trans*-urocanic acid 31
1.5.7 Transepidermal water loss (TEWL), skin hydration and pH measurement 31
1.5.8 Complete blood count 31
1.5.9 Skin and lymph node cell isolation 31
1.5.10 Flow cytometry analysis 32
1.5.11 Monoclonal antibodies used for flow cytometry 32
1.5.12 DNA isolation 32
1.5.13 16S microbiome sequencing 33
1.5.14 16S microbiome analysis 33
1.5.15 Contact hypersensitivity assay 34
1.5.16 Skin sample collection for microarray and histological analysis 34
1.5.17 RNA extraction, ... 34
microarray, and data analysis 34
1.5.18 cDNA synthesis and qPCR 34
1.5.19 Histological analysis 36
1.5.20 Immunohistochemistry 37
1.5.21 Statistical analysis 37

1.6 Results 38
1.6.1 Determination of minimal inflammatory dose (MID 38
1.6.2 UV-B induced physiological changes in the skin: transepidermal water loss (TEWL), skin hydration and pH 39
1.6.3 UV-B converts *trans*- to *cis*-urocanic acid immediately after irradiation 41
1.6.4 Alpha diversity analysis 42
1.6.5 UV-B modulates microbial diversity across various time points after irradiation, as measured by beta diversity analysis 43
1.6.6 Microbial modulation at various time points before and after UV exposure 45
1.6.7 Modulation in abundance of top 5 phyla after UVB exposure 46
1.6.8 UV-B dose-dependently modulates cellular response within the skin 47
1.6.9 UV-B exposure causes systemic effects in monocyte and granulocyte populations in the blood 49
1.6.10 UV-B exposure affects various immune cell population in the skin and lymph node 50
1.6.11 UV-B induces gene expression of antimicrobial peptides S100A8 and S100A9 52
1.6.12 Germ-free mice show significant UV-induced immune suppression of systemic adaptive immune response, by orchestrating local cellular and innate immune response to UV 53
1.6.13 UV-B modulates the cutaneous gene expression in GF and SPF skin.. 60

1.6.14 Canonical pathway analysis of UV-B exposed GF and SPF skin using ingenuity pathway analysis 62
1.6.15 Differential expression of interleukins, chemokines, AMPs and other innate immune response genes in GF and SPF skin after UV-B irradiation 65
1.6.16 Potential upstream transcription regulator genes in UV-B-exposed GF and SPF skin and their gene interaction network 69

1.7 Discussion 71

Part 2 of thesis: Potential link of skin microbiome in pathogenesis of polymorphic light eruption: Expression of antimicrobial peptides 74

2.1 Introduction to polymorphic light eruption 76
2.1.1 Clinical manifestation 76
2.1.2 Photobiologic evaluation: waveband aspects 78
2.1.3 Histology of PLE 78
2.1.4 General immunological features of PLE 79

2.2 Antimicrobial Peptides 80
2.2.1 Properties and diversity of AMPs 81
2.2.2 Mechanisms of action of AMPs 82
2.2.3 Immunoregulatory and non-antimicrobial function of AMPs 83
2.2.4 Potential role of AMPs in pathogenesis of PLE 85

2.3 Hypothesis and Aims 87

2.4 Material and Methods 88
2.4.1 Samples 88
2.4.2 Immunohistochemical staining 88
2.4.3 Quantitative analysis of AMP expression 89
2.4.4 Statistical analysis 89

2.5 Results 90
2.5.1 Increased psoriasin expression in PLE 90
2.5.2 RNase7 is increased in PLE and predominantly expressed in stratum corneum 91
2.5.3 Increased HBD-2 expression in cellular infiltrate in PLE 92
2.5.4 PLE lesions have decreased expression of HBD-3 93
2.5.5 LL-37 is significantly increased in and around blood vessels in PLE and psoriasis 94
2.5.6 Expression levels of AMPs are independent of age 95

2.5.7 PLE lesions share similar AMPs expression profile similar to psoriasis, except for RNase7 and HBD-3 96
2.5.8 AMPs interact with other molecules within the skin 97

2.6 Discussion 98

3 General Discussion 103

4 References 106

License attachments

Abbreviations and Definitions

6-4 PPs – 6,4- photoproducts

8-MOP – Methoxsalen

AD – Atopic dermatitis

AMPs- Antimicrobial peptides

ATP – Adenosine triphosphate

Breg – Regulatory B cell

CAMPs – Commensal associated molecular patterns

CAT – Catalase

CHS – Contact hypersensitivity

CLA - Conjugated Linoleic Acid

CPD – Cyclobutane pyrimidine dimer

DAMPs – Damage associated molecular patterns

DETC – Dendritic epidermal T cell

DNFB - 1-Fluoro-2,4-dinitrobenzene

DTH- Delayed hypersensitivity

GF – Germ-free

HBD- human beta defensin

HLA-DR - Human Leukocyte Antigen – antigen D Related

HPV - Human papillomavirus

ICAM - Intercellular adhesion molecule

IL – Interleukin

ITS – Internal transcribed spacer

LC – Langerhans cell

LDA – Linear discriminant analysis

LefSe- Linear discriminant analysis effect size

LN- Lymph node

LPA – Acyltransferase

LPS - Lipopolysaccharide

LTA - Lipoteichoic acid

LTB - Leukotriene B

MBD- Murine beta defensin

MC – Mast cell

MHC- Major histocompatibility complex

OTU – Operational taxonomic unit

PAMPs – Pathogen associated molecular patterns

PCoA – Principal Coordinates Analysis

PGE2 - Prostaglandin E2

PLE- Polymorphic light eruption

PMA – Propidium monoazide

POD – Peroxidase

PRR – Pattern recognition receptor

QIIME – Quantitative Insights into Microbial Ecology

RNase – Ribonuclease

ROS – Reactive oxygen species

S100 – Calcium binding proteins

SOD – Superoxide dismutase

SPF- Specific pathogen free

T0- Time point 0 (before UV)

T1- Time point 1 (immediately after UV)

T2- Time point 2 (24hr after UV)

TCR – T cell receptor

TEWL – Trans-epidermal water loss

TLR- Toll-like receptor

TNF- Tumor necrosis factor

Treg – Regulatory T cell

UCA – Urocanic acid

UV-R – Ultraviolet radiation

List of figures

Figure 1: The Electromagnetic spectrum from longest wavelength to shortest wavelength2 2

Figure 2: Electromagnetic spectrum of ultraviolet radiation. 2

Figure 3: UVR penetration in the skin. Both UV-B (290-320nm) and UV-A (320-400nm) penetrate the skin. 4

Figure 4: UV-induced immune suppression. 6

Figure 5: Sunburn cells in UV-B exposed (618 mJ/cm^2) mouse skin. 7

Figure 6: Molecular events after UV-R leading to cascade of events, eventually suppressing adaptive immune response. 8

Figure 7: Cytokine network. 11

Figure 8: Overview of Mast cells. 13

Figure 9: Overview of neutrophils. 13

Figure 10: Overview of monocyte differentiation 14

Figure 11: The immune response plays a role in skin tumor growth (Kripke, 1974) 16

Figure 12: Overview of CHS model. 17

Figure 13: Systematic representation of the pathophysiology of contact hypersensitivity. 19

Figure 14: Challenge phase 20

Figure 15: UV-induced systemic induction of CHS. 21

Figure 16: Skin microbial composition in human skin. 22

Figure 17: Potential mechanisms of microbial interference in UV-induced immune suppression. 25

Figure 18: Overview of experimental setup. 29

Figure 19: Minimal inflammatory dose (MID). 37

Figure 20: UV-B induced changes in TEWL and hydration. 39

Figure 21: UV-B isomerizes trans- to cis-UCA. 40

Figure 22: Rarefraction plots. 41

Figure 23: Beta diversity for various doses of UV-B across different time points. 43

Figure 24: LefSe results showing effect of UVB on microbial communities. 44

Figure 25: Boxplots showing relative abundance of top 5 phyla. 45

Figure 26: Effect of UV-B on epidermis and cellular infiltrate. 47

Figure 27: Systemic effect of UV-B on total and differential leukocyte count. 48

Figure 28: Effect of UVB on various immune cell population in the skin. 49

Figure 29: Effect of UVB on various immune cell population in the LN. 50

Figure 30: AMPs expression at different doses. 51

Figure 31: Skin microbiome protects from UV-B induced suppression of induction of CHS..... 53
Figure 32: Microbiome contributes to increased cellular response to UV-B. 55
Figure 33: Immunohistochemical stainings panels. 56
Figure 34: UV exposure boosters the infiltration of skin by neutrophils in SPF mice but macrophages and IL10+ cells in GF mice. 57
Figure 35: UV-B modulates gene expression in GF and SPF skin..... 59
Figure 36: UV induces differential expression of interleukins and chemokines in GF compared to SPF skin...... 64
Figure 37: Effect of UV-B on various upstream regulators and gene interaction. 68
Figure 38: A Maculopapular type of PLE in the V-neck of a young woman. B. Higher magnification of lesions...... 77
Figure 39: Histology of PLE..... 79
Figure 40: Biological function of antimicrobial peptide..... 82
Figure 41: Multifunctional biological properties of antimicrobial peptides. 83
Figure 42: Hypothetical model for pathogenesis of PLE...... 85
Figure 43: Increased psoriasin expression in PLE..... 90
Figure 44: Increased RNase7 expression in PLE..... 91
Figure 45: Increased HBD-2 expression in the dermal infiltrate PLE..... 92
Figure 46: Decreased HBD-3 expression in PLE..... 93
Figure 47: Increased LL-37 expression in PLE..... 94
Figure 48: AMP expression is independent of age and sex..... 95
Figure 49: Heatmap showing expression patterns of AMPs in various diseases...... 96
Figure 50: Effect of AMPs on gene interactions..... 97

List of tables

Table 1: Descriptions of TLR..... 10
Table 2: Monocyte subsets in mouse and humans 15
Table 3: Chemokine receptors expressed on DC and involved in migration to LN..... 18
Table 4: UV-B induced canonical pathways in GF mice 61
Table 5: UV-B induced canonical pathways in SPF mice..... 62
Table 6: UVB induced gene expression of AMPs, TLRs and serotonin signaling genes. 66

Abstract

Human skin apart from functioning as a physical barricade to stop the entry of pathogens, also hosts innumerable commensal organisms, i.e. the skin microbiome. The skin cells and the immune system constantly interact with microbes, to maintain cutaneous homeostasis, despite the challenges offered by various environmental factors. A major environmental factor affecting the skin is ultraviolet radiation (UV-R) from sunlight. By targeting the cells and molecules within skin, UV-R can trigger the production and release of antimicrobial peptides, affect the innate immune system and ultimately suppress the adaptive cellular immune response. However, the role of the skin microbiome in UV-induced immune suppression has been overlooked.

This work addressed the question of microbial involvement in UV-induced immune suppression by using the standard model of contact hypersensitivity in the presence or absence of the microbiome (in germ-free [GF] and disinfected mice). The data indicated that the microbiome inhibits UV-induced immune suppression. Furthermore, the transcriptome analysis (with samples taken 24 hours after UV exposure) showed differential regulation of many genes in the presence or absence of the microbiome, including a predominant expression of pro-inflammatory cytokines versus immunosuppressive cytokines. Moreover, 16s rRNA sequencing revealed that UV exposure indeed affected microbial communities living on the skin. In addition, UV-induced isomerization of urocanic acid from its trans- to cis-form (the latter known to be a strong immune suppressor) in the skin was linked to changes in microbial communities. Furthermore, the work confirmed that UV-B exposure caused epidermal barrier dysfunction as measured by trans-epidermal water loss that could potentially allow microbes or microbial antigens to penetrate the skin.

These findings are also of potential significance for a better understanding of the pathophysiology of polymorphic light eruption (PLE) whose primary trigger remains to be uncovered. PLE may be initiated by elements resulting from UV-induced damage to microbial communities of the skin, leading to a cascade of events eventually resulting in the skin rash of the disease. UV-induced stress on microbial communities of the skin could exacerbate inflammatory responses by inducing the innate immune system through antimicrobial peptides (AMPs) such as psoriasin, RNase7, HBD-2, HBD-3 and LL-37. These AMPs also actively take part in initiating adaptive immunity. Abnormalities in AMP expression have been linked to pathological skin conditions such as atopic dermatitis (AD) and psoriasis. Antimicrobial peptide profiling was carried out in PLE skin samples compared

with that of healthy, atopic, and psoriatic skin. Compared to healthy skin, there was an increased expression of psoriasin and RNAse7 (both mostly in stratum granulosum of the epidermis), HBD-2 (in the cellular infiltrate of the dermis), and LL37 (mostly in and around blood vessels and glands) in PLE lesional skin, a similar expression profile as observed in psoriatic skin and entirely different to that of AD (with little or no expression of psoriasin, RNAse7, HBD-2, and LL37). HBD-3 was downregulated in PLE compared to its high expression in the epidermis of AD and psoriasis.

The role of the skin microbiome in UV-induced immune modulation and the unique profile of differentially expressed AMPs in PLE may be crucial in the pathophysiology of the disease.

Zusammenfassung

Die Haut des Menschen fungiert nicht nur als physikalische Barriere gegen das Eintreten von pathogenen Keimen, sondern beherbergt auch unzählige kommensale Organismen, das Hautmikrobiom. Das Immunsystem und die Zellen der Haut interagieren ständig mit Mikroben, um trotz verschiedener Umwelteinflüsse einen Gleichgewichtszustand aufrecht zu erhalten. Ein wichtiger Umweltfaktor mit großem Einfluss auf die Haut ist die Ultraviolettstrahlung (UV-Strahlung) der Sonne. UV-Strahlung hat einen direkten Effekt auf Zellen und Moleküle in der Haut und kann so die Produktion und Freisetzung antimikrobieller Peptide (AMP) auslösen, das angeborene Immunsystem beeinflussen und schließlich die adaptive zelluläre Immunantwort unterdrücken. Die Rolle des Hautmikrobioms wurde jedoch bisher bei der UV-induzierten Immunsuppression außer Acht gelassen.

Diese Arbeit befasste sich mit der Frage der mikrobiellen Beteiligung bei UV-induzierter Immunsuppression unter Verwendung des Standardmodells der Kontakthypersensibilität in Gegenwart oder Abwesenheit des Mikrobioms (in keimfreien bzw. desinfizierten Mäusen) und zeigte, dass das Mikrobiom die UV-induzierte Immunsuppression inhibiert. Darüber hinaus zeigte eine Analyse des Transkriptoms (an 24 Stunden nach Bestrahlung gewonnenen Proben) eine differentielle Regulation vieler Gene in Gegenwart oder Abwesenheit des Mikrobioms, einschließlich einer vorherrschenden Expression an entzündungsfördernden Zytokinen gegenüber immunsuppressiven Zytokinen. Bei der 16s rRNA-Sequenzierung stellte sich heraus, dass UV-Exposition tatsächlich Auswirkungen auf Mikroorganismen der Haut hat. Darüber hinaus war die durch UV-Einwirkung auf die Haut hervorgerufene Isomerisierung von Urocainsäure von der trans- zur cis-Form (die letztere als starker Immunsuppressor bekannt) mit Änderungen an der mikrobiellen Besiedelung verbunden. Die Arbeit bestätigte auch, dass die Einwirkung von UV-Strahlung eine Dysfunktion der epidermalen Barriere verursachte (gemessen mittels transepidermalen Wasserverlustes), was möglicherweise Mikroben oder mikrobiellen Antigenen das Durchdringen der Haut ermöglichen könnte.

Diese Ergebnisse sind auch für ein besseres Verständnis der Pathophysiologie der polymorphen Lichtdermatose (PLD) bedeutsam, deren primärer Auslöser bisher noch nicht bekannt ist. Laut unserer Hypothese könnte PLD durch Faktoren getriggert werden, die aus UV-induzierten Schädigungen der mirkobiellen Kolonien entstehen. Solche Signale könnten

erzeugt werden, da UV-Strahlung Stress auf mikrobielle Kolonien der Haut ausübt. Dies könnte in weiterer Folge zur Verschlimmerung von Entzündungsreaktionen durch Induktion des angeborenen Immunsystems durch antimikrobielle Peptide (AMPs) wie Psoriasin, RNase7, HBD-2 und LL-37 führen. Diese AMPs können sich aktiv an der Initiierung einer adaptiven Immunantwort beteiligen. Eine abnormale Expression von AMPs wurde bereits mit Hauterkrankungen wie atopischer Dermatitis (AD) und Psoriasis in Verbindung gebracht. Das AMP-Profil von PLD-Hautproben wurde untersucht und mit jenem von gesunder Haut, AD und Psoriasis verglichen. Im Vergleich zu gesunder Haut wiesen PLD-Läsionen eine erhöhte Expression an Psoriasin und RNase7 (beide hauptsächlich in Stratum granulosum der Epidermis), HBD-2 (im zellulären Infiltrat in der Dermis) und LL-37 (hauptsächlich in und um Blutgefäße und Drüsen) auf. Ein ähnliches Expressionsprofil findet man in psoriatischer Haut; jenes von AD ist jedoch anders (wenig bis fehlende Expression von Psoriasin, RNase7, HBD-2 und LL-37). Des Weiteren fanden wir eine verminderte Expression von HBD-3 in PLD, verglichen mit einer sehr hohen Expression in Epidermis und Dermis von AD und Psoriasis.

Die Rolle des Hautmikrobioms bei UV-induzierter Immunmodulation und das einzigartige Profil differentiell exprimierter AMPs bei PLD könnte in der Pathophysiologie der Erkrankung entscheidend sein.

1

Role of skin microbiome in UV-induced immune modulation

1. Ultraviolet radiation

The electromagnetic spectrum of the sun (Figure 1) ranges from gamma rays to radio waves and includes optical radiation. The latter is divided into three major parts: ultraviolet radiation (UV-R) (100 – 400 nm), visible light (400 – 760 nm) and infrared (760 nm and more) (Figure 2). UV-R is one of the most prominent external factor affecting the skin [1] and can be subdivided in UV-A (315 – 400 nm), UV-B (280 – 315 nm) and UV-C (280 – 200 nm). UV-C is blocked by the earth's atmosphere, specifically by the oxygen and ozone in the stratosphere, whereas UV-B and UV-A can reach the surface of the earth [2]. Despite the fact that UV-B makes up to a mere 2-10 % of the radiant energy from the sun to reach the earth's surface, it is the most photochemically active wavelength. UV-R is the most effective and highly carcinogenic factor that interacts with the DNA and lead to alterations within the genomic integrity which affects the normal life processes of all living species ranging from prokaryotes to mammals [3]. However, different species and taxonomic groups have differential tolerance to UV-R and the tolerance is predicted to further diversify and continue throughout this century [4].

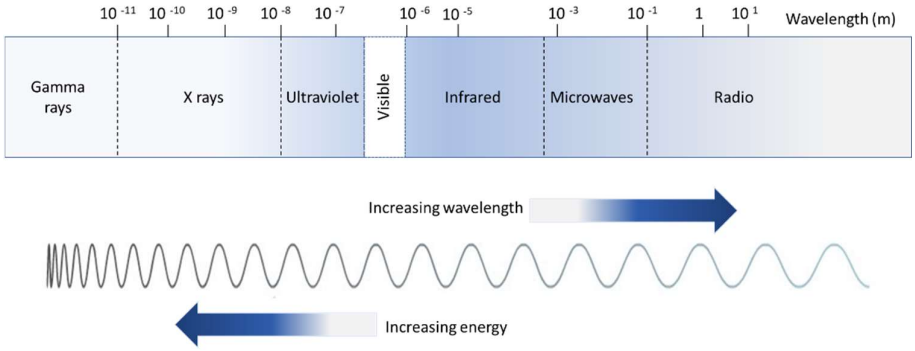

Figure 1: The Electromagnetic spectrum from longest wavelength to shortest wavelength.

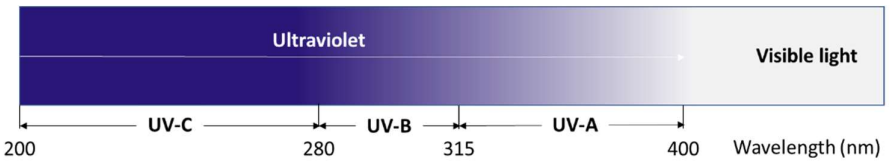

Figure 2: Electromagnetic spectrum of ultraviolet radiation.

1.1.1 UV-A

UV-A constitutes about 95% of the total UV-R reaching the surface of the earth and the transmission of UV-A through windows, sunscreen, and human epidermis is much higher compared to UV-B (Figure 3) [5]. UVA rays are of two types UVA1 (340 – 400 nm) and UVA2 (320 – 340 nm). However, in the skin, the penetration of UV-A through the upper epidermal layers (epidermis and dermis) is about 5-9 times more than UV-B [6] and is known to play a major role in skin aging, wrinkling (photoaging) and may take part in initiating skin cancers and is also considered as carcinogenic. This carcinogenic effect is due to the action of UV-A on various endogenous photosensitizers to produce reactive oxygen species (ROS), which can damage the DNA and the proteins that repair the DNA damage. On the other hand, UV-A is a dominant tanning ray and is widely used in tanning beds. Furthermore, UV-A + psoralen (8-MOP) is widely used in phototherapy.

1.1.2 UV-B

UV-B constitutes about 2-10% [7] of total UV-R reaching the earth surface and penetration can be blocked by glass [7]. However, compared to UV-A, UV-B can only penetrate through the epidermis and not the dermis. UV-B exposure is, however, more photochemically and biologically active and is responsible for sunburn and other physiological changes in the skin's surface which includes tanning. The intensity of UV-B radiation (unlike UV-A) vastly varies depending upon geographic location, time and season. One of the prominent targets of UV-B is cellular DNA, which can absorb UV-B radiation and cause significant adverse effects on organisms such as bacteria [8,9], cyanobacteria, phytoplankton, algae [10], plants [11], animals and humans [12]. Some organisms have evolutionary developed certain UV-absorbing pigments as the first line of defense, though, they cannot prevent UV-R completely from reaching the DNA in superficial tissues [12]. DNA repair enzymatic systems such as superoxide dismutase (SOD), catalase (CAT), peroxidase (POD), vitamins such as C, B and E play additional defense against UV-B [13].

1.1.3 UV-C

UV-C radiation never reaches the earth's surface as it is absorbed in the atmosphere. However, UV-C lamps are widely used as germicidal lamps due to their ability to kill microorganisms [14]. In humans, UV-C is known to be mainly absorbed by the outer dead layers of the epidermis (stratum corneum) and accidental exposure to UV-C can cause corneal burns and mild sunburn in contrast to UV-B.

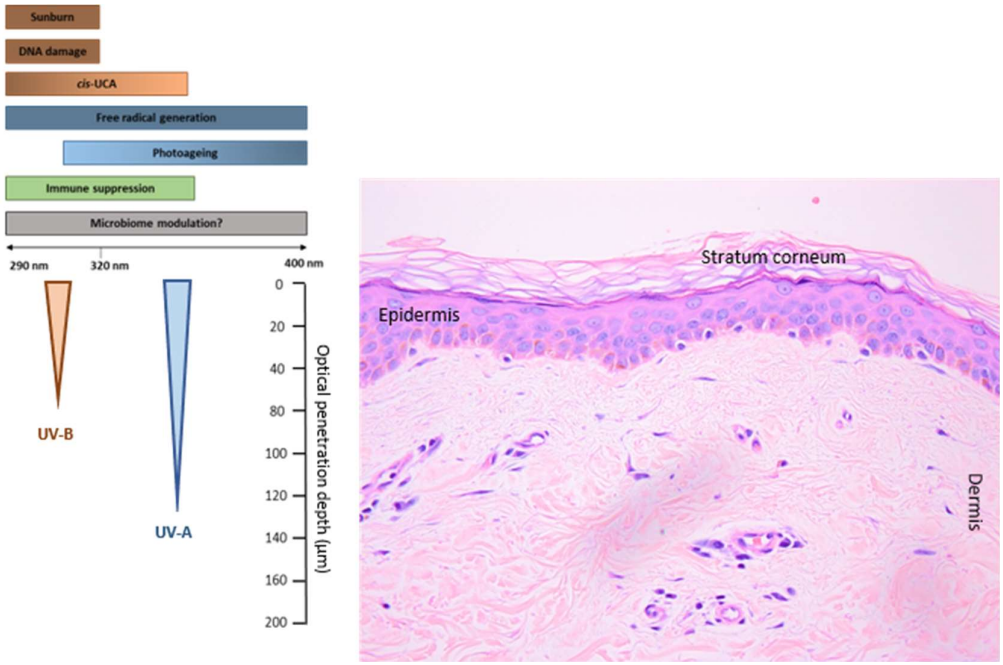

Figure 3: UVR penetration in the skin. *Both UV-B (290-320nm) and UV-A (320-400nm) penetrate the skin. UV-A has greater penetration depth (up to 140 µm) in the skin reaching the dermis. UV-B reaches until basal layers of the epidermis (20- 80 µm). The attenuation of UV light is approximately 5%* [15]. *Reproduced from Patra V el at* [16] *under the terms of Creative Commons Attribution License (CC BY).*

1.2 Photoimmunology

The area of photodermatology involved in investigations of the intricate relationships between UV-R and the immune system is referred to as *photoimmunology*. The foundations of photoimmunology arose from landmark studied from Kripke et al investigating the antigenicity of experimentally UV-induced tumors in syngeneic mice [17] and clinical observations of patients with UV-induced skin cancers [18] . However, the basic understanding of the interaction of UV-R with the immune system has broad implications beyond cancers. The research of photoimmunology has enabled us to understand the mechanisms by which phototherapy works in treating various skin conditions and also to understand the role of the immune system in various photodermatoses.

1.2.1 UV-induced immune suppression

UV-R, especially UV-B (280-315nm) and UV-A (315-400nm) are known to be involved in skin freckling, wrinkling, photoallergic and phototoxic responses and tumor induction and

progression. UV-R has the ability to induce photoproducts such as cyclobutane pyrimidine dimers (CPDs) and eventually leading to mutations, which are linked to carcinogenesis [1]. UV-R mediated immune suppression was first discovered by Kripke et al [19]. This was further confirmed and proved to be T-cell mediated by using contact hypersensitivity (CHS) models in mice [20] and in humans [21-23]. The initial key events that are prominently involved in immune suppression after UV-irradiation are DNA damage [24], the formation of reactive phospholipids like platelet activating factor [25] and isomerization of inactive trans-to water soluble active cis-urocanic acid (UCA) [26]. An early report from our group suggests that cis-UCA can indeed directly modulate skin microbiome [27]. Since UV-R suppresses the immune reaction to antigens of infectious microbes such as *M. lepraemurium*, *bovis BCG*, *C. albicans*, *B. burgdorferi* and *Schistosoma mansoni* [28-30] it can be speculated that exposure to UV-R could enhance susceptibility to infections, however clinical evidence of increased infections after UV-R is very low. This could be due to the fact that UV-R suppresses adaptive immunity but activates innate immunity [31]. One of the important innate key players is AMPs. These are small proteins typically ranging from 10-50 amino acid residues that have potential to neutralize invading microorganisms [32] and mediate adaptive immune response [33-35]. Dysregulation in AMP expression could be linked to many diseases, including photosensitive conditions like PLE [36], where AMPs may be key mediators to maintain homeostasis between host immune system and microbiome. UV-R exposure also leads to infiltration of macrophages and neutrophils [37-39], induces migration of Langerhans cells (LC) from the skin into the draining lymph nodes [40-42] and affects mast cells. Furthermore, regulatory T cells (Tregs) and B cells (Bregs) are recruited and activated [43,44]. All these cells and UV-induced events are known to be involved in immune suppression [45] (Figure 4).

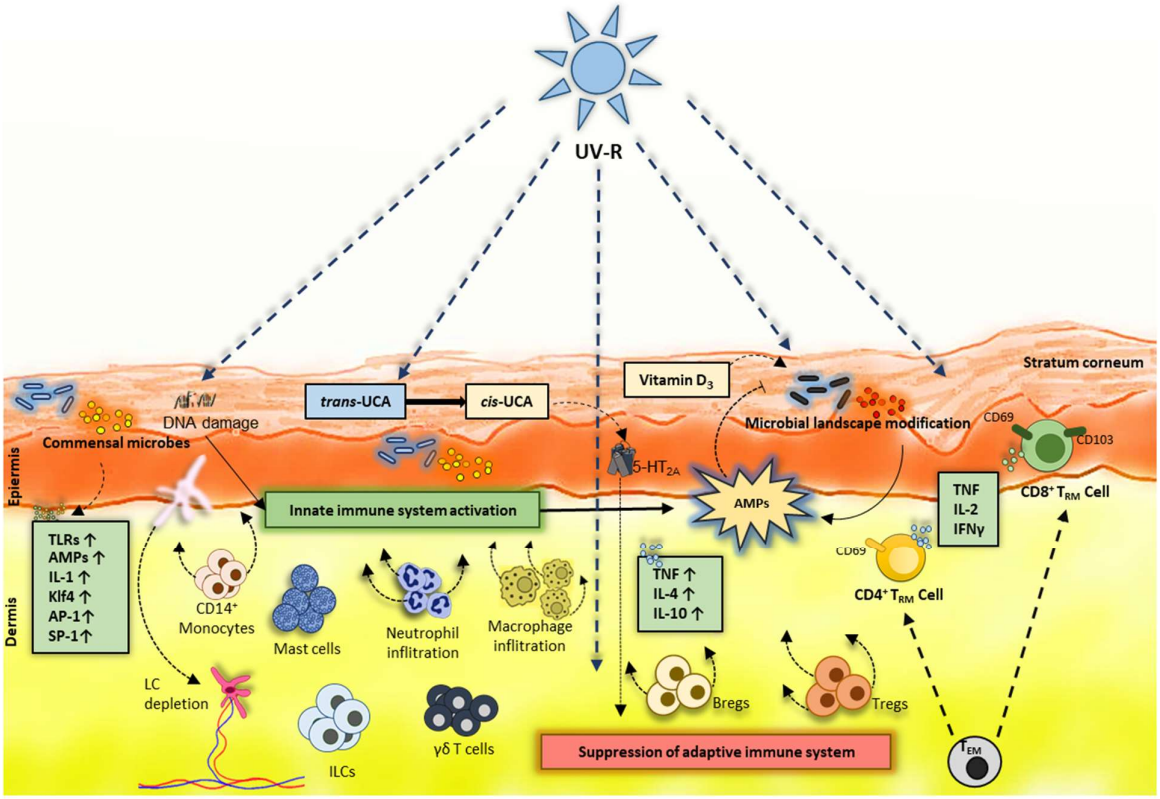

Figure 4: UV-induced immune suppression. *Exposure to UV-R leads to conversion of trans-UCA to cis-UCA. Tumor necrosis factor (TNF) is released by keratinocytes which induce Langerhans cell (LC) migration to the lymph nodes. AMPs are expressed by keratinocytes and various lymphocytes, activating the innate immune system. IL-4 and IL-10 expression lead to neutrophil and macrophage recruitment. Mast cells (MC) degranulates and release various mediators. Tregs and Bregs are recruited to the UV-exposed site. Taken together, these events lead to the suppression of adaptive immune response in the healthy skin. Reproduced from Patra V et al [16] under the terms of Creative Commons Attribution License (CC BY).*

1.2.2 Mechanisms of UV-induced immune suppression

There has been great interest in understanding the mechanisms behind UV-R modulating the immune system. In this introduction, I will briefly focus on the effects of UV-exposure on

(1) Molecular mechanisms of UV-induced cellular apoptosis (2) Innate immune response (3) Adaptive immune response.

1.2.3 Molecular mechanisms of UV-induced cellular apoptosis

DNA is one of the most notable targets of UV-B. There are two important photochemical reactions occurring in DNA after UV-B exposure (i) formations of cyclobutane pyrimidine dimers (CPDs) and (ii) 6-4 pyrimidine-pyrimidine photoproducts (6-4 PPs) [46,47]. If the damaged DNA is left unrepaired, this may result in errors in DNA synthesis and mutations leading to active cellular proliferation and result in skin carcinogenesis. CPDs are highly mutagenic in nature due to their abundance and slow repair [48]; C→T and CC→TT are the most often observed mutations resulting from photoproducts at dipyrimidine sequences in the DNA. These photolesions particularly lead to *p53* mutations resulting in squamous cell carcinoma [49,50]. A surrogate marker for UV-induced DNA damage are sunburn cells (Figure 5), apoptotic cells as a result of UV exposure.

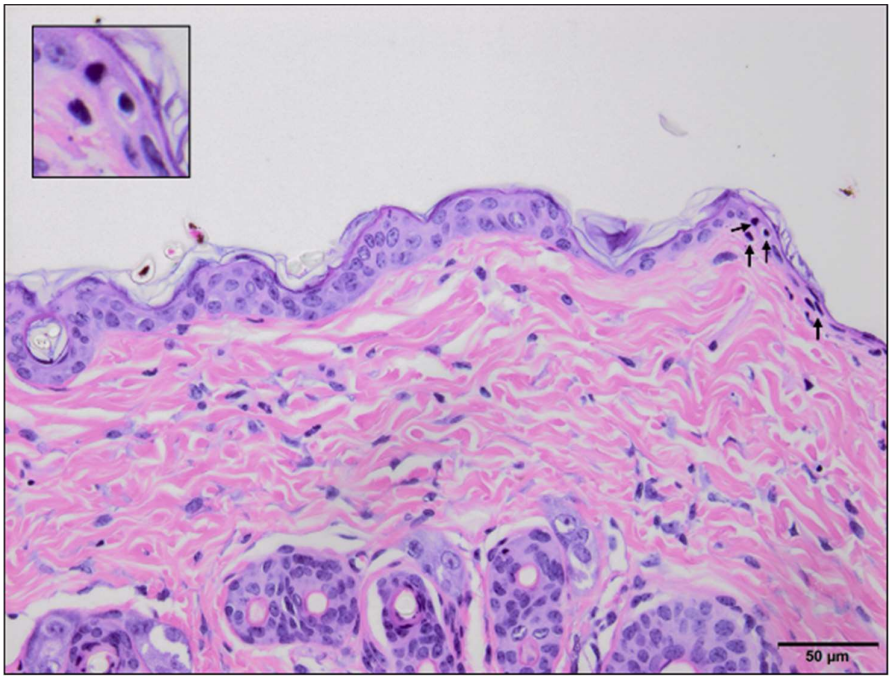

Figure 5: Sunburn cells in UV-B exposed (618 mJ/cm^2) mouse skin*. Hematoxylin and eosin staining for apoptotic cells in the epidermis of irradiated mice. Sunburn cells are indicated by arrowheads.*

1.2.3.1 Modulation of immune responses by UV-R through cellular apoptosis

The epidermis of the skin has a high amount of trans-urocanic acid (UCA) in the stratum corneum, which is normally inactive. Upon UV-R, *trans*-UCA isomerizes to *cis*-UCA, which is known to be a potent immunosuppressive agent [26]. Furthermore, *cis*-UCA can lead to generation of intracellular reactive oxygen species [51,52], cause oxidative DNA damage and lead to immune suppression [53]. That said, Kammeyer A et al., showed that antioxidants abrogate immune suppression caused by cis-UCA[54]. On the other hand, oxidation derivatives of UCA itself can have anti-inflammatory properties [55]. The UV-induced apoptotic bodies (extracellular vesicles generated after apoptosis) are potent inducers of immature LCs, and UV-R is known to cause depletion of LCs, disrupt the migratory ability of LCs which leads to accumulation in the dermis [56]. Moreover, DNA damage in LCs induced by UV exposure can induce the production of IL-10 leading to inhibition of CHS response [57]. LCs are critical for Treg generation and any defect in LCs or Tregs could mediate UV-induced immunosuppression of CHS [58] (Figure 6). LCs after escaping UV-induced apoptosis are known to have reduced capacity to prime $CD8^+$ T cells thus induce tolerance [59]. Therefore, LCs play a major role in generating antigen-specific Tregs, which can mediate UV-induced tolerance in the skin. LCs which are derived from mice deficient in the pro-apoptotic Bid (BH3-interacting death domain protein) can resist apoptosis and ameliorate CHS response [60].

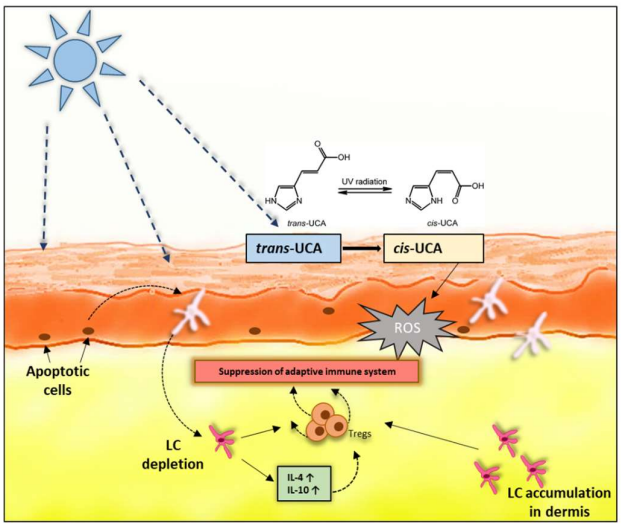

Figure 6: Molecular events after UV-R leading to a cascade of events, eventually suppressing adaptive immune response.

1.2.4 UV-Induced innate responses

UV exposure of healthy individuals leads to suppression of adaptive immune responses. However, no clinical evidence is present for subsequent infections due to suppressed immune response. This may be due to activation of innate immunity in the skin that is the prime sentinal of the immune system and activated immediately after recognizing a wide repertoire of pathogens.

1.2.4.1 UV radiation and antimicrobial peptides

AMPs are one of the key innate immune molecules maintaining healthy homeostasis between the host immune system, skin microbiome and external factors affecting the skin. AMPs in the skin include defensins (α and β), cathelicidin (LL-37), calcium-binding proteins (S100) and ribonucleases (RNase). UV can induce various AMPs such as hBD2, hBD3, RNase7, and S100A7 (Psoriasin) in the skin both *in vitro* and *in vivo* [31]. AMPs are more than just microbicidal, they possess immunomodulating properties, apart from participating in innate immune responses. They actively play a role in adaptive immune responses. The skin innate immunity is greatly enhanced by endogenous AMPs which form a chemical barrier and take part in contributing towards adaptive immune responses [61].

1.2.4.2 Toll-like receptors

Innate immune cells recognize signature molecules of pathogens by expressing pathogen-recognition receptors (PRRs), and these signature molecules are crucial for the survival of pathogens and are known as pathogen-associated molecular patterns (PAMPs). These PRRs recognize PAMPs in skin's compartments and induce production of cytokines for the host defense [62]. One important class of PRRs include Toll-like receptors (TLRs) which are type I integral membrane glycoproteins. TLRs are known to recognize PAMPs that are derived from viruses, pathogenic bacteria and fungi, and parasitic-protozoa. In mice, only TLR1, TLR2, TLR4, TLR5, TLR6, and TLR11 are expressed on the cell surface, whereas TLR3, TLR7, TLR8, and TLR9 are expressed in intracellular vesicles [62-64]. TLRs in collaboration with other innate receptors play an important role in shaping adaptive immune responses. UV-B is reported to activate regulatory B cells via TLR4 signaling and contribute to suppression of CHS responses [43]. In human keratinocytes, UV exposure is known to activate expression of TLR9 [65] and TLR2 in mice [66]. Interestingly, TLR3 can be activated by sensing cellular damage after sunburn [67-69] and contributes to suppressing the immune system.

TLR	Location	PAMPs recognized	Effector cytokines induced
TLR 1 / 2	Plasma membrane (Cell surface)	Triacyl lipopeptides (Bacteria and Mycobacteria)	Inflammatory cytokines (TNF-α, IL-6 etc.)
TLR 2	Plasma membrane (Cell surface)	Peptidoglycan (Gram-positive bacteria), LAM (Mycobacteria), Hemagglutinin (Measles virus), phospholipomannan (Candida), Glycosylphosphophatidyl inositol mucin (Trypanosoma)	Inflammatory cytokines (TNF-α, IL-6 etc.)
TLR 3	Endosome	ssRNA virus (WNV), dsRNA virus(Reovirus), RSV, MCMV	Inflammatory cytokines (TNF-α, IL-6 etc.), type I IFNs
TLR 4	Plasma membrane (Cell surface)	LPS (Gram-negative bacteria), Mannan (Candida), Glycoinositolphospholipids (Trypanosoma), Envelope proteins (RSV and MMTV)	Inflammatory cytokines (TNF-α, IL-6 etc.), type I IFNs
TLR 5	Plasma membrane (Cell surface)	Flagellin (bacteria)	Inflammatory cytokines (TNF-α, IL-6 etc.)
TLR 6 / 2	Plasma membrane (Cell surface)	Diacyl lipopeptides (Mycoplasma), LTA (Streptococcus), Zymosan (Saccharomyces)	Inflammatory cytokines (TNF-α, IL-6 etc)
TLR 7	Endosome	ssRNA viruses (VSV, Influenza virus)	Inflammatory cytokines (TNF-α, IL-6 etc.), type I IFNs
TLR 8 (human)	Endosome	ssRNA from RNA virus	Inflammatory cytokines (TNF-α, IL-6 etc.), type I IFNs
TLR 9	Endosome	dsDNA viruses (HSV, MCMV), CpG motifs from bacteria and viruses, Hemozoin (Plasmodium)	Inflammatory cytokines (TNF-α, IL-6 etc.), type I IFNs
TLR 11	Plasma membrane (Cell surface)	Uropathogenic bacteria, profillin-like molecule (Toxoplasma gndii)	Inflammatory cytokines (TNF-α, IL-6 etc.)

Table 1: **Descriptions of TLR.** LAM: Lipoarabinomannan; WNV: West Nile virus; RSV: Respiratory syncytial virus; MCMV: Murine cytomegalovirus; MMTV: Mouse mammary tumor virus; LTA: Lipoteichoic acid; VSV: Vesicular stomatitis virus; HSV: Herpes simplex virus and CpG: Cytidine-phosphate-guanosine.

1.2.4.3 Cytokines

Cytokines are small proteins that are secreted by various cells that have a specific effect on the interaction among different cells. Cytokines are known by names depending upon cells that secrete them; such as lymphokine (lymphocytes), monokine (monocytes) and adipokine (adipocytes); or their activity such as chemokine (chemotactic activity) or interleukin (produced by one leukocyte to act upon other leukocytes). Similar cytokines can be secreted by different cell types and a single cytokine can act on a wide range of different cells. Furthermore, cytokines are redundant (e.g. similar functions are stimulated by various cytokines). Cytokines are known to act synergistically or antagonistically [70] (Figure 7).

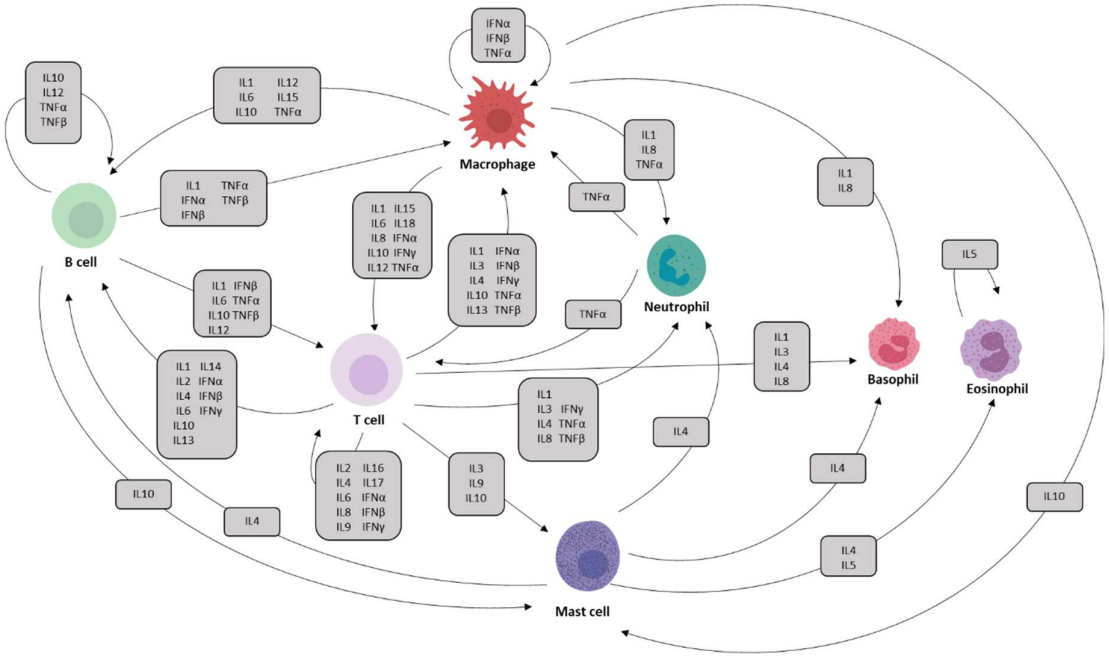

Figure 7: Cytokine network. *Various immune cells including T- and B-cells, neutrophils, basophils, mast cells, eosinophils, and macrophages communicate with each other by secreting various cytokines and play a distinct role in immune response. Reproduced from Zhang et al., 2007 [70] with permission of publisher Wolters Kluwer Health, Inc.*

UV-R is known to cause inflammation in the skin that is linked to the production of cytokines. Cytokines play a prominent role in cellular proliferation and differentiation, cell death and chemotaxis. Interestingly, T cells exposed to UV-R produce inflammatory cytokines which are involved in inducing cellular apoptosis [71,72]. Therefore, cytokines that are produced due to UV-R exposure can be directly involved in local and systemic immune responses. Keratinocytes are one of the most important cells for cytokine productions since they are continuously exposed to UV-R.

1.2.4.4 Langerhans cells (LCs)

LCs are the primary antigen presenting cells that are located in the suprabasal layers of the epidermis at a density of 400-1000 mm^{-2} depending on the anatomical location. The capacity for antigen presentation by LCs is of prime importance in delayed-type hypersensitivity (DTH) and CHS reactions. LCs express HLA-Dr, CD1a, and CD207 (langerin). When LCs encounter antigen or pathogenic microbe they undergo complex activation and maturation and migrate to lymph nodes. These mature LCs can then prime naïve T cells to elicit an immune response [73]. Meanwhile, UV-R exposure is known to alter the process of antigen presentation directly by affecting the epidermal LCs and thus affecting DTH or CHS responses[74]. In humans, UV-R exposure depletes in dose-dependent fashion at least 50% of skin resident LCs ($CD1a^{high}$ LC) after irradiation. However, this depletion in $CD1a^{high}$ $CD207^{-}$ LCs is compensated by the recruitment of $CD14^{+}$ monocytes and two distinct inflammatory dendritic cells, $CD1a^{low}$ $CD207^{-}$ and $CD1a^{low}$ $CD207^{+}$ cells [42].

1.2.4.5 Mast cells

Mast cells are skin resident long-lived cells that provide protection against invading pathogens. Mast cells produce crucial mediators that can orchestrate inflammatory responses to pathogens [75]. Various studies have reported variable effects of UV-R exposure on activated and non-activated mast cells *in vivo* and *in vitro*. Mast cells can release various soluble mediators such as proteases, lipid mediators, cytokines and most notably histamines which contribute to inflammatory responses.

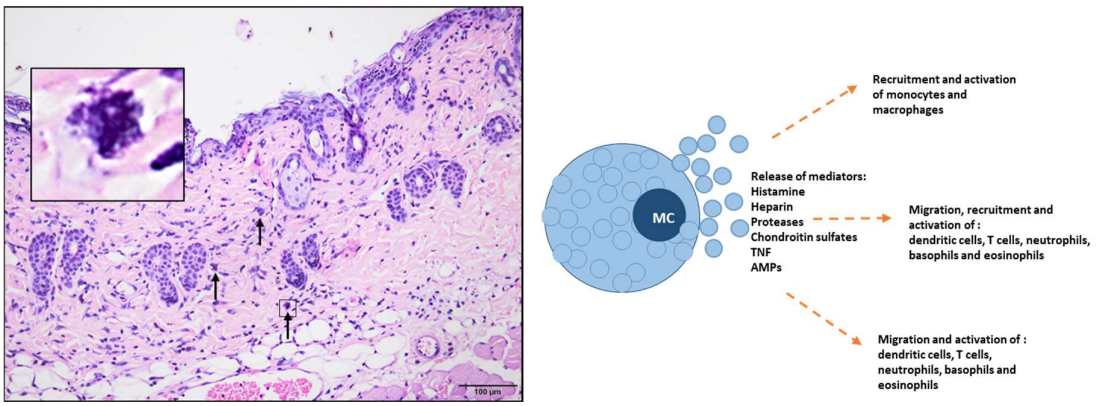

Figure 8: Overview of Mast cells. *H & E image showing mast cells that can release mediators by degranulation in the dermal infiltrate of UV-exposed mouse skin. These mediators are involved in various immune processes including recruitment and activation of various immune cells in the skin.*

Mast cells are critical for UV-induced immune suppression as demonstrated in mast-cell deficient mice (*Wf/Wf*), in which UV-B fails to induce systemic immune suppression [76]. Previous studies report that mast cells are crucial for the immunomodulation via cis-UCA, and formation of cis-UCA is critical to the pathway involved in modulation mast cell activity and degranulation of mast cells by UV-R exposure [77].

1.2.4.6 Neutrophils

Neutrophils are one of the first granulocytic immune cells that travel to the infected site and fight the infection by ingesting microbes and releasing cytotoxic enzymes.

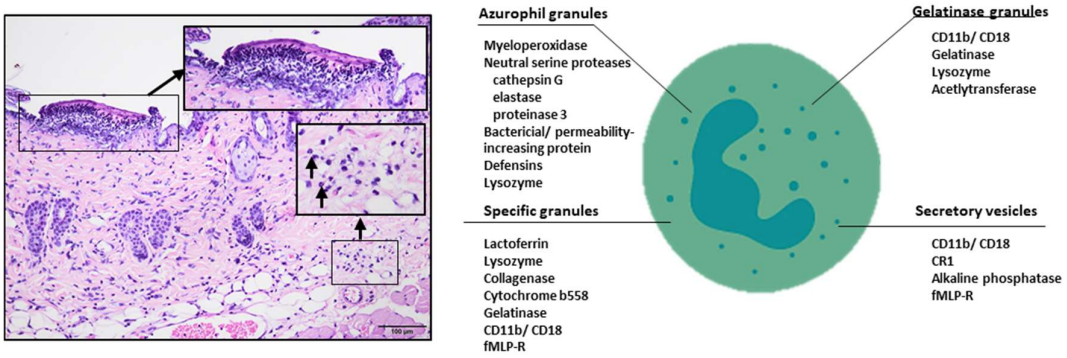

Figure 9: Overview of neutrophils. *H & E image showing neutrophils in the dermal infiltrate and microabscesses of UV-exposed mice skin.*

Exposure to UV radiation leads to a local influx of various immune cells, among which neutrophils are the first to respond and migrate to the irradiated site. However, the functions of neutrophils in UV induced immune suppression are not yet clear. Is it suspected that they could be contributing to multiple processes [78] and the infiltration after UV exposure is due to the signals from damaged skin cells. Infiltrating neutrophils may take part in the removal of these damaged cells by phagocytosis [79] and also contribute to photoaging [80]. Additionally, under certain conditions, neutrophils can secrete a wide range of cytokines. Neutrophils accumulating at UV-irradiated site are known to release IL4 and IL10 which are crucial mediators in UV-induced skin inflammation [78]. Furthermore, a compact accumulation of neutrophils in the epidermis, also known as a neutrophilic abscess can occur in inflammatory conditions such as psoriasis [81].

1.2.4.7 Monocyte/Macrophage:

Monocytes are subsets of white blood cells circulating in the body that are derived from bone marrow cells and differentiate into a wide range of macrophages, dendritic cells, and microglial cells[82].

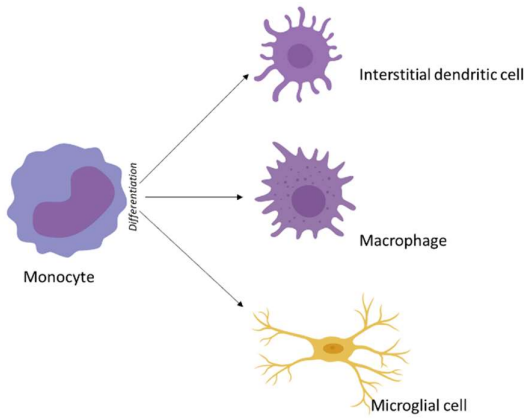

Figure 10: Overview of monocyte differentiation

Monocytes are involved in host defense and play a major role in several inflammatory diseases such as psoriasis. The ability of monocytes to mobilize and traffic to the needed tissue sites is crucial for their functions in mediating immune responses during an infection and driving inflammatory skin diseases[82].

Subset	Markers	Chemokine receptors
Mouse		
$LY6C^{hi}$	$CD11b^{+}CD115^{+}LY6C^{hi}$	$CD11b^{+}CD115^{+}LY6C^{hi}$
$LY6C^{low}$	$CD11b^{+}CD115^{+}LY6C^{low}$	$CX_3CR1^{hi}CCR2^{low}$
Human		
Classical	$CD14^{++}CD16^{-}$	$CCR2^{hi}CX3CR1^{low}$
Non-classical	$CD14^{+}CD16^{++}$	$CX_3CR1^{hi}CCR2^{low}$
Intermediate	$CD14^{++}CD16^{+}$	$CX_3CR1^{hi}CCR2^{low}$

Table 2: Monocyte subsets in mouse and humans

After recruitment to the infected site, monocytes differentiate into macrophages. These macrophages are of two populations, one, which is always resident tissue macrophage (present) and the other major population is newly recruited from hematogenous precursor cells. During inflammation, the number of macrophages increases rapidly and peaks during the granulation tissue formation [83]. These macrophages are involved in antimicrobial effects by releasing inflammatory mediators such as tumor necrosis factor (TNF)-α, nitric oxide and IL-6 [83]. Interestingly, UV-B is known to induce macrophage migration and further involved in IL-10 production to exert an anti-inflammatory environment [84].

1.2.5 UV-induced adaptive immune response

First discovered by Kripke and colleagues landmark studies during the 70s, UV-B was shown not only being carcinogenic but also to suppress the immune responses to syngeneic skin tumors injected into the mice. [85]

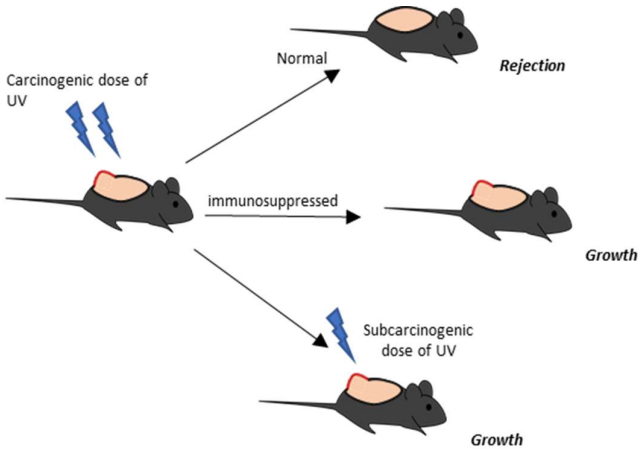

Figure 11: The immune response plays a role in skin tumor growth (Kripke, 1974)

UV-induced skin tumors in mice are extremely antigenic and are rejected when transplanted to genetically matched normal mice (not exposed to UV). However, these same tumors would grow after transplanting into immunosuppressed mice and also UV-irradiated mice. These results indicated that UV radiation not only caused skin tumors but also prevented the rejection by the immune system [85]. Later, it was discovered that UV-induced immune suppression occurred in healthy individuals, a process known to be mediated by T cells [72,86,87]. Single dose UV radiation produces an increase in CD3+ CD4+ T cells in lymph nodes after 24hrs and causes epidermal hyperplasia [88]. Furthermore, UV-R suppresses specific T cell responses in vivo, and also affects B-cell function and reduces specific antibody production [88]. Since the first observation of UV-induced immune suppression, many studies have been performed and the role of T cells has been confirmed in humans and mice by using contact hypersensitivity models.

1.2.6 Contact hypersensitivity assay

CHS is a form of type IV delayed-type hypersensitivity and a classic T cell-mediated phenomenon. CHS reaction to haptens lead to allergic contact dermatitis [89]. Initial skin exposure to a hapten does not lead to any macroscopic skin reaction, but a subsequent exposure to the same hapten will lead to a pruritic rash and swelling within 24hrs in a classic delayed-type hypersensitivity. CHS is both clinically and mechanistically different from immediate hypersensitivity (innate response).

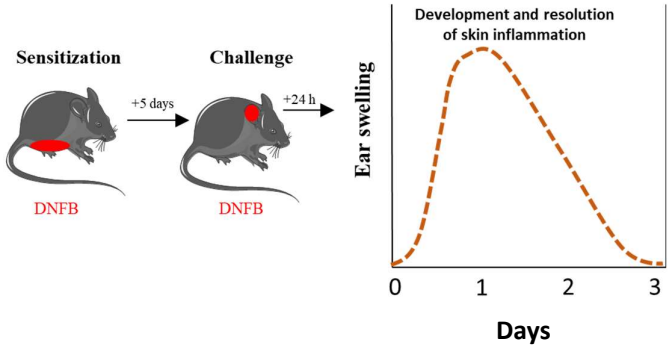

Figure 12: Overview of the CHS model. *Sensitization with topical painting of DNFB on a local site such as the abdomen, and challenge on distal site such as ears with DNFB 5 days later will lead to increased ear swelling due to inflammation.*

CHS is an important experimental model of cell-mediated immune response. When mice are exposed to haptens, it leads to sensitization involving dendritic cells and the LCs which migrate to draining lymph nodes for immune activation. Challenging the mice at a distant site (such as ear) with the same hapten will lead to an inflammatory reaction that peaks usually at 24hrs.

1.2.6.1 Sensitization phase

The haptens used in CHS belong to the class of low molecular weight compounds (<1000). Some of the haptens belong to active synthetic molecules, heavy metal ions, and drugs. The small size of the haptens allows them to penetrate the skin and this can be facilitated if the skin is already compromised by a disease such as atopic dermatitis. Sensitization starts with the entrance of the haptens through epidermis and identification by skin antigen-presenting LCs. This recognition of haptens leads to internalization and endosomal processing of the particular hapten. These processed haptens are presented on the surface of LCs and become associated with major histocompatibility complex I (MHC I) or II (MHC II) molecules, thus activating LCs as observed *in vitro*[90] and *in vivo*[91]. This activation of LC leads to cell

maturation and cytokines responsible for this maturation are proinflammatory cytokines such as IL1β and TNF-α (usually produced in lower quantities in resting state) with IL1β taking the center stage in CHS reaction among other costimulatory molecules (ATP/PGE2, LTB4, ROS, ICAM-1). IL10 is functionally opposite to the aforementioned cytokines. IL10 is responsible for suppression of the costimulatory molecules and inhibiting the production of pro-inflammatory cytokines. The role of IL10 in suppressing CHS reaction is shown by injecting it after sensitization, reducing induction of IL1β and TNFα [92]. These inhibitory effects of IL10 are involved directly in limiting antigen presentation functions of LCs, which in turn prevents tissue damage and inflammation. The matured LC migrate towards the lymph node (LN) (where a high density of T cells resides) which is triggered by the actions of IL1β and TNFα. By the time LCs reach the LN, they are fully mature. Chemokines play a major role in homing the LC to LN (Table 3).

Immature DC		**Mature DC**	
Receptor	*Chemokine*	*Receptor*	*Chemokine*
CCR1	CCL3,5,7,8,13,14,15,23	CCR7	CCL19,21
CCR2	CCL2,7,8,13	CXCR5	CXCL12
CCR4	CCL17,22		
CCR5	CCL3,4,5,8,11,13,14		
CCR6	CCL20		
CXCR4	CXCL12		

Table 3: Chemokine receptors expressed on DC and involved in migration to LN. *Adapted from [93]*

After the arrival of matured LCs, antigen presentation takes place. Receptors of naïve T cells recognize the fragments bound to the surface of LC (bound to MHC-I and MHC-II). This binding of specific antigen receptors to peptide fragments leads to specific $CD4^+$ and $CD8^+$ T cell proliferation and maturation[94 95]. These matured T cells acquire novel molecular keys (such as a cutaneous lymphocyte-associated antigen [CLA]), that lets them to extravasate from blood vessels. Once CLA is acquired, these activated T cells are drawn into circulation,

and this completes the process of sensitization [96]. The sensitization process lasts up to 10-15 days in humans and 5-7 days in mice [94].

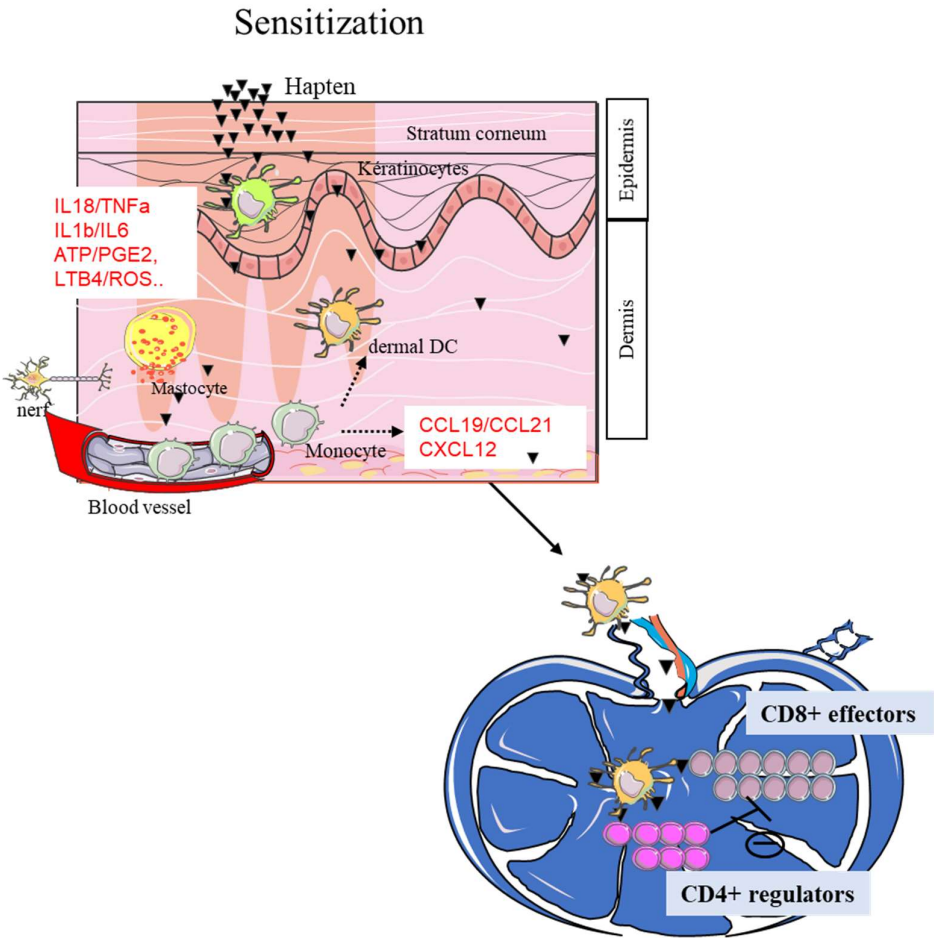

Figure 13: Systematic representation of the pathophysiology of contact hypersensitivity. *Sensitization phase: Hapten penetrates through the skin, inducing a local inflammatory reaction whereby the innate immunity is activated including hyphenation of the proteins, followed by the release of various pro-inflammatory mediators such as IL-1β, TNF-α, IL-18, ATP, PGE2, LTB4, ROS, and histamines by skin-resident cells. Leukocytes from blood are rapidly recruited to the skin which include CCR2+ monocytes that are then differentiated into DCs. These haptenized DCs undergo activation/maturation and migrate into LN whereby they activate specific $CD8^+$ T cells. Figure reproduced from Vocanson M et al, 2009 [94] with permission (see license attachment) from John Wiley and Sons.*

1.2.6.2 Elicitation phase

The elicitation phase of CHS is triggered when the hapten is re-applied (challenge) to the skin. CHS hapten, small molecule enters cells (keratinocytes', LCs) binds to endogenous proteins to be processed into MHC1 addressing CD8+ T cells; in contrast to larger antigens injected in DTH reactions processed by professional APCs to be presented in MHC II addressing mainly CD4+ T cells .The antigen presentation to hapten-specific T cells induces local clonal proliferation and differentiation, followed by an accelerated accumulation of effector T cells at the challenged site. Antigen presentation is performed by LCs, keratinocytes, mast cells, endothelial cells, and macrophages[97]. CD8+ cytotoxic T cells are the main effector cells of the CHS response and are recruited to the challenged site. Their activation in the skin leads to the development of eczematous lesions[94].

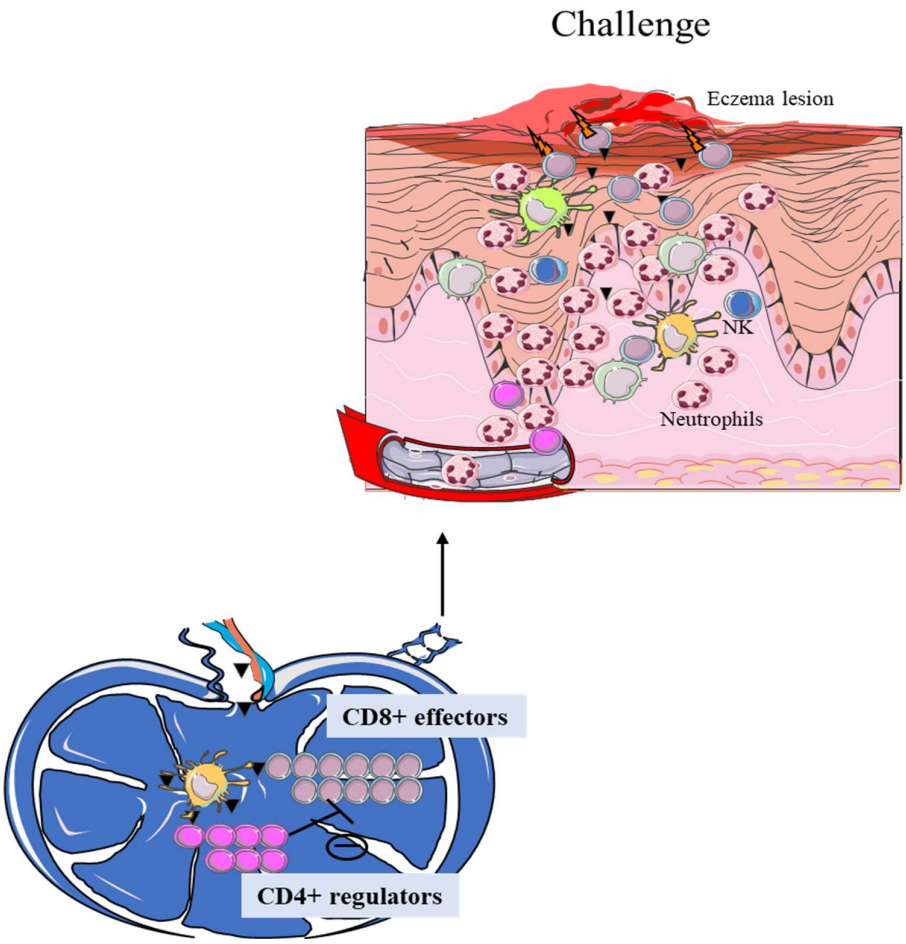

***Figure 14: Challenge phase**: Re-exposure to the same hapten leads to rapid activation of innate immunity as depicted above, along with secondary responses (due to existing specific IgM molecules and T cells). After the protein is haptenized in the skin, hapten-specific IgM antibodies are involved in the generation of C5a, which activates mast cells to produce TNF-α and serotonin. Skin-resident cells secrete inflammatory mediators such as IL-18, IL-1β, TNF-α, ATP, PGE2, histamine, and CCL2. Blood leukocytes are recruited, including hapten-specific effector T cells within 6-12 hrs. Keratinocytes apoptosis is induced by hapten-specific effector $CD8^+$ T cells and new inflammatory mediators (CXCL9, CXCL10) are released by resident-skin cells, mostly by mast cells (TNF-α, CXCL-8) which induce an influx of a second wave of leukocytes including mostly of neutrophils. Eczematous lesions appear within 24-48 hrs. Figure reproduced from Vocanson M et al, 2009 [94] with permission (see license attachment) from John Wiley and Sons.*

The induction of CHS response is suppressed when the hapten is applied epicutaneously after UV-R exposure directly to the irradiated area like dorsal skin (local immune suppression) and/or to an unirradiated distal area, usually abdomen (systemic immune suppression)[98]. The induction of systemic immune suppression generally requires higher doses of UV-R compared to local immune suppression. UV-B is known to cause defects in antigen presentation, which in turn will lead to failure of T cell differentiation and proliferation, thus affecting the immune response to hapten.

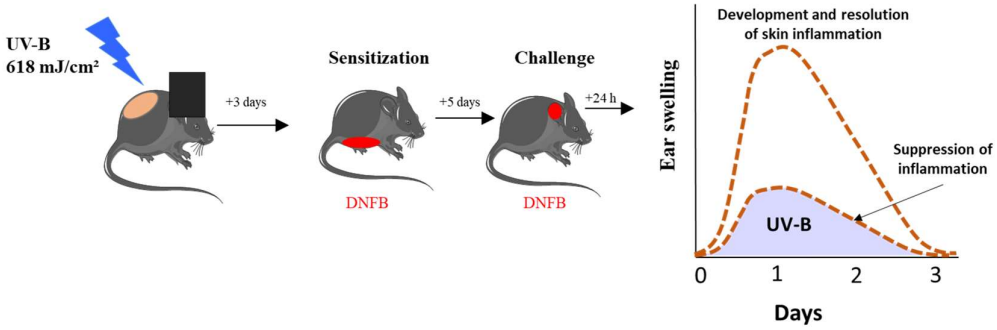

***Figure 15: UV-induced systemic induction of CHS.** Irradiation with UV-B (ears protected from exposure) and 3 days later sensitization with DNFB on distal site such as the abdomen, and challenge with DNFB 5 days later will lead to significantly reduced ear swelling due to immune suppression.*

1.3 Skin microbiome

Human skin is one of the largest organs of the body and has the largest epithelial surface close to 25 m^2 (including appendages) [99], with a diverse physical, chemical and biological ecosystem. The epithelial surface harbors abundant and diverse microbial species (bacteria, fungi, viruses, archaea) and engages in a mutualistic relationship with these microbes[61]. Is it estimated that around 10^{10} bacterial cells inhabit the entire skin of the human body, with 1 million bacterial cells residing per square centimeter of the skin [100]. The majority of these microbes are transients or commensals (causing no harm). Opportunistic and/or pathogenic bacteria (in cases of infection) also exist within the skin. The diversity of skin microbiome is partly due to the diverse nature of the skin ecosystem, influenced by humidity, moisture, temperature, pH, lipids, and sebum content[101]. Despite having a robust immune system, with a strong ability to rapidly detect and eliminate foreign invaders, it is intriguing that an innumerable number of microbes resides on the surface and sub-epidermal compartments [61] [101].

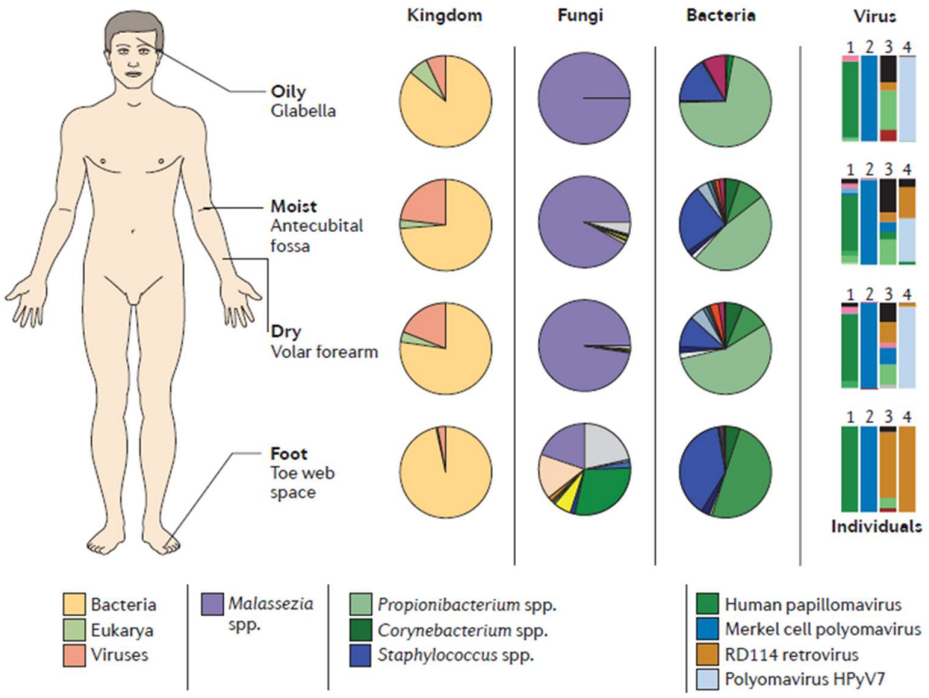

Figure 16: Skin microbial composition in human skin. *Image reproduced from Byrd A et al., 2018 [102] with permission (see license attachment) from Springer Nature.*

Sequencing the 16S small-subunit ribosomal RNA gene, revealed that skin is colonized by a wide range of bacterial species, mostly dominated by *Proteobacteria, Actinobacteria, Bacteriodetes* and *Firmicutes* [103]. The bacterial colonization depends topographically as several studies indicate specific communities of bacteria are associated with moist, dry or sebaceous environments within the skin. The moist areas of the skin, such as umbilicus, axillary vault, inguinal crease, gluteal crease, foot etc. have an abundance of *Staphylococcus* and *Corynebacterium* species and these microbes prefer increased humidity. The dry areas such as buttocks and forearms show a highly intertwined abundance of *Actinobacteria, Proteobacteria, Firmicutes*, and *Bacteriodetes.* Moreover, these dry skin sites are known to be colonized with gram-negative bacteria, which were initially thought to be very rare on the skin. Compared to the gut or oral cavity, there is a higher phylogenetic diversity of bacteria in these dry skin sites [104,105]. Sebaceous sites are mostly known to harbor fewer bacterial populations due to the harsh microenvironments. The forehead, area behind the ears, inside of the nose are few examples of sebaceous environments with lower bacterial phylotype richness [105]. *Propionibacterium* species are observed to be dominant in areas like hair shaft and follicle [61,105].

Skin is colonized by a wide diversity of fungal species which contribute to health and disease. The genomic methods to characterize fungal species are very limited in comparison to that available for bacteria. Findley et al[106] describes the fungal species residing in the skin by using ITS1 (internal transcribed spacer 1 region) and 18s rRNA (phylogenetic marker within the ribosomal RNA). Malassezia genus was observed to be dominant across 11 different core body sites (back, occiput, external auditory canal, inguinal crease, retroauricular crease, glabella, manubrium, nare, antecubital fossa, volar forearm, hypothenar palm, plantar heel, toe nail, and toe-web space). The plantar heel was observed to have the highest fungal diversity, including *Malassezia, Aspergillus, Cryptococcus, Rhodotorula, Epicoccum* among others [61,106].

Probst et al[107] reported the lesser known archaeal communities in the skin by sequencing 16s rRNA and observed 4% of microbial genes were of archaeal 16s rRNA genes. Around 90% of all the observed operational taxonomical units (OTUs) consisted of phylum Thaumarchaeota with the rest being Euryarchaeota. Recent studies [108,109] indicate the potential role and importance of archaea in health and diseases[61].

One of the less investigated subsets of skin microbiome are skin-related viruses and viral-like particles, that cannot be cultivated and do not show any consensus sequences to be detected using molecular tools. However, in recent years there has been increasing evidence that skin harbors resident or short-lived viruses, such as human alpha, beta, and gamma papillomaviruses (α-HPV, β-HPV, and γ-HPV) [110,111]. Functional metagenomic methods have also revealed new viruses related to *Polyomoaviridae* family [112]. These studies show that healthy skin has the presence of cutaneous viral microbiome, which might be involved in certain proliferative skin diseases[61].

1.3.1 Skin microbiome and immunity dialog

The skin microbiome and the immune system are in constant communication with each other to support tissue homeostasis. To carry out this homeostasis, the skin's immune system has to be tailored to the appropriate threat, as any immune response to skin commensal could lead to inflammation and disease formation [113]. To execute these functions, the skin has been equipped with numerous immune cells (innate and adaptive immune system)[113]. An acute damage to the skin will lead to the production of ligands/antigens/PAMPs/DAMPs, which can activate keratinocytes and result in the subsequent release of inflammatory mediators. In these conditions, LPA (product of *Staphylococcus epidermidis*) can indeed reduce the level of inflammation and be part of wound healing by binding to TLRs [114] and more recently it has also been described that, immunogenicity to microbial LPS can lead to autoimmunity [61,115]. Skin microbiome can indeed control and regulate the expression of a wide range of innate immune sensors such as AMPs and gene expression of various immune regulators [116,117]. The mechanisms by which AMPs shape the skin-resident microbes remains elusive, as these AMPs can be induced by both UV-R and skin microbiome. This complex multidirectional interaction might be key to unlock the pathophysiology of various inflammatory skin diseases and can give an insight into the physiology of healthy skin[61].

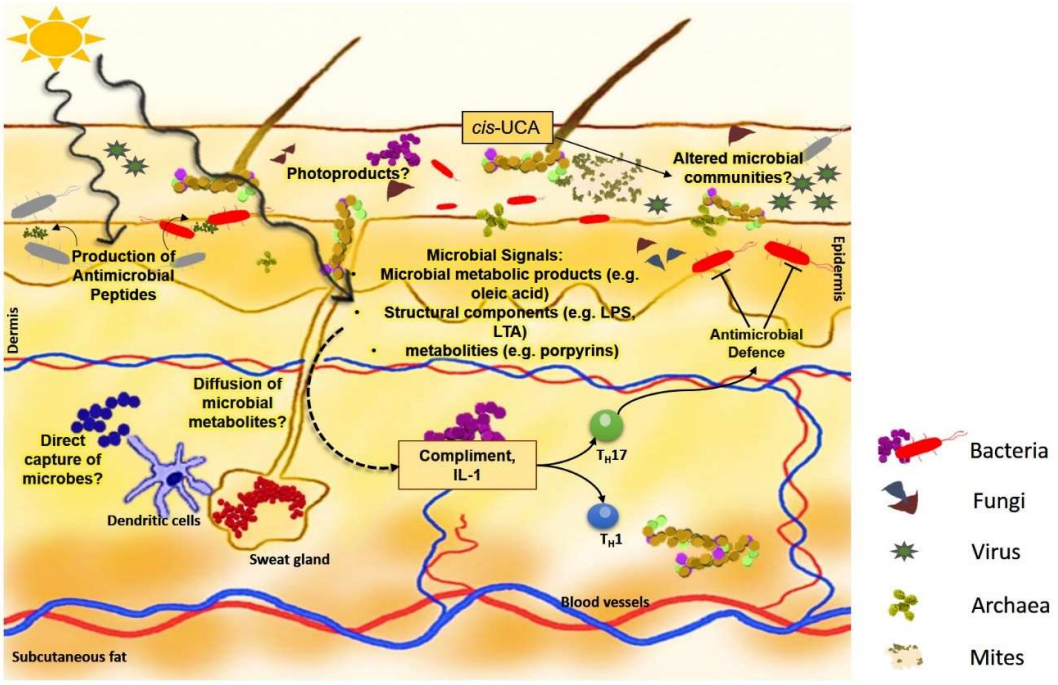

Figure 17: Potential mechanisms of microbial interference in UV-induced immune suppression. *Microbiome, consisting of bacteria, fungi, viruses, archaea, and mites, covers the skin surface as well as colonizes in appendages and glands. This cutaneous microbiome encounters similar UV-R as skin cells do. UV-R could directly alter the microbial communities on the skin, by producing microbial photoproducts such as pyrimidine dimers and/or 6-4 photoproducts, leading to microbial killing. At sub-toxic levels, UVR may initiate a pathogen/damage-associated molecular pattern (PAMP/DAMP) response. Such a response may result in the expression of various microbial signals such as oleic acid, LPS and/or porphyrins, affecting the overall immune signaling cascade, leading to inflammation, and altered immune response. Microbial metabolites can also exert an effect on dendritic cells which can recognize or can be involved in the direct capture of microbes. Moreover, microorganisms can produce natural AMPs directly or can control AMP production by keratinocytes and their production can be increased by exposure to UV-R. UVR-induced cis-UCA could not only contribute to induction of altered immune response but also indirectly change the microbial load, by affecting the microenvironment through yet unknown pathways. In addition, the microbiome can also induce complement and IL-1 set under stress by UV-R and together with directly induced microbial signals influence the skin immunity*

by induction of various cytokines such as that of the Th17 pathway. Said so, keratinocyte effector function could be influenced by production of IL-17, leading in a circle to altered AMP production, and release, in turn affecting the microbiome. Reproduced from Patra V el at [61] under the terms of Creative Commons Attribution License (CC BY).

1.4 Hypothesis and Aims

Much of the skin microbiome at the sun-exposed body sites are directly exposed to UV-radiation, either completely or during most of its life cycle. Exposure to UV can impose profound changes in microbial species and furthermore lead to a chain of events leading to immune suppression. In healthy individuals, UV-R is known to activate the innate immune system and suppressing the adaptive immune arm[16,61]. Furthermore, UV-R is directly linked to many pathological skin diseases such as polymorphic light eruption, and skin cancers.

On the other hand, skin microbiome is known to educate and control the skin's immune system by various mechanisms and signaling pathways. Dysbiosis in resident skin microbiome leads to many inflammatory skin diseases such as atopic dermatitis, acne among others. Interestingly, a recent study reports the contribution of skin microbiome to differentially regulate the gene expression in the skin, most notably for the genes encoding TLRs, AMPs, genes related to IL1 family [117]. Furthermore, the microbiome is also involved in regulating genes responsible for epidermal differentiation and development and influence wound healing [117,118]. However, the effects of UV on the resident skin microbiome and the role of skin microbiome in UV-induced immune suppression or modulation has been overlooked.

In this thesis, the aim was to extend the current knowledge of UV-induced immune suppression with following questions:

- What is the skin microbial (bacteria) alterations at different doses of UV-B by 16S rRNA sequencing?
- What is the UV-B induced physiological changes and immune infiltration within the skin?
- What is the role of skin microbiome in UV-induced immune suppression to contact allergen?
- What is the molecular signature of UV exposure, with and without the presence of microbiome?

1.5 Material and Methods:

1.5.1 Animals:

Cesarean born, axenic 4-8 weeks old female C57/BL6J mice were bred at the Core Facility for Germfree Research (CFGR) at Karolinska Institutet, Stockholm, housed in a sterile environment and regularly monitored to ensure their germ-free status. All short-term experiments with axenic mice were conducted in ISOcage Positive cages from Tecniplast, using the appropriate SOPs at CFGR, Karolinska Institutet. Protocols involving the use of germ-free animals were approved by the Regional Animal Research Ethical Board, Stockholm, Sweden (Stockholms norra djurförsöksetiska nämnd), following proceedings described in EU legislation (Council Directive 86/609/EEC). Animal husbandry was in accordance with Karolinska Institutet guidelines and approved by the above-mentioned board (Ref: N190/15). For disinfection studies, 4-8 weeks old female C57/BL6J (stock: 00064) mice were purchased from Charles-River Laboratories, Sulzfeld, Germany. Five mice per experimental group were housed in autoclaved cages. Sterile food and water were provided to all the animals. All animal protocols were also approved by the Austrian government, Federal Ministry for Science and Research approved animal procedures, through protocol number BMWFW-66.010/0137-WF/V/3b/2014. Animal experiments adhered to 3R policy to ensure use of minimum numbers of animals to maximize data mining.

1.5.2 Skin disinfection:

Shaved dorsal skin of mice was disinfected using 2% chlorhexidine- and 70% isopropyl alcohol- pre-soaked wipes (purchased from Clinell #CA2CSKIN). Two fresh wipes were subsequently rubbed gently each for at least 30sec on the dorsal skin of the mice 24hrs and 1 hr. prior to UV-B irradiation and control mice.

1.5.3 UV-B source and irradiation:

The backs of the mice were shaved using an electric clipper 24hrs prior to UV-B exposure. UV radiation was performed using a Waldmann 236 light source (Waldmann Medizintechnik, Villingen-Schwenningen, Germany), equipped with two Waldmann UV6 fluorescent tubes (emission range 280–360 nm; peak, 320 nm) and positioned upside down on top of the cage. The mean UVB irradiance of the lamp was 1.9 mW/cm^2, as measured by a Waldmann UV photometer with a UV6 detector head appropriate to the radiation device.

A dose of UV-B radiation of 618 mJ/cm^2 (average time of exposure 5 min 42 sec) was given to the animals. During the UV exposure, ears of all the mice of CHS experiments were shielded by covering with black electric tape. All the procedures were performed under sterile conditions and using a laminar air flow unit.

1.5.4 Skin sampling for microbiome analysis

Skin swabs were collected from shaved backs of the mice using BD CultureSwab™ EZ Collection and Transport System soaked with sterilized 0.15M NaCl and 0.1% Tween-20 [119]. The tips of swabs were then cut off under sterile conditions into a sterile 1.5 ml reaction tube. PMA™ (propidium monoazide) (Biotium, #40013) was added to the reaction tube and left at room temperature for 5 min in dark and subjected to photo activation for 15 min using PMA-Lite™ LED Photolysis Device (Biotium, #E90002). Unused swabs soaked in sterile buffer were used as negative control. The samples were then frozen at -80ºC at once until further processing.

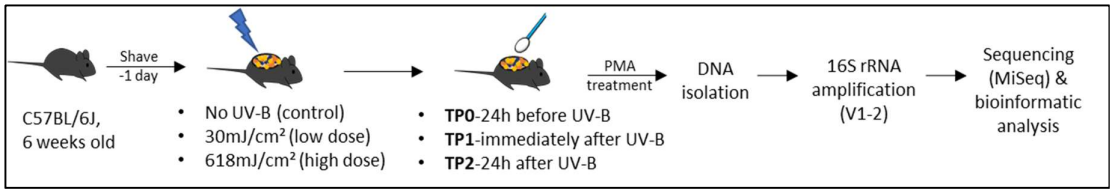

Figure 18: Overview of the experimental setup.

1.5.5 Skin sampling for urocanic acid quantification:

1-2 Tape strips (D100 - D-Squame Standard Sampling Discs, Clinical & Derm) were used to collect a sample before and after UV-B exposure. Tape strips were collected in a sterile tube and snap frozen immediately in liquid nitrogen and stored at -80º until further processing. The tape strips were extracted with 500 µl methanol at 20°C for 10 min with 800rpm on a Thermomixer (HLC, KTR-133) shaker. The extracted samples were dried overnight at room temperature in a speed vac concentrator (SAVANT, SC250EXP). Samples were re-suspended in 500 µl H2O with 0.5 % formic acid (FA), centrifuged at 6°C with 2500 rpm (Heraeus, Multifuge 3LR), and stored at 6°C in auto sampler before analysis with LC-MS. To compare the *trans*- and *cis*-UCA values a calibration line was measured within a concentration range of 0.00586 µM up to 3 µM cis/ trans-UCA.

1.5.6 Liquid chromatography (LC)/MS for analysis of *cis* and *trans*-urocanic acid

The processed mouse skin tape strips samples were separated on a Phenomenex Kinetex EVO C18 2.1 x 150 mm x 2.6 µm column, thermostated at 45°C in an Advanced UHPLC system from Bruker. Isocratic elution was done with H2O 0.1% FA at a flowrate of 130 µL min-1 for 6 min per run. Autosampler tray was kept at 6°C and 5 µl of the sample was injected. After chromatographic separation, the samples were analyzed by EVOQ triple quadrupole (Bruker) mass spectrometer in positive ESI mode. Ion source parameters were: source voltage 4 kV, cone temperature 350°C, heated probe temperature 300°C, cone gas flow of 20 arbitrary units, heated probe gas flow of 40 arbitrary units, and nebulizer gas flow of 60 arbitrary units. Peak areas were calculated by MS data review (Bruker) for all detected analytes.

1.5.7 Transepidermal water loss (TEWL), skin hydration and pH measurement:

TEWL was measured using open chamber Tewameter® TM 300 probe, by gently applying it on the skin surface for 30s. Skin hydration or moisture was measured using a Corneometer® CM 825 probe and pH using the Skin-pH-Meter PH 905 probe. All the probes were connected to Cutometer® dual MPA 580 (Courage and Khazaka Electronic GmbH, Köln, Germany) and data collected using the MPA software.

1.5.8 Complete blood count:

Blood was collected by retroorbital puncture from the mice in EDTA coated vials and were processed immediately using the cell counter analyzer- MELET SCHLOESING LABORATORIES.

1.5.9 Skin and lymph node cell isolation

Skin biopsies and brachial lymph nodes were collected, cut in small pieces, and incubated at 37°C, 45min or 20min, respectively, in a digestion media (RPMI 1640 medium supplemented with 2 mM L-glutamine, 10 mM 4-(2-hydroxyethyl)-1-piperazineethanesulfonic acid (HEPES) (all from Life Technologies, Carlsbad, California, USA), 10% fetal calf serum (FCS; Lonza, Basel, Switzerland), collagenase type 1 (121.9 CDU/ml; Sigma-Aldrich, Saint-Quentin Fallavier, France) and DNase (2 KU/ml; Sigma-

Aldrich, Saint-Quentin Fallavier, France). Cells were passed through a 100µm cell strainer (ThermoFisher Scientific, Dardilly, France) to obtain single cell suspensions. Cell viability was determined by trypan blue exclusion.

1.5.10 Flow cytometry analysis

Isolated single cell suspensions were stained using fluorescently labeled monoclonal antibodies (mAbs) and fixable viability staining was performed to exclude dead cells from the analysis. Stained cells were analyzed on an LSRFortessa flow cytometer (BD Biosciences, Franklin Lakes, New Jersey, USA), and data were analyzed using FlowJo software (Treestar, Ashland, Oregon, USA). Total cell numbers were calculated based on the numbers of viable cells determined by trypan blue exclusion during the isolation process.

1.5.11 Monoclonal antibodies used for flow cytometry

The antibodies used for flow cytometry included CD11c (cl:HL3), CD11b (cl:M1/70), MHC-II (cl:2G9), CD64 (cl: X54,5/7,1), CD86 (cl: GL1), Ly6G (cl: 1A8), CD8b (cl: H35-17.2), CD103 (cl:M290) from BD Biosciences, CD45.2 (clone(cl): 104), CD244 (cl: m2B4(B6)458.1) from Biolegend, CD40 (cl: 1C10), PD-1 (cl: J43), CD69 (cl : H1-2F3) from Ebioscience, TCRab (cl: H57-597) from Invitrogen, Epcam (caa7-9G8), CD83 (cl: REA304) from Miltenyi, TIM-3 (cl: 215008) from R&D Systems. Cell viability was analyzed using a Fixable Viability Dye eFluor™ 450 (eBioscience, #65-0863-14; San Diego, California, USA).

1.5.12 DNA isolation

Total DNA was isolated from the frozen skin swabs with both mechanical and enzymatic lysis. The samples were thawed and transferred to a sterile Magna Lyser green bead tubes (Roche, Manheim, Germany) and bead beat for mechanical lysis at 6000 rpm for 30 secs for two times in a MagNA Lyser Instrument (Roche, Mannheim, Germany). Unused swabs and unused buffer tubes without swabs served as negative controls for sampling and DNA isolation. The samples were further subjected to enzymatic lysis by incubating with 20 µl lysozyme at 37ºC for 1 hr. Further processing was performed using QIAamp ® DNA mini kit (Qiagen, Germany) per manufacturer's instructions. Total DNA was eluted in 35 µl of buffer AE provided in the kit. Total DNA was stored at -20ºC until PCR amplification. All the procedures were performed under sterile conditions.

1.5.13 16S microbiome sequencing

16s rRNA library preparation, quantitation, and sequencing were performed as recently published by Klymiuk et al [120]. Briefly, 5 µl of total DNA was used for PCR amplification with the target-specific primers 27F 5'- AGAGTTTGATCCTGGCTCAG - 3' and R357 5' – CTGCTGCCTYCCGTA -3' (MWG, Ebersberg, Germany). PCR reaction was of initial denaturation at 95°C for 3 minutes followed by 32 cycles of denaturation at 95°C for 45 seconds, annealing at 55°C for 45 seconds and extension at 72°C for one minute. Final extension was performed at 72°C for seven minutes and PCR reactions were performed in triplicates. Triplicates were pooled and 5 µl visualized on a 1% agarose gel for amplification success. Normalization, indexing, pooling of the individual PCR products and purification of the final library were performed as described in Klymiuk et al [120]. The library was quantified using the QuantiFluor ONE dsDNA Kit (Promega, Mannheim, Germany) according to manufacturer's instructions and visualized on an Agilent 2100 Bioanalyzer (Agilent Technologies, Waldbronn, Germany) using a high sensitivity DNA assay according to manufacturer's instructions. The 6 pM libraries were sequenced on a MiSeqII desktop Sequencer (Illumina, Eindhoven, Netherlands) with v3 chemistry for 600 cycles and 20% PhiX control DNA and FastQ files were used for data analysis.

1.5.14 16S microbiome analysis

Raw reads were processed in a two-step procedure: First, sequences were pre-processed (including steps of trimming, removal of low quality, short and homopolymeric sequences as well as of sequences containing undefined bases) and quality filtered (denoised, chimera and contaminant removal) using mothur (1, version 1.23) according to the developer's protocol [2, accessed June 2016]. Default and recommended parameters were used if not indicated otherwise. Second, the remaining high-quality sequences were further processed with QIIME (3, version 1.9.0). Operational taxonomic units (OTUs) were established by QIIME's open reference OTU-picking strategy [4] using UCLUST (OTU clustering distance 0.03) against the Greengenes [5, version 13.8] reference database for taxonomic classification of representative sequences. Sequences were rarefied to a minimum sequencing depth per sample of 756 reads. Alpha diversity was assessed by the number of observed species (observed_otus), Chao1, and Faith's phylogenetic diversity index (PD_whole_tree) implemented in QIIME's core. diverstiy workflow. Beta diversity was

evaluated by principal coordinate analysis (PCoA) based on unweighted UniFrac [6] distances calculated within QIIME's core diversity script and plotted in GraphPad Prism Version 7. Linear discriminant analysis (LDA) was performed by LEfSe [7, version 1.0]. Statistical comparison of alpha-diversity metrics (within QIIME's core.diverstiy workflow) was performed using an unpaired t-test and 999 Monte-Carlo permutations. Bonferroni correction was used to account for multiple comparisons. Non-parametric ADONIS (QIIME compare. Categories) was used to test for significant differences of beta-diversity based on the unweighted UniFrac distances. Significant differences in relative abundances of taxa between groups were calculated using linear discriminant feature analysis by LEfSe. P-values ≤ 0.05 were considered statistically significant if not indicated otherwise.

1.5.15 Contact hypersensitivity assay:

Groups of mice were sensitized (3 days after UV exposure) with 50µl of freshly prepared 0.5 % 1-Fluoro-2,4-dinitrobenzene (DNFB; Sigma #D1529) in acetone on the shaved abdomen. Five days later the ears were challenged with 20 µl of freshly prepared 0.25 % of DNFB in acetone. Ear thickness before and 24hrs after the challenge was measured using spring-loaded engineer's micrometer (Mitutoyo) to calculate ear swelling and the following formula was used for calculating percent suppression of CHS:

$$\boldsymbol{CHS = \left[1 - \left(\frac{Ear\ swelling\ of\ UV+\ senstized+mice}{Ear\ swelling\ of\ UV-\ sensitized+mice}\right) * 100\right].}$$

1.5.16 Skin sample collection for microarray and histological analysis:

Group of 3 GF or SPF mice were irradiated with a single dose of UV-B (618 mJ/cm^2) on the shaved dorsal skin. 24hrs later the mice were sacrificed, and skin samples were collected and fixed in 4% formaldehyde and paraffin-embedded for histological and immunohistochemical analysis. Parts of the skin samples were snap frozen in liquid nitrogen and stored at -80º C until RNA isolation.

1.5.17 RNA extraction, Microarray, and data analysis:

Total RNA was extracted using the miRNeasy Kit (Qiagen, Hilden, Germany; Cat. No. 217004) including DNase treatment steps on the column according to the protocol. We obtained RNA quality of a RIN between 5 and 6 (checked on the BioAnalyzer BA2100 (Agilent; Foster City, CA; Cat. No. 5065-4476)). GeneChip® Mouse Gene 2.0 ST Arrays

(Affymetrix; Santa Clara, CA; Cat No. 902118) was used for the whole transcript; additionally, we used 500ng of the total RNA for the amplification since the RNA included fragmentation. The protocol was followed according to the manual. The amplified cDNA was analyzed using the BioAnalyzer BA2100 (Agilent, Foster City, CA) and RNA 6000 Nano LabChip (Agilent; Foster City, CA; Cat.No. 5065-4476). The given fragment size of < 2000nt over all samples was satisfying for ss-cDNA synthesis, fragmentation, and labeling according to the manual. We hybridized 18h at 45°C as suggested by the manual while rotating in the hybridization oven. Washing and staining (GeneChip® HT hybridization, Wash, and Stain Kit; Affymetrix, Santa Clara, CA; Cat No. 900720) were done with the Affymetrix Genechip® fluidics station 450 according to the manual (protocol on fluidics station: FS450_0002). Arrays were then scanned with the Affymetrix GeneChip scanner GCS3000. For the evaluation of the hybridization controls and pre-analysis Affymetrix Expression Console EC 1.3.1. was used – no technical outlier arrays were detected. Raw data are available at the Gene Expression Omnibus (GEO; accession number GSE117359). Statistical analysis was done with the Partek Software v.6.6 (Partek Inc, St Louis, MO). CEL files with the probe intensity data are imported using robust multichip average (RMA) algorithm. This includes background correction, quantile normalization across all arrays, median polished summarization based on log-transformed expression values. Differences among groups are tested with 1-way ANOVA.

1.5.18 cDNA synthesis and qPCR:

Total RNA (1µg) extracted for microarray was used to prepare cDNA using the Script cDNA synthesis kit (#1708890; Bio-Rad Laboratories). Reverse transcription (RT) was then performed on the 1µl RNA sample by adding iScript reagents including 4µl 5x iScript reaction mix, 1µl iScript reverse transcriptase, and nuclease-free water to a reaction volume of 20µl. The reaction was incubated for priming at 25°C for 5 min, RT at 42°C for 30 min, and RT inactivation at 85°C for 5 min. 1:5 diluted cDNA was used for qPCR. PCR was performed in 384-well Hard-Shell ® PCR plates (#HSP3805, Bio-Rad Laboratories). 1 µl of cDNA, 5 µl of iTaq ™ universal SYBR® Green Supermix (#1725121, Bio-Rad Laboratories), 1 µl 10 pM forward primer, 1 µl 10 pM reverse primer and sufficient nuclease-free water was in used in a total reaction volume of 10 µl. mRNA was then quantified using quantitative PCR on a CFX384 Touch Real-Time PCR Detection System (Bio-Rad Laboratories). Primer pairs used are listed below. Expression of mRNA was analyzed using the change-in-cycle-threshold (ΔCT or ΔΔCT) method.

Gene	Sequence (5'->3')
IL10	CCA AGC CTT ATC GGA AAT GA CCA AGC CTT ATC GGA AAT GA
IL1β	CAG GCA GGC AGT ATC ACT CA AGG TGC TCA TGT CCT CAT CC
IL17a	AGC TGG ACC ACC ACA TGA AT AGC ATC TTC TCG ACC CTG AA
Ccl3	CCC GAC TGC CTG CTG CTT CT GAT CTG CCG GTT TCT CTT AGT CA
Ccl7	GCATGGAAGTCTGTGCTGAA AGAAAGAACAGCGGTGAGGA
S100A3	GTGAGTTCCGGGAGTGTGAC TGGCAGTAGAGACAGAGGCT
S100A4	GCTGCCCAGATAAGGAACCC TGCGAAGAAGCCAGAGTAAGG
S100A7	TGAAGGGTCCATCAGTCA CTAGTAGAGGCTGTGCT
S100A8	TGTCCTCAGTTTGTGCAGAATATAAA TCACCATCGCAAGGAACTCC
S100A9	GTTGATCTTTGCCTGTCATGAG AGCCATTCCCTTTAGACTTGG
mBD1	CCAGATGGAGCCAGGTGTTG AGCTGGAGCGGAGACAGAATCC
mBD3	GCATTGGCAACACTCGTCAGA CGGGATCTTGGTCTTCTCTA
mBD4	GCAGCCTTTACCCAAATTATC ACAATTGCCAATCTGTCGAA

1.5.19 Histological analysis:

Paraffin-embedded skin samples were sectioned (3.5 μm) and stained for H&E. Cellular infiltrates in the dermis was measured using an ocular grid with area coverage of 0.25 mm^2 at 5 randomly selected sites per sample. Epidermal thickness and epidermal layers were

determined at 5 randomly selected locations per H&E sample under a microscope at 40x magnification. All the measurements were performed in a blinded fashion. Finally, the results were averaged per mouse and per treatment group for the statistical analysis. Images of stainings were acquired with a DP71 digital camera (Olympus, Vienna, Austria), attached to an Olympus BX51 microscope.

1.5.20 Immunohistochemistry:

FFPE tissue sections (3.5 µm) were deparaffinized and rehydrated for immunohistochemical staining. Slides with tissues sections were incubated for heat-induced antigen retrieval in Dako Target Retrieval Solution Citrate pH 6.0 (Dako S2369) or Dako Target Retrieval Solution pH 9,0 (Dako S2367) for 30 minutes in a steamer. The staining was then performed manually at 4°C antibody incubation using the Dako REAL™ Detection System, Peroxidase/AEC, using antibodies directed against: anti-CD3 (1:200; #ab16669, Abcam, Cambridge), anti-Ly6c (1:500, ab15627, Abcam, Cambridge) and anti-IL10 (1:400, ab189392). ImmPRESS™ HRP Anti-Rat IgG (Peroxidase) Polymer Detection Kit (MP-7444, Vector Laboratories, California, USA) was used as secondary antibody for anti-Ly6c and anti-IL10 antibodies. F4/80 (1:200, MA5-16630, Thermo Scientific) staining was performed using EXPOSE mouse- and rabbit-specific HRP detection IHC kit (ab80436, Abcam, Cambridge) according to manufacturer's instructions. Images of stainings were acquired with a DP71 digital camera (Olympus, Vienna, Austria), attached to an Olympus BX51 microscope.

1.5.21 Statistical analysis:

Mann-Whitney Test was used to determine statistical significance between groups in CHS experiments and histological analyses. For microarray analyses, 1way ANOVA with FDR < 5% was used for filtering genes. Differentially expressed genes were filtered when $p < 0.05$ and fold change ±2. Unpaired T-test was used to determine statistical significance for qPCR analysis. Statistical analysis was performed using GraphPad Prism version 7 (GraphPad). Statistical significance was set at p-value of <0.05.

1.6 Results:

1.6.1 Determination of minimal inflammatory dose (MID)

To determine the minimal inflammatory dose, the mice were shaved, and UV-B was given every 24hrs with a 40% increase of dosage. To measure the MID, dorsal skin thickness was measured 24hrs after every exposure, and skin swelling was determined. Dunn's multiple comparison test revealed significant swelling starting at 316 mJ/cm^2 (MID) up to 618 mJ/cm^2 (2x MID).

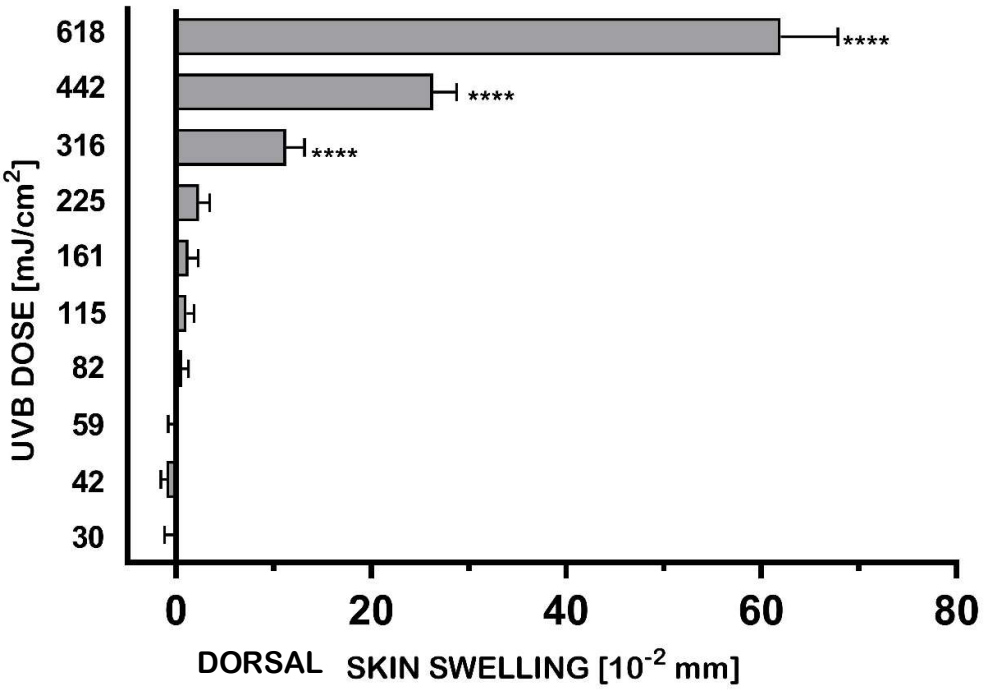

Figure 19: Minimal inflammatory dose (MID). *C57/BL6J SPF mice were irradiated on the shaved dorsal skin every 24hrs with 40% increase in daily UVB dose to determine MID (minimum dosage of UVB required to produce a skin swelling after 24h). Data shown represented mean ± SEM. N=5 per experimental group; p-value determined by Dunn's multiple comparisons test. * P< 0.05: ** P ≤ 0.01; *** P ≤ 0.001*

1.6.2 UV-B induced physiological changes in the skin: transepidermal water loss (TEWL), skin hydration and pH

Exposure to UVR leads to cutaneous damage which includes oxidation of biomolecules along with depletion of antioxidants. Stratum corneum, the main barrier against external hazards is particularly susceptible to UV-induced damage and barrier perturbation. This defect in barrier function could perhaps lead to microbial or microbe-associated antigen penetration into the skin and subsequent immune response. TEWL was used (amount of water that evaporates passively through the skin), which is widely used to characterize the skin barrier function and skin hydration (moisture content) and pH after different doses of UV-B and different time points. Significantly increased TEWL and skin hydration was observed only in mice exposed to high dose at immediately after UV exposure (T1) ($p=0.0001$) compared to unexposed mice. The levels of TEWL and skin hydration normalized 24hrs after (T2) UV exposure. No change in skin pH was observed at any dose and time point.

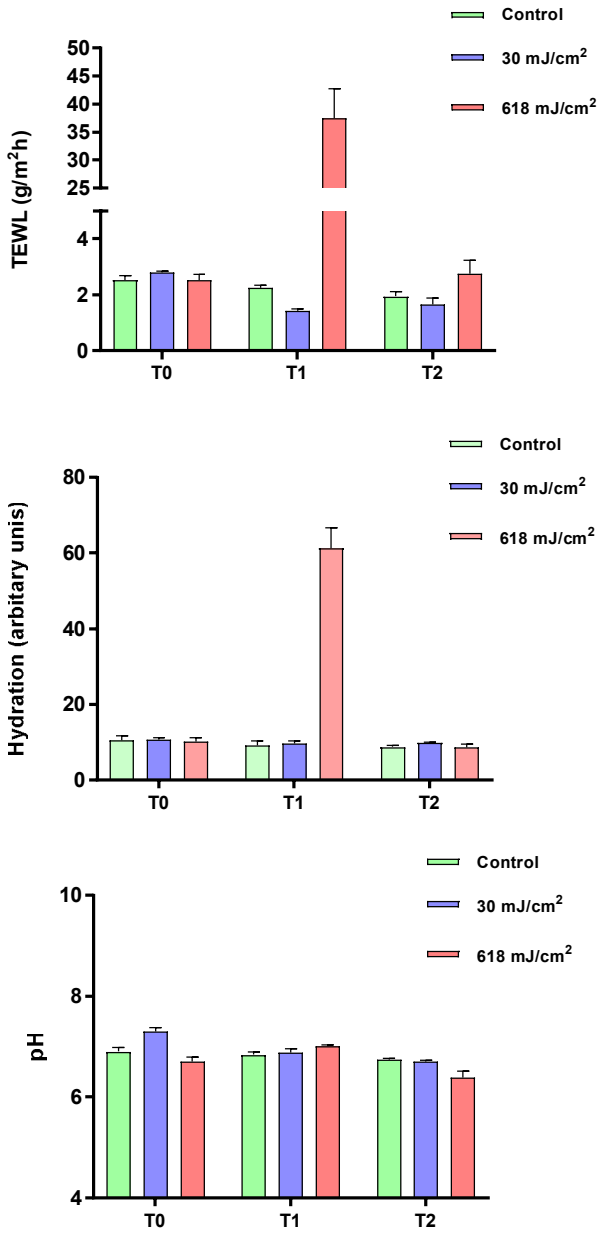

Figure 20: UV-B induced changes in TEWL and hydration. *C57/BL6J SPF mice were irradiated on the shaved dorsal skin with 30 mJ/cm² (low dose) and 618 mJ/cm² (high dose) and one group were left unirradiated (control). TEWL, skin hydration and pH were measured using appropriate probes with Cutometer® dual MPA 580 at different time points. A significant increase was seen in TEWL (p=0.0001) and hydration (p=0.0001) for high dose at T0 compared to control group. No changes were seen in pH at different doses and time points. N=5 mice per group. Data shown represents mean± SEM. 2way ANOVA was used to measure statistical significance between groups.*

1.6.3 UV-B converts *trans*- to *cis*-urocanic acid immediately after irradiation

One of the early events in the skin after UV irradiation is isomerization of inactive *trans*- to active *cis*-UCA[16]. *cis*-UCA is long known to be immune suppressive[16]. To determine the levels of formation of *cis*-UCA after different doses of UV-B, tape strips were collected and quantified for *trans*- and *cis*-UCA by mass spectrometry. The ratio of *cis*-UCA/*trans*-UCA was observed to be significantly higher immediately (T1) after UV-B exposure. Both low dose (p=0.0323) and high dose (0.0001) showed increased amounts of *cis*-UCA compared to control. At T2 (24hrs after UV-R) cis-UCA was only detected in the mice that received a high dose (p=0.0306, compared to control group), whereas low dose and control group showed no significant amounts of cis-UCA.

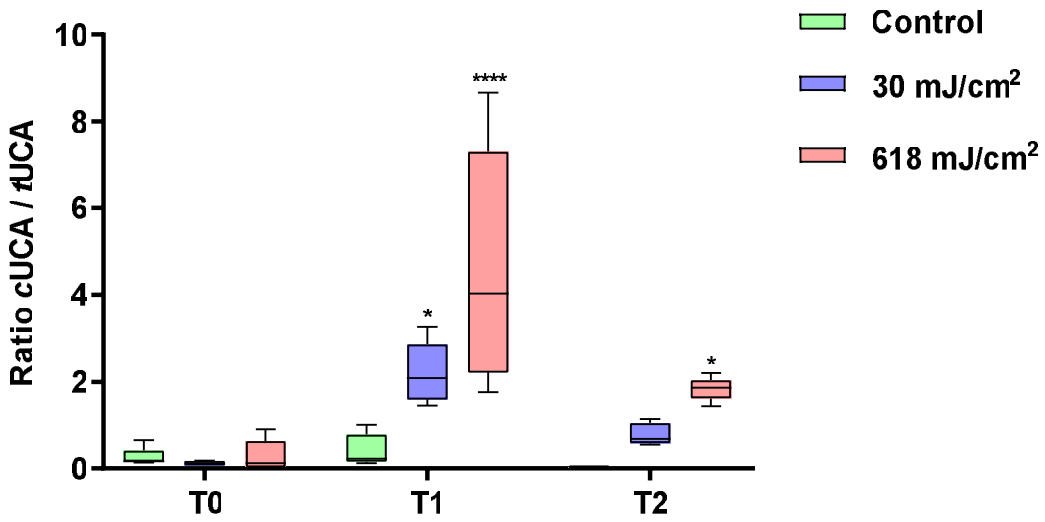

Figure 21: UV-B isomerizes trans- to cis-UCA. *C57/BL6J SPF mice were irradiated on the shaved dorsal skin with 30 mJ/cm^2 (low dose) and 618 mJ/cm^2 (high dose) and one group was left unirradiated (control). 2 tape strips were collected from each mouse and the amount of UCA was quantified using Liquid chromatography (LC)/MS (see methods). Both low dose and high dose significantly isomerized trans-to cis-UCA compared to control group at T1. However, at T2 cis-UCA was only detected in mice that received a high dose. N=5 mice per group. Data shown represents mean± SEM. 2way ANOVA was used to measure statistical significance between groups. * P=0.0323: **** P =0.0001*

1.6.4 Alpha diversity analysis

Alpha diversity is a measure of a number of taxa or species richness. Rarefactions were performed to a depth of 11750 reads. At the maximum subsampling depth of 11750 reads, the mean number (including all time points) of observed species was 290 for the control group, 196 for the low dose UV group and 249 for the high dose UV group. Rarefaction curves for richness in all the samples with plateau at the maximum depth is shown, indicating an adequate sampling procedure.

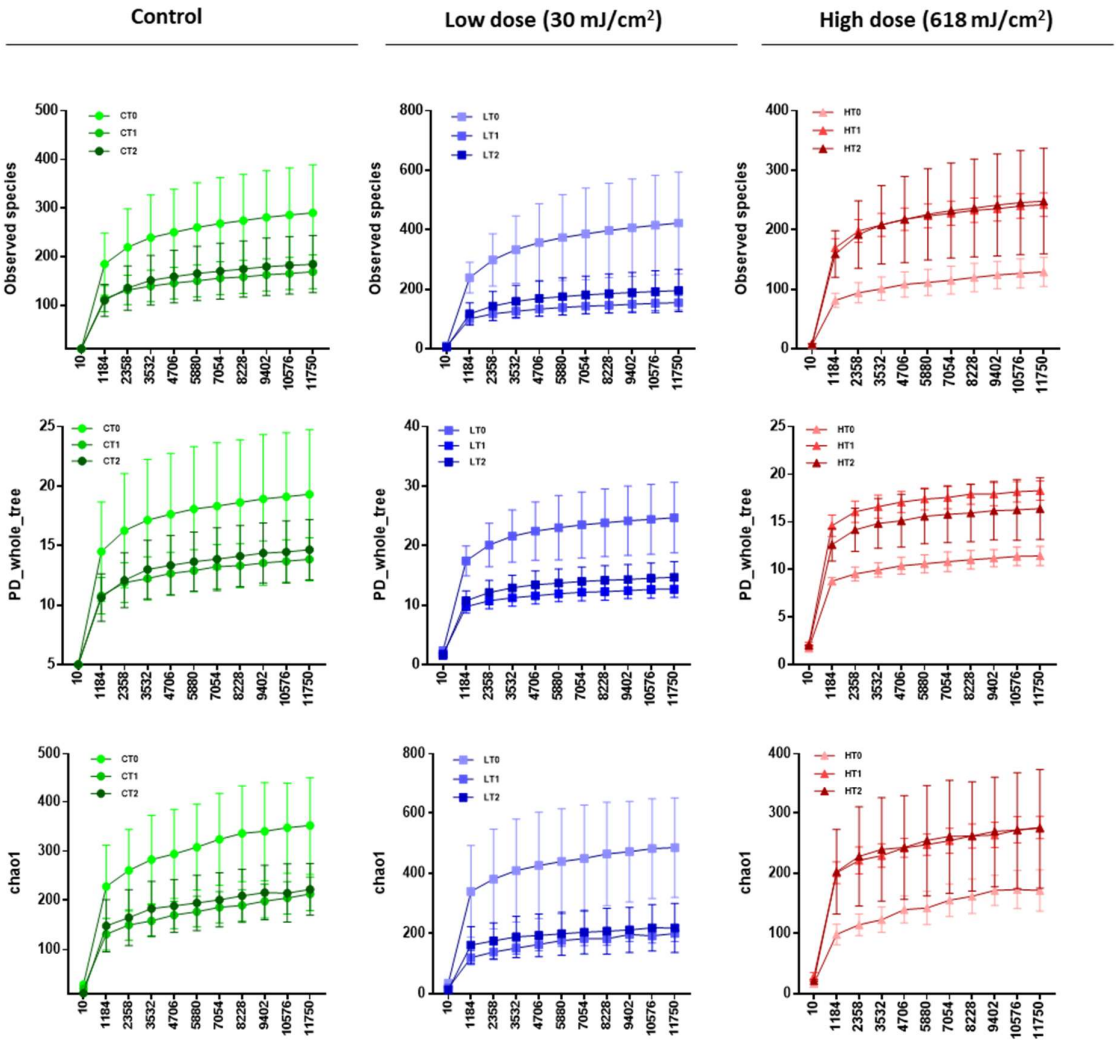

Figure 22: Rarefraction plots. *Rarefaction plots of all time points and treatment groups (one curve per experimental group (n=5)) showing curves reaching an asymptote at the cut-off of 11750 reads. Rarefaction curves (number of observed species, whole tree, and chao1 on Y-axis) for various time points (TP0, TP1, TP2).*

1.6.5 UV-B modulates microbial diversity across various time points after irradiation, as measured by beta diversity analysis

Beta diversity measures the diversity between samples, which is a way to quantify how similar or dissimilar are the samples and is represented by a distance matrix which is further used to do *Principal Coordinate Analysis (PCoA)*. This results in an ordination plot with multiple dimensions, where a particular sample is represented as a point and the distance between the points show the similarity of those samples (points closer correspond more similarity). UV-B exposure to the mice revealed both low dose and high dose significantly affected the diversity between various time points as seen below. A clear clustering was observed in low dose- and high dose-treated mice at TP1 and TP2. Whereas the control group remained heterogeneous in nature and showed no clear clustering of the orbs.

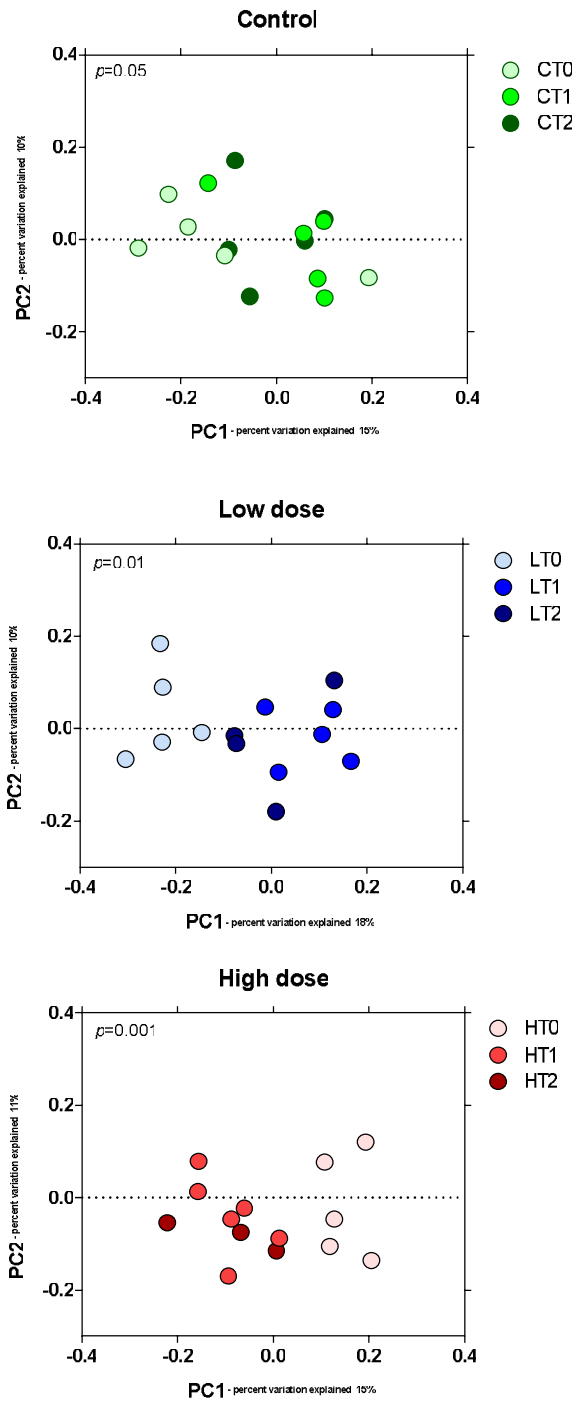

Figure 23: Beta diversity for various doses of UV-B across different time points. *A: 2D PCoA of the microbial communities in the control group (unirradiated) showed no clustering. B. Low dose group showed clear clustering before (LT0) and after irradiation (TP1 & TP2) p=0.01. C. High dose group also showed different clustering of microbial communities before and after irradiation with p=0.001.*

1.6.6 Microbial modulation at various time points before and after UV exposure

Comparative analysis was performed using linear discriminant analysis (LDA) effect size (LefSe). Data showed changes within microbiome even for unexposed mice, which could perhaps be an artifact from swab or a cage effect. However, there was a significantly increased abundance before (T0) and after UVB exposure (T2) both at a low dose and high dose suggesting that UVB exposure indeed modulates microbial communities.

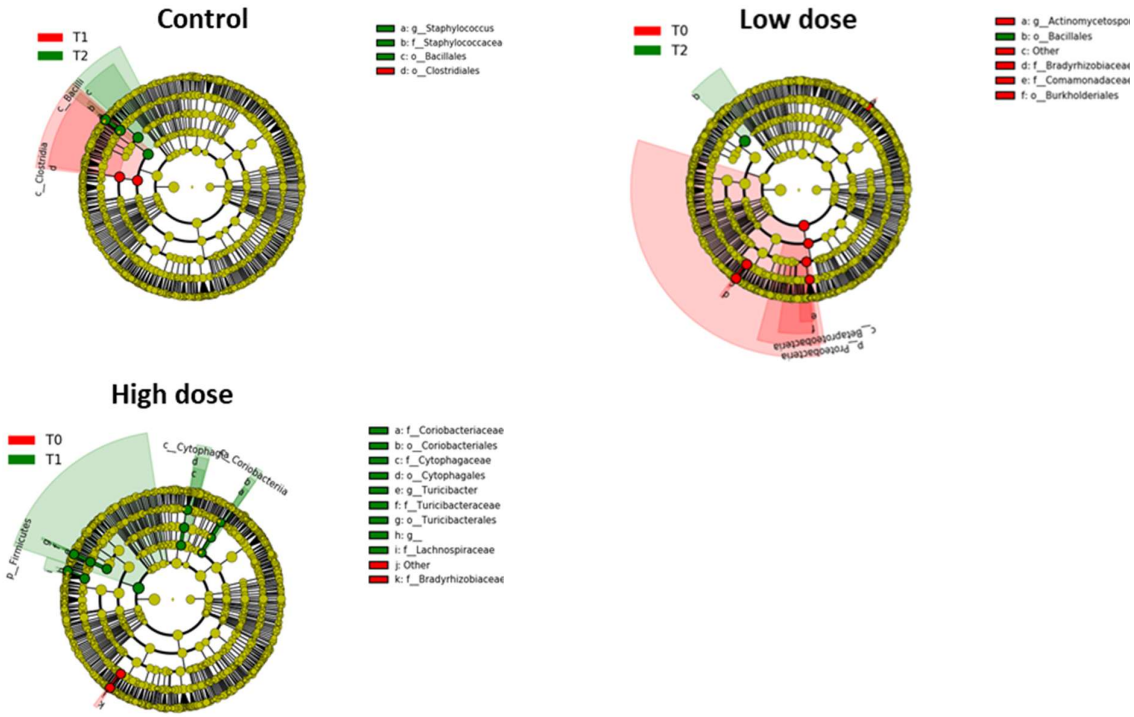

Figure 24: LefSe results showing effect of UVB on microbial communities. *Taxonomic representation of statistically and biologically consistent microbial communities are plotted. Alpha value was set at 0.01 and LDA cut-off was performed at 5.*

1.6.7 Modulation in abundance of top 5 phyla after UVB exposure

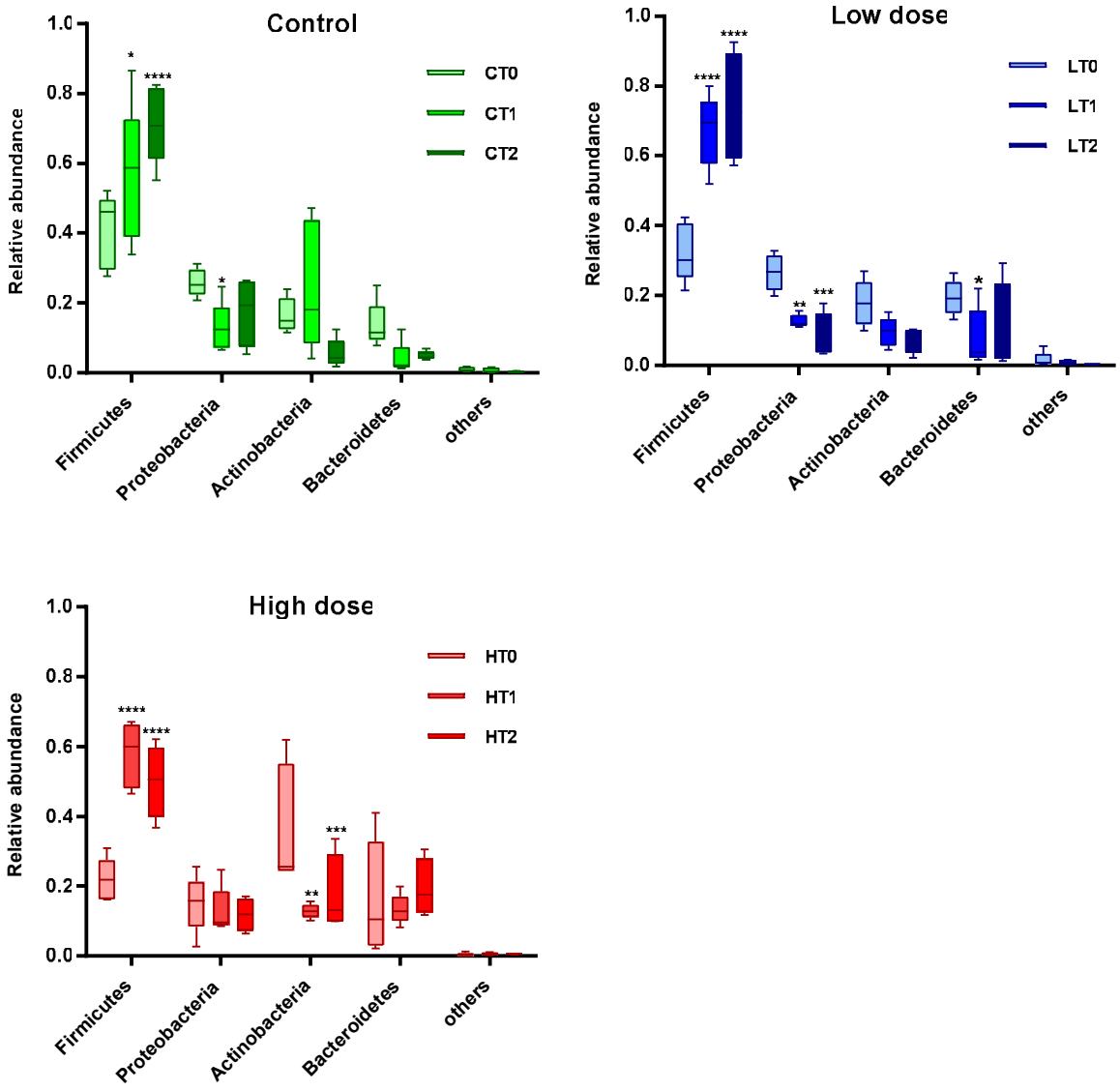

Figure 25: Boxplots showing relative abundance of top 5 phyla. *Relative abundance of top5 significant phyla after various doses and time points are plotted. N=5 per groups. Data are represented as mean ± SEM. 2Way ANOVA was used to calculate the statistical significance. * P= 0.0167, ** P= 0.0068, *** P= 0.0006, ****P= 0.0001*

1.6.8 UV-B dose-dependently modulates cellular response within the skin

UV-B exposure leads to increased epidermal response as measured by epidermal thickness, epidermal layers, sunburn cells. These results suggest, this phenomenon to be dose-dependent. High dose (618 mJ/cm^2) exposure leads to a significant increase in epidermal thickness, layers, cellular infiltrate which includes neutrophils and mast cells. An increased neutrophil-driven microabscesses (data not shown) was observed in high dose-treated mice, and not in control or low dose groups. Collectively these results showed that UV-B significantly affects the epidermal response to UV depending upon the dose, and subsequently leads to immune modulation and microbial alterations.

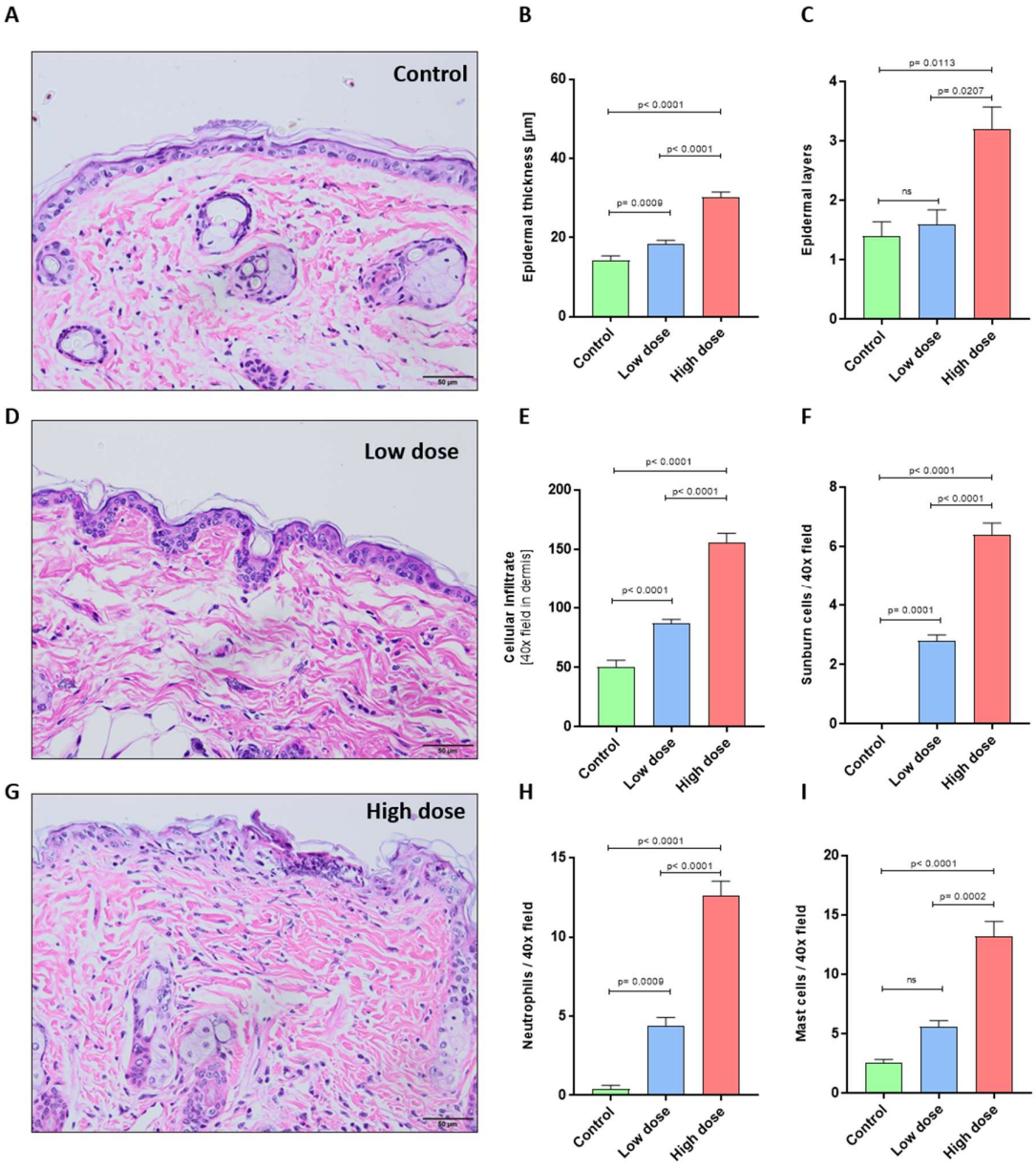

Figure 26: Effect of UV-B on epidermis and cellular infiltrate. *Exposure to different doses of UV-R led to increased epidermal thickness, layers, cellular infiltrate in the skin (A, D and G). High dose UV-R was significantly stronger in eliciting an epidermal response in the skin compared to low dose or unirradiated skin (B-I). N=5 mice per treatment groups. Data represented as mean ± SEM. P-values were calculated using the 2Way ANOVA statistical test.*

1.6.9 UV-B exposure causes systemic effects in monocyte and granulocyte populations in the blood

Complete blood count is widely used laboratory practice to examine the systemic effects of various treatments. The blood count of the mice was monitored after irradiation (24hr after UV exposure). Though there were no significant differences in the total count of leucocytes and percentages of lymphocytes in the blood, monocytes and neutrophils/granulocytes showed the major difference after the low dose and high dose irradiation. Collectively this data suggests that UV-B influences immune cells in the blood, potentially contributing to causing a systemic effect.

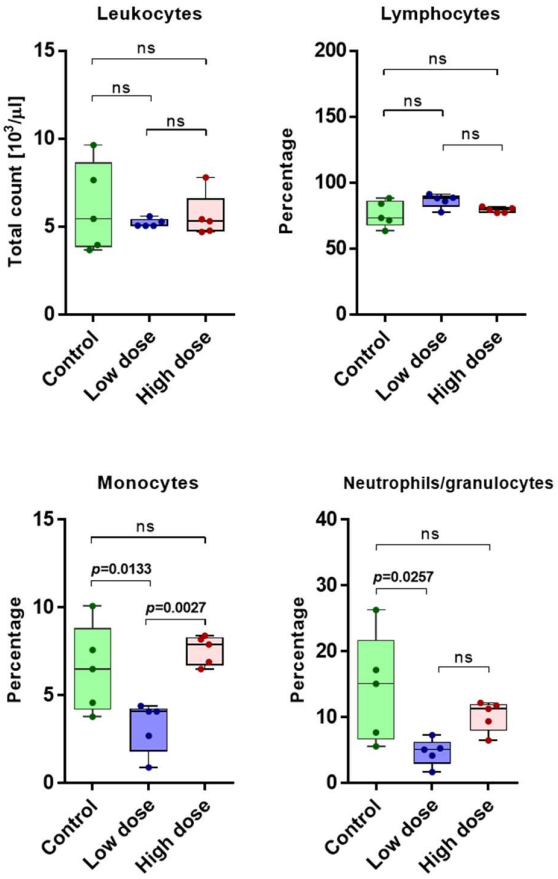

Figure 27: Systemic effect of UV-B on total and differential leukocyte count. *Total leukocytes were counted per $10^3/\mu L$ from N=5 mice per experimental groups and the percentage of monocytes and neutrophils were calculated and plotted. 2Way ANOVA was used to determine statistical significance.*

1.6.10 UV-B exposure affects various immune cell populations

UV exposure is known to modulate the immune responses by acting on various cells and molecules. Groups of mice were irradiated with various doses of UVB and harvested skin and lymph nodes 24hrs later. Cells were extracted as described in methods and stained for various immune cell markers and analyzed using flow cytometry. Interestingly the data showed a reduction of antigen presenting cells (DCs) in the skin, which goes in line with previous reports [42,74] and increased infiltration of inflammatory monocytes and neutrophils into the skin at a high dose of UVB.

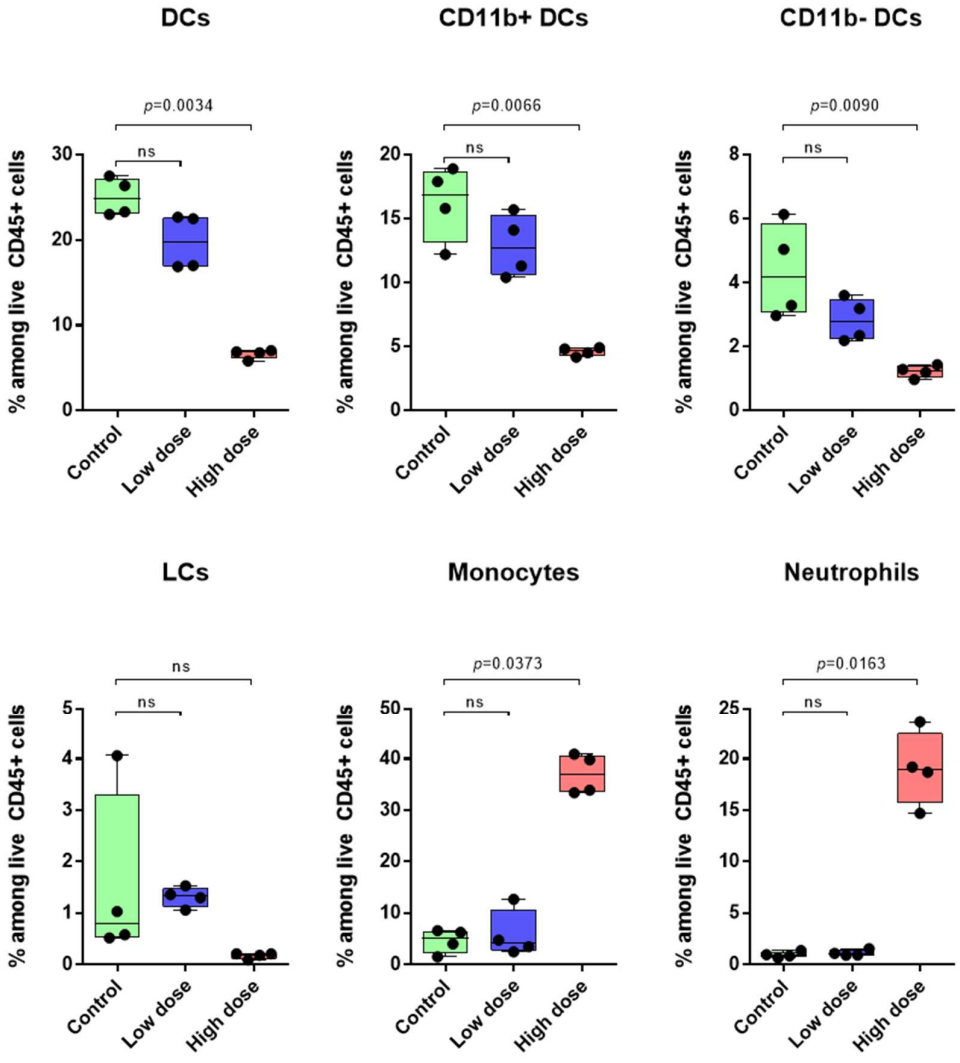

Figure 28: Effect of UVB on a various immune cell population in the skin. *24hrs after UVB exposure skin was harvested and stained for the various immune cell population. N=5*

per group. Data represented as mean ± SEM. 1way ANOVA was performed to determine statistical significance.

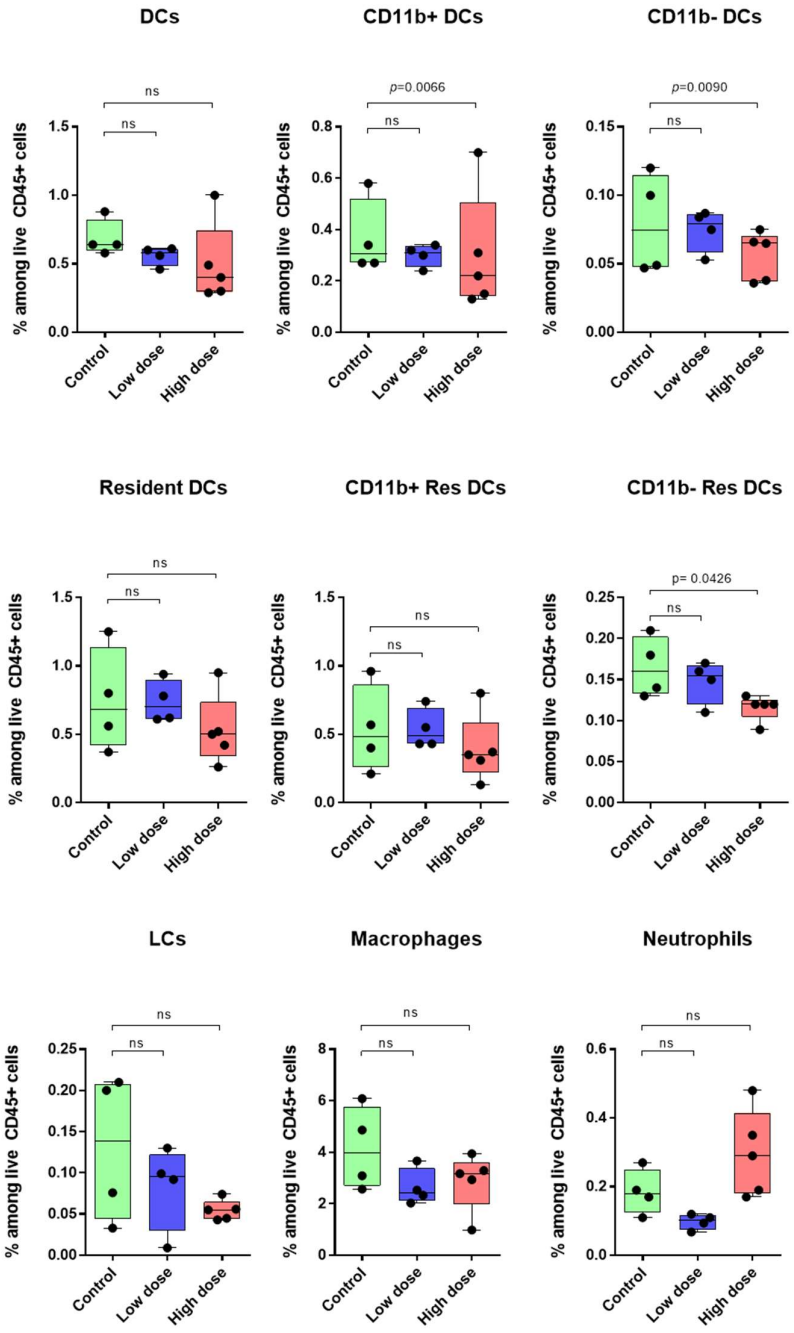

Figure 29: Effect of UVB on a various immune cell population in the LN. *24hrs after UVB exposure draining LNs were harvested and stained for the various immune cell population. N=5 per group. Data represented as mean ± SEM. 1way ANOVA was performed to determine statistical significance.*

1.6.11 UV-B modulates gene expression of antimicrobial peptides S100A7 and S100A8

AMPs are the key innate immune molecules to defend against microbes and maintain a healthy homeostasis in the skin. UV-R is known to upregulate certain AMPs in the skin such as beta-defensin -2, -3 ,4, RNase7 and psoriasin (S100A7) [31] in human keratinocytes and subjects. Gene expression of murine beta-defensin 1, -3 and -4, S100A7, S100A8 and S100A9 was investigated. No significant changes in murine beta-defensins after UV exposure were observed. However, increased expression of S100A7 (p=0.046), and decreases S100A8 (p= 0.0077) after high dose was seen. Low dose showed no significant expression in any of the AMPs.

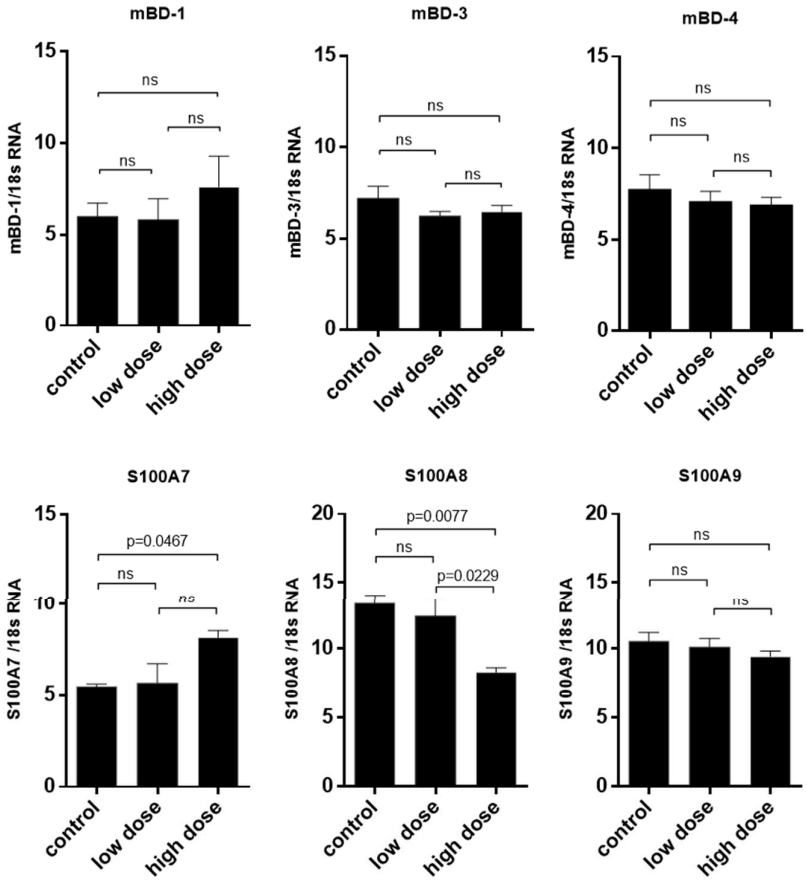

Figure 30: AMPs expression at different doses. *Quantitative real-time PCR was performed for various AMPs. 18s RNA was used as a housekeeping gene. A significant difference was seen for S100A7 and S100A8. 2way ANOVA was performed for statistical analysis. (n=5 mice per group).*

1.6.12 Skin microbiome limits UV-induced suppression of systemic adaptive immune response, by orchestrating local cellular and innate immune response to UV

GF mice and disinfected-SPF mice were used to study the effect of skin microbiome on cellular and immune response to UV-B. The data indicate that the presence of skin microbiome reduces UV-induced suppression of CHS (Figure 31). GF mice exposed to UV-B prior to sensitization with DNFB showed significantly reduced CHS response (measured by macroscopic ear swelling) compared to SPF mice (71% vs 40%; p=0.0317) (Figure 31B). Furthermore, to replicate these observations, cutaneous disinfection the skin (at the site of irradiation) was done. This was consistent with the results in disinfected-SPF mice which also showed an increased CHS suppression after UV-B compared to non-disinfected control mice (Figure 31C). To understand the early molecular events after UV-exposure, tissue samples were taken from the UV-irradiated dorsal skin site 24hrs after exposure. Histological analysis of the dorsal skin sections (Figure 32B-E) revealed that UV-irradiated skin of GF and SPF mice showed an increase in epidermal thickness compared to the unexposed skin (Figure 32F). No significant difference was seen in unexposed GF and SPF mice, which also go well in line with a recently published report [117]. However, UV-B induced epidermal thickness (Figure 32F), epidermal layers (Figure 32H) and cellular infiltrate (Figure 32G) was significantly greater in SPF mice compared to GF mice. This difference in epidermal response to UV could be due to the fact that UV-induced cellular response happens in a sterile environment in GF mice, resulting in host-derived damage-associated molecular patterns. Whereas, in SPF mice, host-derived along with microbial-associated molecular patterns could amplify the epidermal response to UV-exposure [118]. This is consistent with our observations that UV exposure boosted neutrophilic infiltration in SPF mice to a greater degree than it did in GF mice, as evidenced by increased numbers of microabscesses (built up mainly by neutrophils) in the epidermis (Fig. 34B) and densely scattered neutrophils in the dermis (Fig. 34C). No significant differences in neutrophil numbers were observed in the unexposed skin of GF versus SPF skin. In parallel, UV-exposed GF skin showed increased numbers of $Ly6c^{+}$ cells (i.e., activated macrophages in inflammatory tissues) and $F4/80^{+}$ cells (i.e., matured tissue macrophages) in the dermis, compared to SPF skin (Fig. 34F & G). Moreover, the anti-inflammatory cytokine IL10 was expressed at significantly higher levels in UV-exposed GF skin than in SPF skin (mostly in the cellular infiltrate in the dermis), despite a higher baseline expression of this cytokine in SPF mice. Indeed, it has been recently reported that the microbiome can trigger the expression of IL10 in SPF mice [117] (Fig. 34H).

No significant difference was observed in the numbers of sunburn cells, mast cells, and $CD3^{+}$ cells (most likely dendritic epidermal T cells) in UV-exposed and unexposed GF skin compared to SPF skin (Fig. 33-34 A, D, E).

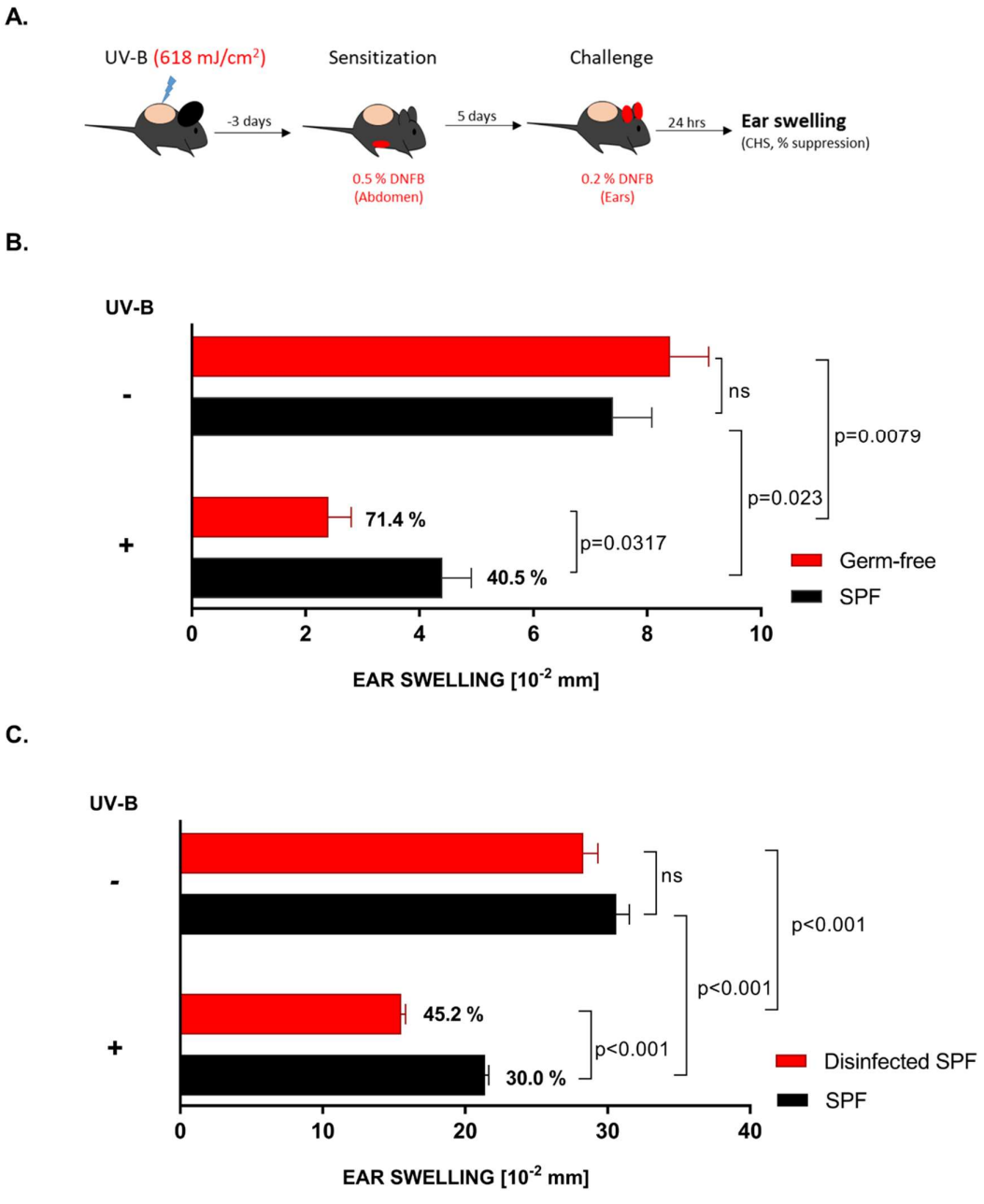

Figure 31: Skin microbiome protects from UV-B induced suppression of induction of CHS. *(A) GF, disinfected SPF or control SPF mice were subjected to CHS model as described in detail in materials and methods. (B & C) The ear swelling differences between UV-B-irradiated and non-irradiated mice, with relatively more immune suppression in GF compared to SPF (71.4% vs 40.5%) and in disinfected SPF mice compared to non-disinfected mice (45.2% vs 30.0%) indicate the immune protection by microbiome. Data shown represent mean ± SEM. N=5-10 per experimental group, p-value determined by Mann-Whitney Test.*

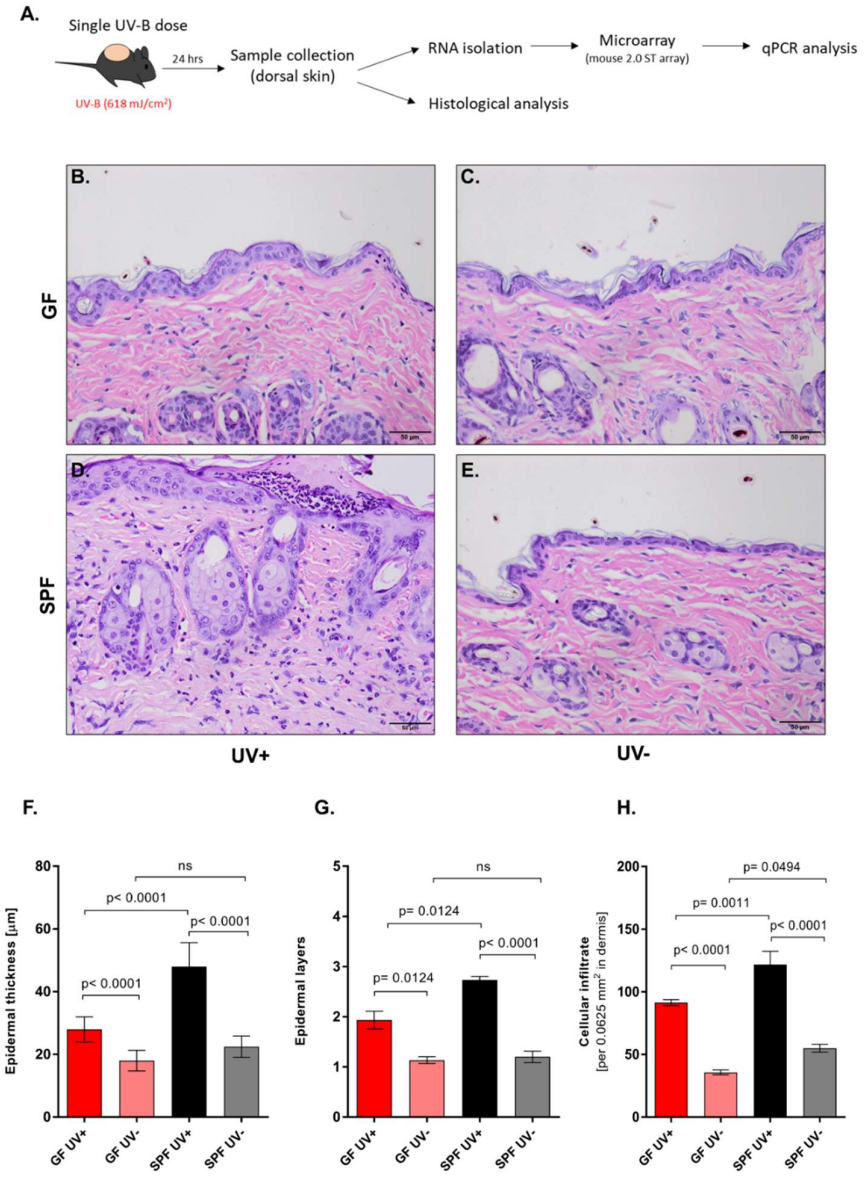

Figure 32: Microbiome contributes to increased cellular response to UV-B *(A) A single dose of UV-B (618 mJ/cm²) was given to the shaved dorsal skin of GF and SPF mice 24hrs before tissue collection. (B-E) Representative hemotoxylin and eosin stainings of formalin-fixed paraffin-embedded skin sections are shown and indicate a UV-induced increase in (F) epidermal thickness, (G) epidermal layers and (H) cellular infiltrate comparing GF and SPF skin. Data shown represent mean ± SEM. N=3 per experimental group; p-value determined by 2-way ANOVA.*

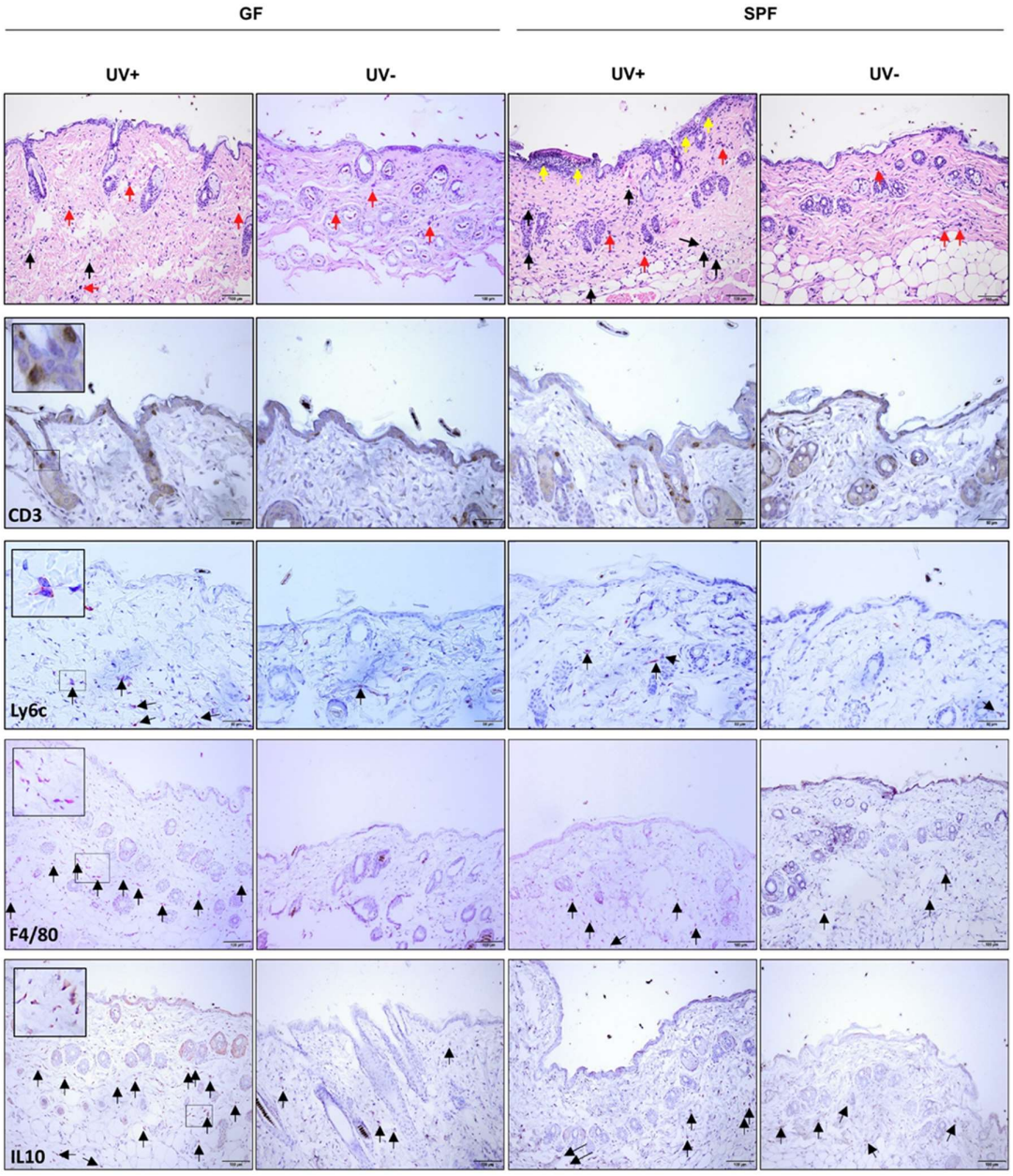

Figure 33: Immunohistochemical stainings panels.

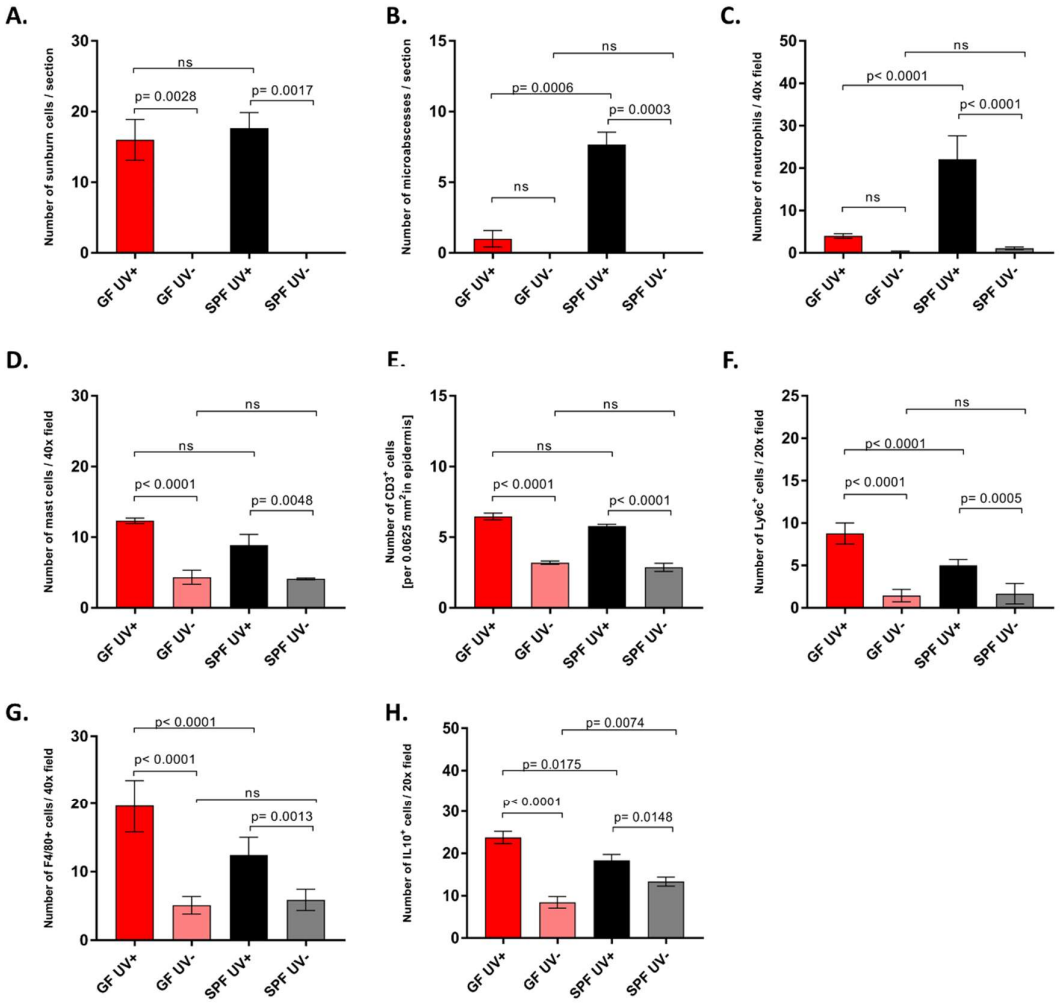

Figure 34: UV exposure boosters the infiltration of skin by neutrophils in SPF mice but macrophages and IL10+ cells in GF mice. *Quantitative analysis showed increased numbers of (B) epidermal microabscesses and (C) increased neutrophil infiltration in UV-exposed SPF compared to GF skin. In contrast, UV-exposed GF skin showed higher numbers of (F) Ly6c, (G) F4/80 and (H) IL10+ cells. Beside a slight increase of IL10+ cells in the skin of SPF mice, no differences were seen in baseline levels of (A) sunburn cells, (D) mast cells and (E) $CD3^+$ cells between SPF and GF skin. Data shown represent mean ± SEM; N=3 per experimental group; p-value determined by 2-way ANOVA.*

1.6.13 UV-B modulates the cutaneous gene expression in GF and SPF skin

To analyze the impact of UV-B in the presence or absence of microbiome on the gene expression microarray of the UV-exposed and unexposed skin of GF and SPF mice was performed. Biological replicates of UV-exposed GF and SPF skin cluster together as demonstrated by principal component analysis (Figure 35A) compared to the unexposed groups. To analyze the upregulated and downregulated gene, the distribution was set to FDR 5%, $p< 0.05$ and fold change of ±2. Total of 1075 genes was upregulated, and 794 genes were downregulated in response to UV-B treatment in GF mice. In comparison, 539 genes were upregulated, and 325 genes were downregulated in SPF mice (Figure 35B). With this regard, a recent study has revealed differential gene expression (2820 genes) using RNA sequencing in GF and SPF skin [117], indicating that microbiome can regulate gene expression within the skin. A similar number of differentially expressed genes (2414 genes) in the unexposed skin GF compared to SPF skin was observed in this dataset. GO terms of the filtered genes were obtained using gene ontology enrichment analysis and visualization tool (GOrilla) [121] and the resulting GO terms and p-values were used as input for REVIGO [122] for visualizing the scatterplots for biological processes (Figure 3C) in GF and SPF mice. The Biological process GO terms enriched in the gene set contained terms related to “defense response” (GO: 0006952), “immune system process” (GO: 0002376), “response to external stimulus” (GO: 0009650), “leukocyte migration” (GO: 0050900), “chemokine-mediated signaling pathway” (GO: 0070098).

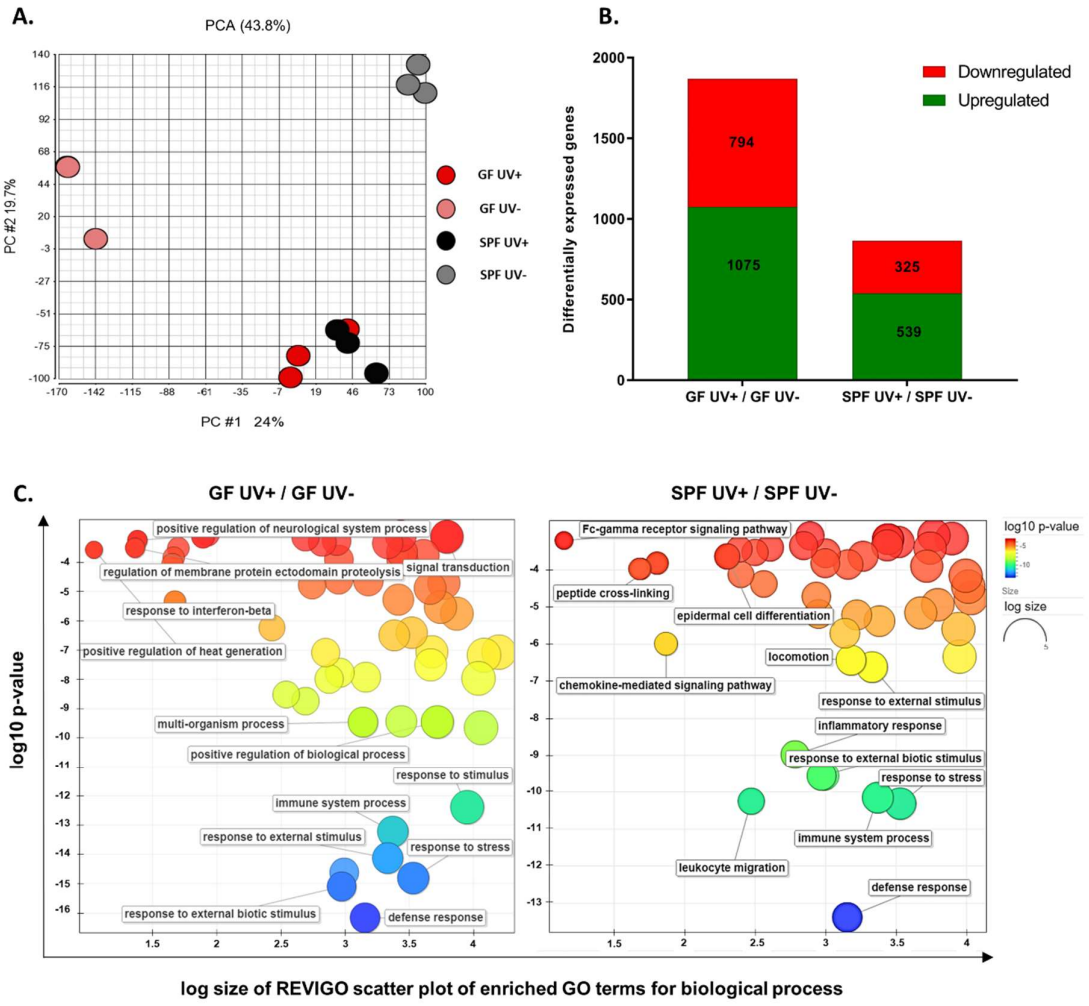

Figure 35: UV-B modulates gene expression in GF and SPF skin. *(A) The 2-dimensional principal component analysis was done using Partek. Each point corresponds to a specific sample hybridized on one microarray containing 53617 probesets. Points that are closer together (GF UV+ and SPF UV+) represent similar genome than that of points that are far apart (GF UV- and SPF UV-). (B) The number of UV-B induced differentially expressed, upregulated or downregulated genes with p< 0.05 and FC ±2 are plotted for GF and SPF skin. (C) GO enrichment analysis summarized and plotted using REVIGO scatter plots for biological processes UV-induced differentially expressed genes in GF and SPF skin. The scatterplot shows the clusters in two-dimensional space by applying multidimensional scaling for the input GO terms. Log10 p-values of GO terms are shown in the y-axis (indicated as colors) and log size (frequency of the GO term in the database, bubbles of more general terms are larger) on the x-axis.*

1.6.14 Canonical pathway analysis of UV-B exposed GF and SPF skin using ingenuity pathway analysis

To understand the functions of regulated genes and their roles in biological processes a reliable bioinformatics approach, Ingenuity Pathway Analysis (IPA) (Ingenuity, CA) was used. The results of the canonical pathway analysis by IPA are shown in Table 4 & 5. The top 5 activated pathways activated by UV-B exposure in GF mice belong to TREM1 signaling, the role of NFAT in the regulation of the immune response, P13K signaling in B lymphocytes, dendritic cell maturation, leukocyte extravasation signaling, and inhibited pathways are PCP pathway, basal cell carcinoma signaling, PPAR signaling and LXR/RXR. The top 5 UV-B activated pathways in SPF mice belonged to acute phase response signaling, TREM1 signaling, LPS/IL-1 mediated inhibition of RXR function, toll-like receptor signaling, cholecystokinin/gastrin-mediated signaling and inhibited pathways are LXR/RXR activation, PPAR signaling role of NFAT in regulation of the immune response, IL-17A signaling in airway cells, 14-3-3-mediated signaling. We also analyzed disease and functions by IPA for both GF and SPF mice exposed to UV-B. Taken together these results highlight some profound and substantial differences in activation of various biological pathways and how the skin initially responds to UV-B exposure in the presence or absence of microbiome on the skin.

Ingenuity Canonical Pathways	Total genes	p-value	z-score
TREM1 Signaling	18/69	3.16E-06	**4.24**
Role of NFAT in Regulation of the Immune Response	22/170	1.15E-02	**3.58**
PI3K Signaling in B Lymphocytes	16/124	2.88E-02	**3.50**
Dendritic Cell Maturation	27/159	7.94E-05	**3.40**
Leukocyte Extravasation Signaling	23/202	3.80E-02	**3.27**
IL-6 Signaling	24/124	2.24E-05	**3.13**
FcÎ³ Receptor-mediated Phagocytosis in Macrophages and Monocytes	13/90	2.00E-02	**3.05**
NF-Î°B Signaling	25/168	1.10E-03	**3.00**
CD28 Signaling in T Helper Cells	18/118	3.98E-03	**3.00**
Toll-like Receptor Signaling	13/70	2.40E-03	**2.71**
iCOS-iCOSL Signaling in T Helper Cells	18/110	1.82E-03	**2.67**
PKCÎ¸ Signaling in T Lymphocytes	17/120	1.05E-02	**2.67**
Retinoic acid Mediated Apoptosis Signaling	8/43	1.55E-02	**2.65**
Acute Phase Response Signaling	25/157	3.98E-04	**2.56**
Actin Cytoskeleton Signaling	24/217	4.68E-02	**2.50**
Role of Pattern Recognition Receptors in Recognition of Bacteria and Viruses	20/127	1.66E-03	**2.50**
UVA-Induced MAPK Signaling	14/99	1.95E-02	**2.50**
Interferon Signaling	6/30	2.45E-02	**2.45**
Oncostatin M Signaling	6/33	3.80E-02	**2.45**
NF-Î°B Activation by Viruses	13/86	1.41E-02	**2.31**
Death Receptor Signaling	17/88	3.47E-04	**2.18**
Role of IL-17F in Allergic Inflammatory Airway Diseases	9/37	1.62E-03	**2.12**
PCP pathway	8/62	0.04677	**-2.12**
Basal Cell Carcinoma Signaling	12/69	0.00603	**-2.65**
PPAR Signaling	18/89	0.00013	**-3.30**
LXR/RXR Activation	19/108	0.00055	**-3.64**

Table 4: UV-B induced canonical pathways in GF mice.

Ingenuity Canonical Pathways	Total genes	p-value	z-score
Acute Phase Response Signaling	21/157	1.6218E-07	**3.15**
TREM1 Signaling	12/69	4.7863E-06	**2.89**
LPS/IL-1 Mediated Inhibition of RXR Function	21/197	6.9183E-06	**2.33**
Toll-like Receptor Signaling	12/70	5.6234E-06	**2.12**
Cholecystokinin/Gastrin-mediated Signaling	8/97	0.02137962	**2.12**
Inflammasome pathway	4/19	0.00389045	**2.00**
Oncostatin M Signaling	4/33	0.02818383	**2.00**
MIF Regulation of Innate Immunity	4/38	0.04466836	**2.00**
LXR/RXR Activation	19/108	6.9183E-09	**-2.67**
PPAR Signaling	10/89	0.0011749	**-3.16**

Table 5: UV-B induced canonical pathways in SPF mice.

1.6.15 Differential expression of interleukins, chemokines, AMPs and other innate immune response genes in GF and SPF skin after UV-B irradiation.

Gene intensities values of interleukins with $p< 0.05$, FC±2 were used to plot the expression heatmap of each mice using the online heat mapper tool (http://www.heatmapper.ca/) [123]. Genes are clustered by average linkage and distance measurement was done using the Euclidean method. Fold change values are plotted for GF UV+ / GF UV- and SPF UV+ /SPF UV- groups. Most notable changes in gene expression are for IL20rb, IL22ra1, IL34, IL20ra, IL12rb2, IL1f10, IL22ra2 which are differentially expressed without any UV-treatment (Figure 36A). However, after a single UV-B dose, significant flipping of the expression of these genes in both GF and SPF skin (Figure 36B) was seen. Genes for IL1b, IL6, IL24 were highly expressed in SPF compared to GF after UV-B treatment. On the other side, IL20ra, IL12rb2, IL22ra1, IL22ra2, IL34, and IL20rb are downregulated by UV-B by a greater degree in SPF skin compared to GF skin. However, the gene expression of IL20rb, IL34, IL1f9, IL2rg, IL15ra, Il16, IL13ra1, IL31ra, IL1f6, IL2rb, IL7r, IL10ra, and IL1f8 was increased in GF skin compared to SPF skin (Figure 36B). Furthermore, the genes for most chemokines were upregulated after UV-B exposure in both GF and SPF skin. However, a complete flipping of Ccr4 for both GF and SPF skin (Figure 36C) was observed. The expression of almost all the genes for chemokines was higher in SPF skin with few exceptions such as Cxcl16 And Ccl6, Ccr2, Ccr5, Ccl9 which were expressed similarly in both GF and SPF skin. The expression of other genes such as Ccl7, Cxcl1, Cxcr2, Ccl2, Ccl3, Cxcl5, Cxcl2, Ccr1, Ccl12 is significantly higher in SPF skin compared to GF after UV-B treatment (Figure 36D). Innate immune genes such as AMPs, TLRs, and serotonin-related genes were differentially regulated by UV-B in GF and SPF skin (Table 6). A total of 11 genes for AMPs (S100 family, DEFB and RNase) were differentially expressed in GF and SPF skin after UV-B exposure. Additionally, TLR13 and TLR1 were significantly

upregulated in SPF skin compared to GF skin. Furthermore, serotonin signaling receptor gene HTR2A and SLC6A4 was upregulated in GF skin compared to SPF skin.

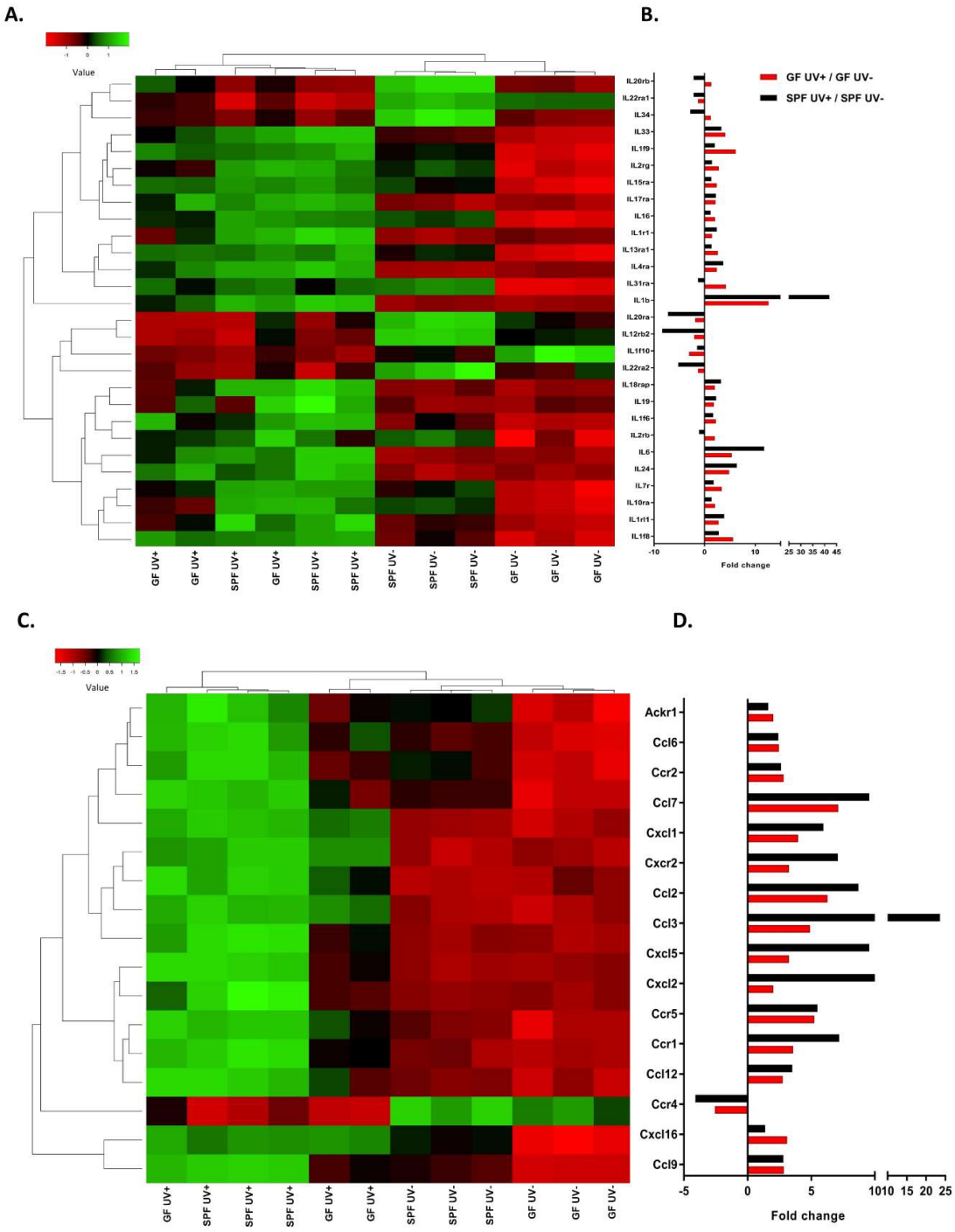

Figure 36: UV induces differential expression of interleukins and chemokines in GF compared to SPF skin. *(A) (C) RMA intensities from microarray were used to construct heatmap, using heat mapper (http://www.heatmapper.ca/). The genes are clustered by average linkage and distance measurement was done using the Euclidean method. Gene expression fold change for various (B) interleukins and (D) chemokines due to UV-B treatment in GF and SPF skin is shown in the bar graph.*

Gene	GF UV+ / GF UV-		SPF UV+ / SPF UV-	
	p-value	Fold change	p-value	Fold change
Antimicrobial Peptides				
S100A7A	3.199E-06	**-13.00**	0.0192862	**1.93**
S100A3	1.288E-06	**-31.34**	0.0426101	**1.91**
S100A4	1.202E-07	**4.12**	0.0019311	**1.44**
S100A8	0.303135	**1.39**	8.363E-05	**9.01**
S100A9	0.0046878	**2.65**	0.0001055	**5.90**
DEFB8	0.459292	**-1.40**	0.0011003	**-8.45**
DEFB3	0.0713878	**1.31**	0.0005708	**2.05**
DEFB14	2.649E-05	**4.81**	7.909E-06	**6.36**
DEFB6	0.0007831	**2.14**	0.464353	**-1.12**
DEFB14	2.649E-05	**4.81**	7.909E-06	**6.36**
RNASEL	0.0002004	**2.20**	0.0862219	**1.27**
RNASET2B	1.404E-07	**-2.42**	0.535204	**-1.03**
RNASET2A	1.103E-07	**-2.42**	0.419315	**-1.04**
RNASE1	0.0003325	**-2.55**	0.0010736	**-2.19**
Toll-like receptors				
TLR13	0.0282753	**2.77**	0.0018269	**5.72**
TLR1	0.0646121	**1.70**	0.0123469	**2.22**
Serotonin signalling genes				
HTR2A	0.0006754	**2.05**	0.0725447	**1.32**
SLC6A4	0.0028866	**1.29**	2.125E-06	**-2.05**

Table 6: UVB induced gene expression of AMPs, TLRs and serotonin signaling genes.

1.6.16 Potential upstream transcription regulator genes in UV-B-exposed GF and SPF skin and their gene interaction network

The upstream regulator analysis within IPA analyzes linkage to differentially expressed genes through coordinated expression and identifies potential upstream regulators which have been experimentally observed to participate in gene expression [124]. The analyses of significant upstream regulators in GF and SPF skin response UV-B exposure showed 6 genes: EP400, SMAD3, IL1b, AGO2, TNF, IL10RA (Figure 37A). We found that EP400, SMAD3, IL1b, AGO2, and TNF were highly upregulated in SPF skin compared to GF. Intriguingly, after UV-B exposure IL10RA was highly activated in GF compared to SPF skin. In contrast, the expression of pro-inflammatory molecule IL1B was more dominant in UV-B-irradiated SPF compared to GF skin. GeneMANIA [125] (https://genemania.org/) was used to predict the interactions and functional association of the upstream regulator genes. We found several target genes including IL10, CMA1, MAP2K3, CCL3, CCL4, NFKBIA, IL10RB, TNFAIP3, HSPA1L, IFNG, NFKB2, FOSL1, IL7R, CLEC7A, CD44, IL6, FOS, CYTIP, CLN8, CD83 interacting physically or co-expressed together. Notably, these genes are involved in cytokine activity, inflammatory response, positive regulation of defense response and response to molecule of bacterial origin (Figure 37B). qPCR analysis was done for genes within the dataset and target genes observed in gene network of upstream regulators and we found a significantly higher expression of IL10 and S100A4 in GF skin compared to SPF skin after UV-B exposure. However, expression of IL-17a, IL-1b, Ccl3, Ccl7, S100A3, and S100A9 was downregulated by UV-B in GF skin compared to SPF skin (Figure 37C).

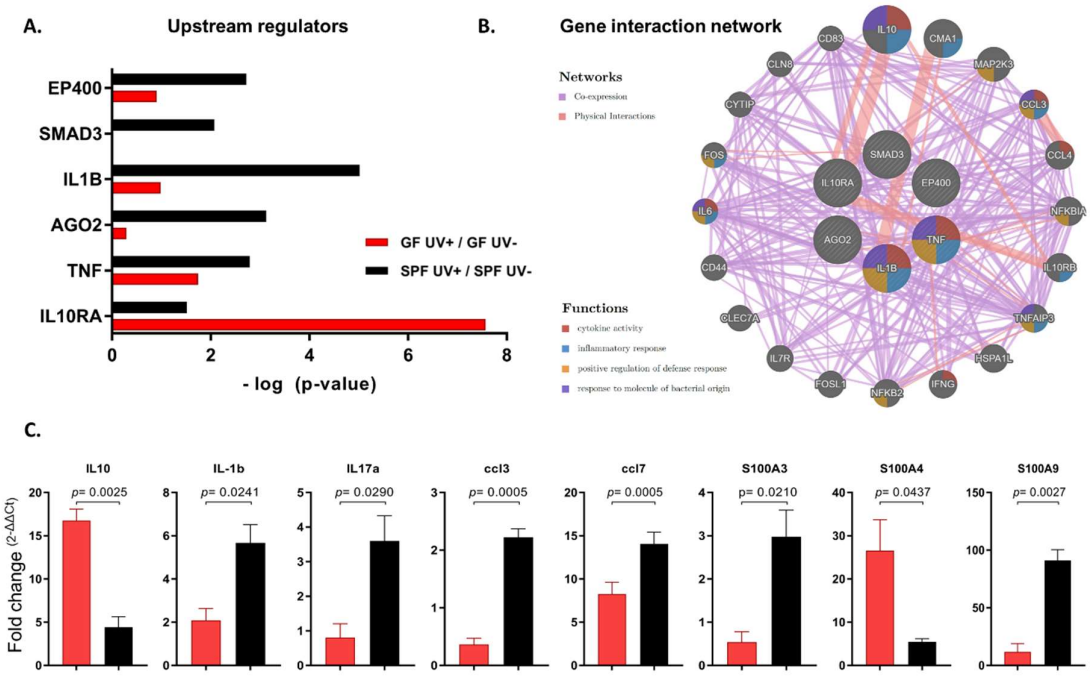

Figure 37: Effect of UV-B on various upstream regulators and gene interaction. *(A) Predicted upstream regulators enriched in UV-B treated GF and SPF skin identified by microarray analysis. The filtered (prediction activation state and p< 0.05) upstream regulators are plotted based on their -log (p-value). (B) Gene interaction network of upstream regulators was done using geneMANIA. The genes involved in various functions are represented in colors. Co-expression and/or physical interactions are also shown in the network. (C) qPCR analysis was done for selected genes from the dataset and gene network of upstream regulators. qPCR was performed in triplicates. Data shown represent mean ± SEM. N=3 per experimental group; p-value determined by unpaired T-test.*

1.7 Discussion:

The skin is one of the most exposed parts of the human body and constantly experiences numerous environmental hazards. One of the hazardous entities affecting the skin and its barrier function is UV-R. UV-R is known to cause skin photoaging and skin cancer. UV-B, in particular, is known to affect the morphology of the epidermis, permeability barrier, lipids, lead to increased transepidermal water loss and decreased hydration [126].

This study shows an increased TEWL and skin hydration after doses of UV-B (30 and 618 mJ/cm^2) compared to unexposed mice which go well in line with the previous report [127]. This suggests that UV-B causes an epidermal barrier dysfunction, that could potentially lead to penetration of microbes or microbial antigen into the skin. Exposure to UV increased epidermal thickness, layers and cellular infiltrate (mostly mast cells and neutrophils) at the high dose of UV-B in SPF mice. This could be due to the fact that UV-B could potentially act on the skin-resident microbiome and in turn lead to innate immune activation to control the inflammation [31,42,61,67]. To evaluate the effect of UV-B on skin microbiome, groups of mice were irradiated with varying doses of UV-B (30 mJ/cm^2 and 618 mJ/cm^2). 16s rRNA sequencing was performed to determine bacterial populations affected by UV-B exposure. Significant modulation of bacteria was observed by alpha and beta diversity analysis. Firmicutes were most sensitive to UV-B (both low dose and high dose, as well as in controls), significant increase in prevalence and decrease in proteobacteria (only in low dose). These changes in microbial composition run parallel to immune infiltration in the skin, with increased infiltration of inflammatory monocytes and neutrophils in high dose groups, alongside emigration of antigen presenting cells and upregulation of genes expressing AMPs [42].

The impact of UV-R and immune system was first described in the landmark studies conducted by Margaret Kripke and colleagues during the 1970s [17]. These studies showed that mice lost the ability to reject subcutaneously implanted, syngeneic immunogenic tumors due to an immunosuppressive environment after UV-exposure. To illuminate the immune suppression effects of UV-R, CHS and DTH models were established and immune responses were found suppressed in those models, now known to be mediated by specific regulatory T-cells [87] and B-cells [43]. This study shows that the microbiome of the skin profoundly modulates the effect of UV-B on the immune system.

As demonstrated by this study in GF and disinfected mice, the presence of microbiome reduces UV-induced immune suppression as measured by suppression of induction of CHS (Figure 1). Notably, the initial cellular response to UV-B differed between GF and SPF mice. SPF mice showed increased epidermal hyperplasia and dermal cellular infiltration (Figure 2), despite the fact that there was no overall difference in cellular damage as measured by sunburn cells as surrogate markers. Furthermore, dendritic epidermal γδ T cells (DETCs) are known to be activated after exposure to UV and to be involved in limiting DNA damage [128]; however, no significant differences in epidermal $CD3^+$ cells between UV-exposed GF and SPF skin were observed. This indicates that the presence of microbiome affects the response of the skin to UV-B exposure.

Indeed, transcriptome analysis revealed the differential regulation of genes after UV-exposure in the presence vs absence of microbiome, resulting in a predominance of pro-inflammatory cytokines such as IL1β**,** IL6, IL18rap vs immunosuppressive cytokines such as IL10, IL10ra, IL20rb, IL7r. Indeed, recent work has shown microbes or microbial products are able to induce immunoregulatory effects [114], protect against UV-induced skin neoplasia [129], and modulate gene expression in the skin and can influence the epidermal development and differentiation [117] and wound healing [118]. Moreover, it is known that certain skin resident microbes and microbial products can regulate the expression of AMPs [116]. Furthermore, UV-R can also directly induce expression of certain AMPs within the skin [31] and possibly at least in part by pro-inflammatory cytokines[130]. In this study, significant difference in modulation of AMP expression in UV-exposed GF compared to SPF skin was found. This modulation of AMPs in GF skin could greatly contribute to cellular and humoral cytokine production and immune response in the skin. Increased expression of TLR13 in UV-exposed GF skin, which is an important macrophage receptor [131] was observed. Increased activated macrophages (Ly6c+) infiltration in UV-exposed GF skin compared to SPF skin was also seen. Intriguingly, macrophages can produce large amounts of the anti-inflammatory cytokine, IL10 that was upregulated in UV-exposed GF skin. Moreover, serotonin signaling genes HTR2A and SLC6A4 are significantly upregulated in GF skin compared to SPF skin. It has been previously published that serotonin signaling is crucial in UV-induced systemic immune suppression but not local inflammation [132]. This supports the observation of increased UV-induced immune suppression, but the weaker epidermal response and cellular infiltration in GF compared to SPF mice. A previous study has shown that sensitization through UV-exposed skin induces Tregs and these UV-induced Tregs

suppress immune response via production of IL-10 [133]. GF mice are known to have increased number of cutaneous Foxp3^{+} Tregs compared to SPF mice [134].

After exposing skin to UV-R, IL10 is secreted by keratinocytes to some extent, but a large amount of IL10 is produced by bone marrow-derived macrophages infiltrating the skin [135,136]. In the gene expression and gene-interaction analysis, the skin of UV-exposed GF mice showed high expression of IL10 and its receptors (IL10RA, IL10RB) compared to SPF mouse skin. IL10 inhibits production of IL1α, IL1β, IL6 by monocytes [137]; this is consistent with data showing increased gene-expression of IL10 and its receptor IL10ra and reduced expression of IL1β and IL6 in UV-exposed GF skin and an opposite effect is observed in SPF skin, with increased expression of IL1β (linked to contact hypersensitivity [138]), and IL6 and reduced IL10. Interestingly, IL20rb was seen to be upregulated in UV-exposed GF skin, whereas was downregulated in SPF skin. IL20rb is known to play a major role in signaling related to cutaneous inflammatory response and also to reduce production of IL1β [139]. Previous research has shown that commensal microbes can augment IL1 signaling and subsequently promote effector T cell functions [134]. This data indicated increased IL1β expression in SPF skin, most likely directly induced by microbes and further amplified by UV-exposure [140]. Moreover, IL34 which is known to stimulate monocyte and macrophage development and proliferation [141] was highly expressed in UV-exposed GF skin and downregulated in SPF skin. IL7r which is known to block innate and adaptive inflammatory response [142] was highly expressed in the skin of UV-exposed GF compared to SPF mice.

Alongside, UV-exposure increased the expression of various chemokines in SPF skin, compared to GF skin. This data showed increased expression of Ccl7, Cxcl1, Cxcr2, Ccl2, Ccl3, Cxcl5, Cxcl2, Ccr1, Ccl12 which goes well in line with previously published research, [143,144] and suggesting that UV-exposure induces chemokine production that mediates the recruitment and activation of immune cells. A high expression of pro-inflammatory chemokines Ccl2 and Ccl3 [145] induced by UV-B in SPF skin was observed. Furthermore, SPF skin increased levels of Cxcl5 which is known to be involved in UV-B induced hypersensitivity in humans and rats and causes local inflammation by infiltrating neutrophils and macrophages to the skin [144], consistent with observation of increased cellular infiltrate in SPF compared to GF skin. Ccr4, which is expressed on Foxp3+ Tregs is critical for suppressing cutaneous inflammatory response [146] and Ccr4$^{-/-}$ mice exhibit a stronger CHS response compared to wild-type mice [147]. UV-B suppressed the expression of Ccr4 slightly more in the skin of SPF compared to GF mice in this study. A decrease of Ccr4 expression

could impair DC-T-cell interaction and ultimately lead to enhanced inflammation in the skin [147,148]. This data is consistent with the observations of the topical application of *S.epidermidis* on the skin resulting in modulation of cytokines such as Ccl3, Ccr2, Cxcl2, IL18rap, IL1β, IL6 [149]. In this study these cytokines proved to be upregulated in UV-exposed SPF compared to GF skin.

The limitation of GF model is to separate effects of distal gut microbes from skin resident microbes, as it could be possible that gut microbiome can influence the response of the skin though circulating microbial products or metabolites and further modulate the immune response [150-152]. However, the fact that this study shows increased immune suppression in disinfected compared non-disinfected mice supports the importance of skin microbiome for directly modulating the immune response to UV-B (independent from gut microbiome). 16s microbiome analysis showed differences within the bacterial communities in control (UV-unexposed) group. This could be attributed to experimental artifacts such as shaving the mice, or the skin swabs used. In addition, cage effect could be another key issue for the differences observed in T0 in control, low dose and high dose groups. Studies shows that husbandry and caging can indeed modify microbial composition at significant levels [153]. Further studies need to minimize the cage effect by housing the mice together in a single cage for several weeks and to increase the sample size significantly to minimize the experimental artifacts. Moreover, PMA used in this study to exclude dead cells during sampling could also lead to experimental artifacts. Studies have shown that long-term DNA storage can also lead to variations in the results of microbial population analyses between different samples [120,154].

Taken together, a more local pro-inflammatory environment is induced in the skin by UV-B in the presence than in the absence of microbes. These findings are crucial for understanding UV-induced skin carcinogenesis and go in line with a recent report [129] showing a protective effect against skin cancer by the common skin commensal *Staphylococcus epidermidis.*

2

Potential link of skin microbiome in pathogenesis of polymorphic light eruption: Expression of antimicrobial peptides

Disclosures

Parts of this thesis have been published in:

- Patra V and Wolf P. **Microbial elements as the initial triggers in the pathogenesis of polymorphic light eruption?** Exp Dermatol 2016 Dec;25(12):999-1001

- Patra V, Mayer G, Gruber-Wackernagel A, Horn M, Lembo S, Wolf P. **Unique profile of antimicrobial peptide expression in polymorphic light eruption lesions compared to healthy skin, atopic dermatitis, and psoriasis.** Photodermatol Photoimmunol Photomed. 2018 Mar;34(2):137-144.

Permission to reproduce published text and figures have been obtained via RightsLink® from the publishers.

2. Introduction to polymorphic light eruption

Polymorphic light eruption (PLE) was first described by Epstein in 1942 under the name of prurigo aestivalis [155]. PLE is the most common photodermatosis that affects around 10-20% of the young female population in temperate climates [156-160]. PLE patients develop pruritic and nonscarring lesions as early as few hours to days after the first exposure to sunlight, mostly in early spring or summer. The lesions with varying morphology, usually subside in few days when exposure to sunlight is avoided [156,158]. As the summer progresses PLE patients may experience natural hardening due to repeated exposure to sunlight. This often results in less likeliness to develop lesions, and/or less lesion severity [157]. PLE patients usually develop the lesions in sun exposed parts that are normally covered during winter like the upper chest, neck and the arms [156,159,161].

2.11 Clinical manifestation

As the name of the disease implies ("polymorphic"), the lesions are generally of varying morphology (among individuals) which includes popular, papulo-vesicular, plaque, erythema multiforme (EM)- like and insect bite-like (strophulus) [162]. The crucial differential diagnoses include solar urticaria, lupus erythematous and photosensitive EM[162]. However, within individuals, the lesions are monomorphic in nature [156,162]. In addition, a variant of PLE known as PLE sine eruption with intense pruritus on the sun-exposed skin has been reported [163,164]. Systemic symptoms such as headache, chills and fever, nausea can be associated with PLE [165], however it is still unclear if these symptoms are directly related to PLE or associated with an accompanying sunburn. Indeed, UV exposure can lead to production of IL-1 an IL-6, which are known for endogenous pyrogenic activity [166,167]. Recently it is reported that PLE lesions have an increased expression levels of IL-1[168].

A

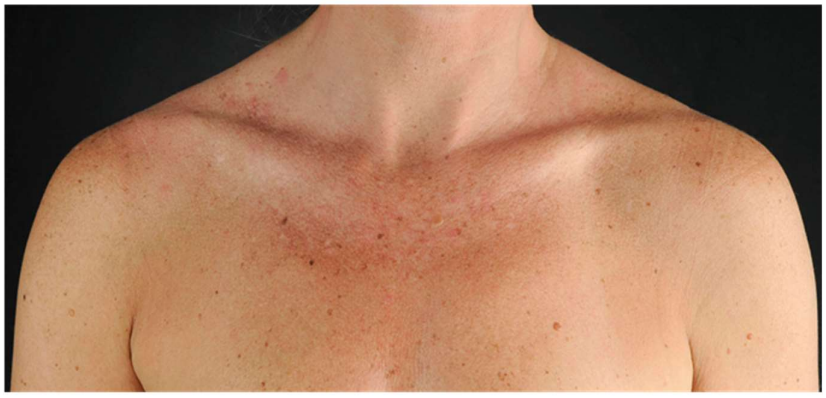

B

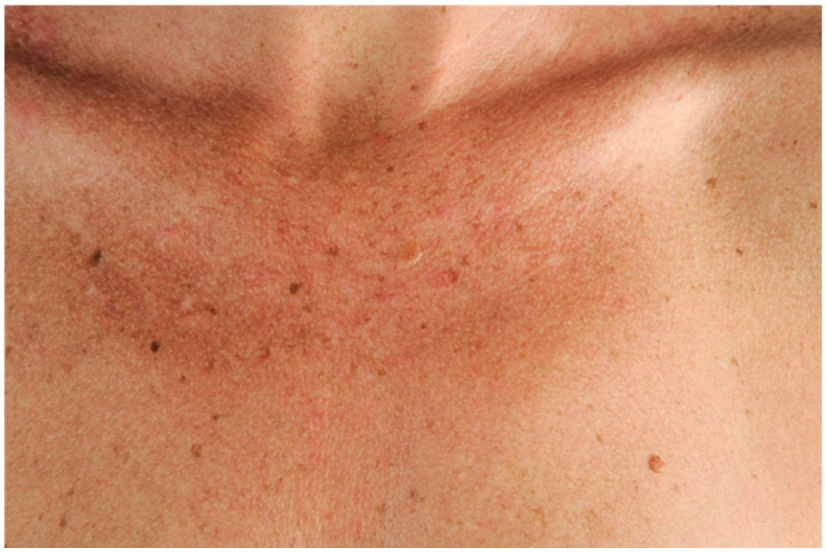

Figure 38: A Maculopapular type of PLE in the V-neck of a young woman. B. Higher magnification of lesions.

2.1.2 Photobiologic evaluation: waveband aspects

The UV waveband action spectrum to elicit PLE is quite broad. Most of the patients developing PLE are sensitive to UV-A, but UV-B alone can induce PLE lesions [159]. PLE patients show sensitivity to UV-A waveband of sunlight penetrating through glass windows, and lack of protection from UV-B absorbing sunscreen can indeed substantiate the role of UV-A in triggering the disease [169-171]. It has been reported that sunburn is not crucial in development of PLE [156] and higher incidence of PLE is observed in temperate areas with higher levels of UV-A during spring and autumn [158], supporting the importance of UV-A in disease induction and progression. Epstein reported that repeated exposures of UV-A or UV-B are required to provoke PLE, rather than a single exposure [163,171]. This concept underlies the basis of photo-provocation of PLE in a clinical setting and to confirm the diagnosis by reproducing PLE [156,163].

2.1.3 Histology of PLE

The histology of PLE is nonspecific and greatly depends on the clinical morphology (Figure 39). Spongiotic microvesicles are usually seen in papulo-vesicular type along with subepidermal edema and lymphoid perivascular infiltrate in dermis[172]. On the other hand, in EM-type PLE, vacuolar alteration of cells at the epidermal junction can be seen [172]. An increased immune response to UV has long been thought responsible for the pathogenesis of the disease. The cellular infiltrate of PLE is mainly composed of activated CD4+ T cells, being consistent with a delayed type hypersensitivity reaction [173] up to 72 hours in early lesions, and CD8+ T cells in established lesions, which is consistent with underlying mechanisms of PLE involving cellular mediated immune response [174]. This predominantly lymphocytic perivascular cellular infiltrate is linked with increased numbers of macrophages and dendritic cells (DCs), along with Langerhans cells (LCs) 5 hours after UV exposure.

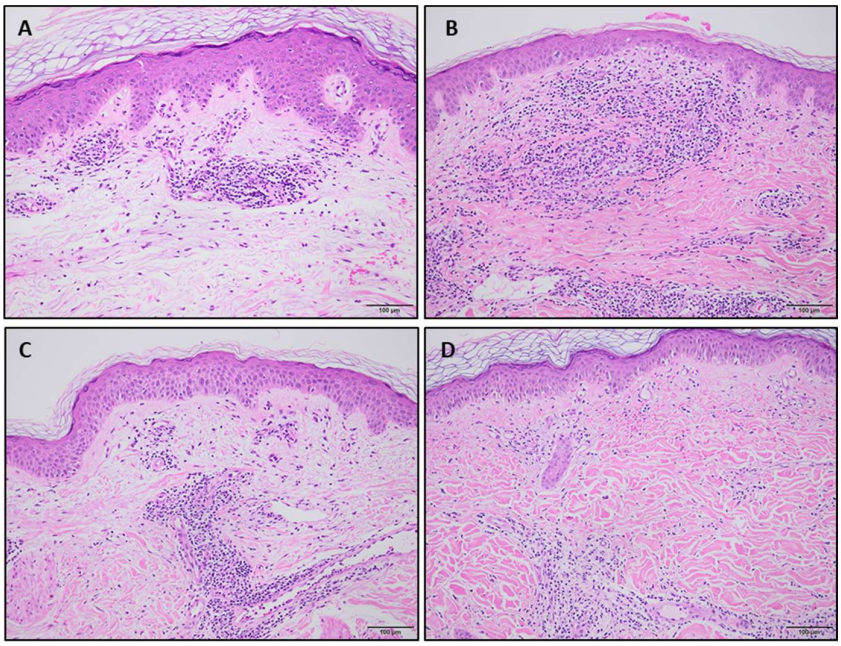

Figure 39: Histology of PLE*. Hematoxylin-eosin staining shows an increased subepidermal edema and predominantly lymphoid perivascular infiltrate in dermis. Slight vacuolar alteration of cells and liquefaction degeneration at dermal and epidermal junction is visible.*

2.1.4 General immunological features of PLE

The exact cause and pathogenesis of PLE is currently unknown, but a resistance to UV-induced immune suppression and immune reaction to neoantigens are thought to be involved [156]. UV-R exposure modifies proteins and DNA in the skin, thereby creating new or altered skin components that could be recognized as antigen by the immune system [206].

In healthy skin, the ability to generate immune responses (T-cell mediated) to contact allergens is significantly suppressed by exposure to UVR [23,175,176] and immune tolerance can be established. This UV-induced tolerance is hapten-specific and the sensitization potential to another hapten is not affected. Thus, PLE could be result of decreased UV-induced immune suppression, allowing the response to a photo antigen. UV-induced suppression of CHS (in healthy subjects) is associated with production of various cytokines such as TNF-α, IL-4, IL-10. Emigration of LCs from epidermis and subsequent infiltration of HLA-DR+/CD11b+/CD1a- macrophages is a key feature observed in healthy subjects after UV-B exposure [177]. UV-B exposure creates a local environment with changes in cytokine

expression that are favorable to development of type 2 helper (Th2) cells [178]. Along with the depletion of CD1a+ LCs after UV exposure, CD36+ CD11b+ CD1- cells infiltrate the dermis in healthy subjects, which is not observed in PLE [179]. These CD11b+ macrophage like cells play an important role in inducing immune suppression and tolerance [156,162]. Moreover, unlike in healthy subjects, in PLE patient's failure to recruit CD11b+ CD68 - neutrophils has been reported. As neutrophils are important in immune suppression due to their capacity to produce IL-4 and IL-10 [162,163] and decreased neutrophil infiltration in PLE skin could lead to a failure in suppressing the immune response. Mast cells are recruited after exposure to UV and are crucial in signaling such as activation of regulatory T cells (Tregs) that lead to immune suppression. It has been that reported that the skin of PLE patient contain lower number of mast cells than the skin of healthy subjects. This may play a role in pathogenesis of PLE. Furthermore, mast cell-derived cytokines such as IL-10, can contribute to recruiting Tregs. Indeed, PLE skin shows low Treg infiltration, suggesting potential role of mast cells in PLE [180,181].

2.2 Antimicrobial Peptides

AMPs are small proteins, known to have microbicidal activity. AMPs are commonly found from prokaryotes to human and are known to be conserved evolutionarily. Lysozyme was the first reported protein in 1922 by Alexander Fleming, which had antimicrobial function. AMPs are present in all the species of life that are studied for this activity. AMPs since then, have been characterized extensively and more than 2995 AMPs have been currently deposited in antimicrobial peptide database (http://aps.unmc.edu/AP/main.php) and more are being discovered. AMPs are mostly produced by the cells in constant exposure to microorganisms. In the skin there are two main classes of AMPs, i.e., β-defensins and cathelicidins. In humans LL-37 is the only cathelicidin found, which is expressed by various epithelial cells and keratinocytes in inflamed skin [34]. Apart from defensins and cathelicidins, skin also constitutively expresses a wide range of AMPs like RNase 7 (ribonuclease 7), S100A7 (Psoriasin, calcium binding protein), and dermcidin (that is sweat gland derived). AMPs are produced during inflammation or in cases of infection. The production of these AMPs, including beta defensins, cathelicidins, ribonucleases and S100 proteins, are triggered by various pathogen or damage associated molecular patterns (PAMPs/DAMPs), exogenous microbial danger signals like Toll-like receptor (TLR) agonists, or endogenous mediators of inflammation such as TNF-α, IL-1, IFN-γ and IL-17 [35,182-184]. It is also known

that UV-R induces production of AMPs, as essential components and triggers of the innate immune system. Studies have shown that UV-R induces human beta defensin 2 (hBD2), hBD3, ribonuclease 7 (RNase7), S100A7 (psoriasin), S100A12 and elafin by keratinocytes *in vitro* and *in vivo* [31,33,34,185-187]. One mechanism of UV-induction of AMPs could involve production of the active form of Vitamin D [188]. Alternatively, or in concert with this, Vitamin D_3 itself could be suppressing adaptive immune responses [189] and/or tempering inflammatory events in UV-exposed skin[161 190] .

2.2.1 Properties and diversity of AMPs

AMPs usually consist of 10-50 amino acid residues. AMPs contain amino acid distribution and hydrophic residues that align in three dimensions and form variable structures[191]. These amino acid structures are water soluble and hydrophobic in nature. AMPs can be classified based on their structures: α-helical (e.g.: human cathelicidin peptide), β-sheets (bactenecins and defensins), and extended AMPs (histidine, arginine, glycine or tryptophan)[191].

Not only the skin produces the AMPs but also microbes can produce various AMPs in order to control the growth of other resident microbes. However, the AMPs produced by microbes are fairly distinct from that produced by mammalian AMPs. Some prominent microbial AMPs are cationic peptide polymyxin B (by *Bacillus polymyxa*)[192] and noncationic glycopeptide vancomycin (*Amycolatopsis orientalis*)[193]. Cholera and diptheria toxins, bacteriolytic enzymes such as lysostaphin and hemolysins, bacteriocins are few other examples of AMPs produced by bacteria. In mammalian species, AMPs vary considerably[191]. For instance, in humans α-defensins are the most prevalent host defense peptides produced by neutrophils but are completely absent in neutrophils of mice and cattle. Defensins are the most quickly evolving groups of mammalian peptides and show significant variations in the properties and hundreds have been identified so far. In contract, very less variation has been observed in the AMP cathelicidin family. Mammalian cathelicidins include bactenecins (Bac5 and Bac7) and rabbit CAP18[191].

2.2.2 Mechanisms of action of AMPs

The capacity of AMPs to kill and neutralize microbes depends on their ability to physically interact with microbial membranes or cell walls. Since AMPs generally have positive charge along with hydrophobic amino acids, which lets them bind to negatively charged microbial membranes. This binding of AMPs to microbial membrane results in its non-enzymatic disruption, and subsequent killing of the microbe. The AMP selectivity for specific species is due to the differential composition of the cell membranes among different microbes.

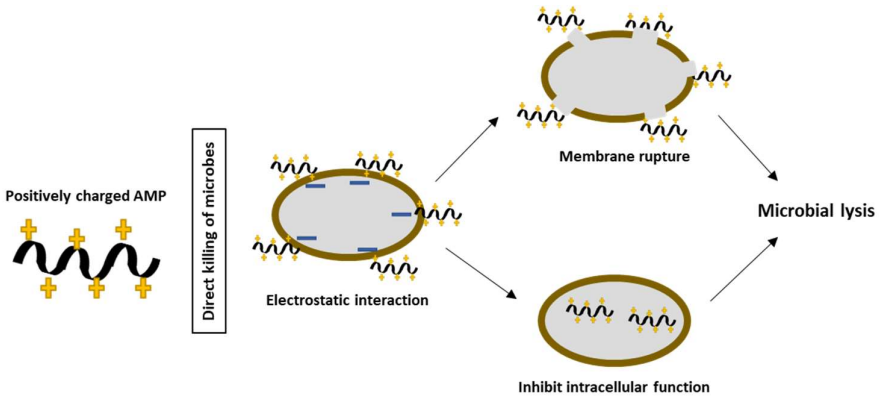

Figure 40: Biological function of antimicrobial peptide*. AMPs can selectively bind to membrane by electrostatic interactions, and either disrupt the membrane directly or indirectly by inhibiting the intracellular function by entering the microbe.*

Similar to defensins, most cathelicidins are able to disrupt the membrane of microbes by binding to them. LL-37 (cationic, α-helical), is known to bind to microbial cell membrane by electrostatic interactions, followed by its insertion, leading to membrane disruption[34].

Some AMPs are known to cause membrane disruption by enzymatic digestion, such as lysozyme, which hydrolyses the beta-glycosidic linkage between N-acetylmuramic acid and N-acetyl glucosamine in the peptidoglycan (present in bacterial cell walls), and phospholipase A2 (PLA2) which are known to be secreted from human platelets neutralizes invading pathogenic bacteria by hydrolyzing the bacterial membrane phospholipids. Meanwhile, some AMPs (such as LL37, indolicidin, buforin 2) are known to cross the lipid bilayer and kill the microbe by inhibiting its intracellular functions.

Skin is colonized by diverse species of microbes, most of the commensals are required to maintain a healthy homeostasis with the host. It is intriguing that the adaptive immune

system can indeed target all the microbes, yet the microbes reside in the skin. These resident microbes block the peptide attachment to their membrane which increases their survivability on the skin, evading the immune system.

2.2.3 Immunoregulatory and non-antimicrobial function of AMPs

One of the hallmark features of AMPs apart from killing microbes, is their ability to interact and modulate adaptive immune system[187]. For example, AMPs can take part in chemotactic activity, attract leukocytes, modulate cellular responses to TLRs, stimulate angiogenesis, trigger monocyte development and differentiation, and induce expression of cytokines [33-35,184,187]. LL-37 is known to attract neutrophils, monocytes, mast cells and T cells. α-defensins are able to chemoattract CD45RA+ naïve T cells, whereas β-defensins are chemotactic for CD4+ CD45RO+ T cells and DCs[34]. These interactions and the constitutive expression of AMPs in the skin are able to increase host's responsiveness to self-antigens, that can lead to autoimmune diseases such as psoriasis and rosacea.

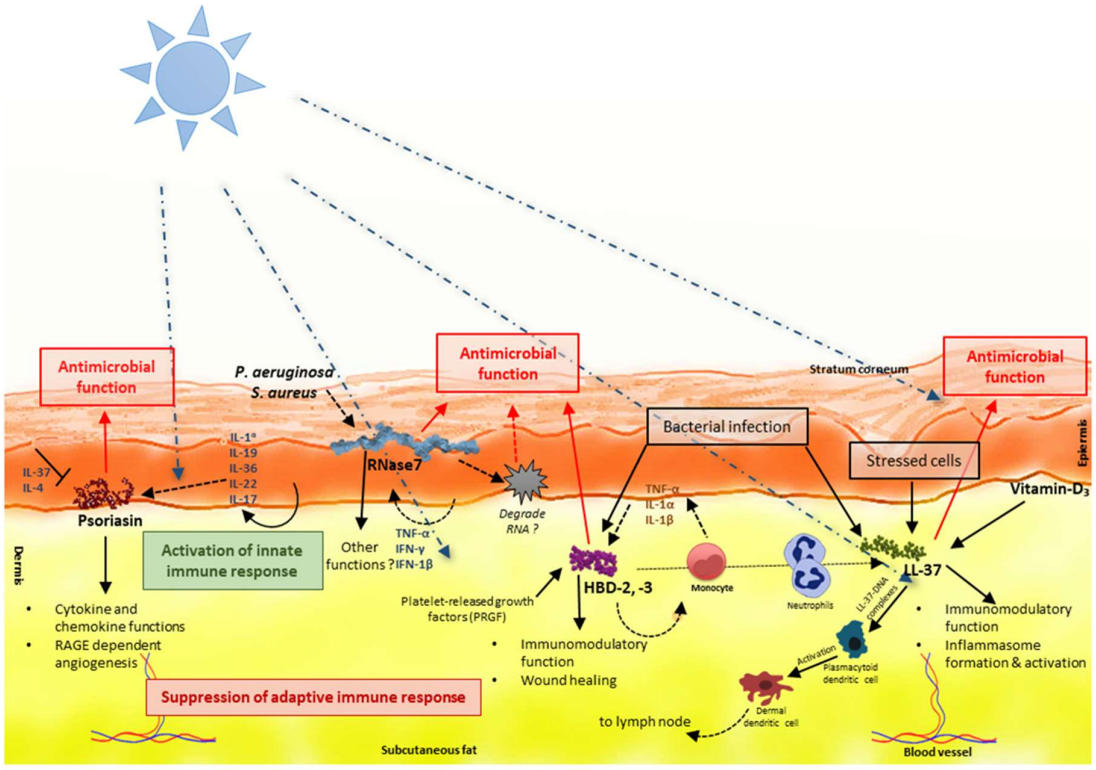

Figure 41: Multifunctional biological properties of antimicrobial peptides. *UV-R is known to activate innate immunity and suppress adaptive immunity in healthy skin or under normal*

physiological behavior. UV-R is known to induce various AMPs such as Psoriasin, RNase7, HBD-2, -3 and LL-37 among many others. Psoriasin is known to be in nucleus or in cytoplasm and can be upregulated by bacteria, UV-R and interleukins. Apart from antimicrobial effects, psoriasin can induce chemotaxis of neutrophils and T cells. RNase7 shows ribonuclease activity and is constitutively produced by keratinocytes. The production of Rnase7 can be induced by microbial stimuli or various proinflammatory cytokines (TNF-α, IFN-γ, IFN-1β). Human beta-defensins (HBD-2, -3) are mostly expressed in epithelial cells, but can be expressed in other cells such as monocytes, macrophages and dendritic cells. HBD-2 is induced by UV-B, microbial infections and/or pro-inflammatory stimuli (LPS, TNF-α, IL-1α and IL-1β). HBD-3 is more potent than other HBDs in killing a broad range of microorganisms at low concentrations. HBDs are also actively involved in modulating innate and adaptive immune responses. LL-37 is the only cathelicidin produced in humans (mostly in granulocytes). LL-37 can be induced by UV-B, vitamin-D_3, stress signals and microbial stimuli. It is known to activate dermal dendritic cells and the inflammasome pathway, ultimately modulating immune responses.

2.2.4 Potential role of AMPs in pathogenesis of PLE

Pathogen/damage associated molecular patters (PAMPs/DAMPs) can be released due to UV-induced stress on the skin microbial communities and/or skin cells, these PAMPs/DAMPs can therefore trigger and exacerbate inflammatory responses by inducing the innate immune system [194], for example by producing antimicrobial peptides (AMPs) (Fig 42). Photo-provoked PLE patients show an upregulation of AMPs such as Psoriasin, RNase7 and HBD-2 [195]. PLE patients pre-treated with calcipotriol show reduction in PLE symptoms[196] , interestingly, it is known that the beneficial effects of calcipotriol is due to the modulation of AMP regulation via TH17 pathways[195]. AMPs are the key molecules in maintaining a healthy homeostasis with the skin microbial communities and the immune system. It is known that photosensitive patients have lower serum vitamin D_3 levels [195,197]; this low vitamin D_3 levels could lead to microbial community alteration via dysregulating AMPs in the skin (Fig 42).

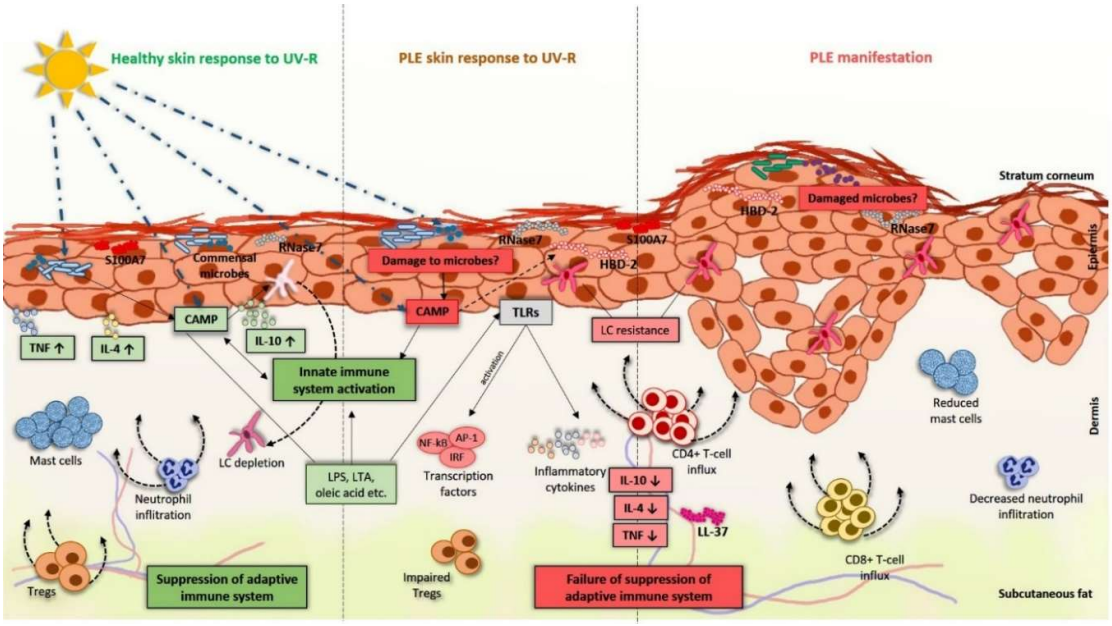

Figure 42: Hypothetical model for pathogenesis of PLE. *Exposure of the skin to ultraviolet radiation (UV-R) leads to the production of commensal-associated pattern (CAMP). They are usually buried intracellularly, but upon secretion from dying human cells or microbial communities of the skin, they may exacerbate inflammatory responses by inducing the innate immune system through producing antimicrobial peptides (AMPs) such as S100A7*

(psoriasin), HBD-2, RNase7 and LL-37. This increase in AMPs can promote in a vicious circle the activation of adaptive immune responses and exacerbate the inflammatory responses. In addition, UV-R can also directly lead to microbial killing, resulting in the production of microbial signaling molecules such as lipopolysaccharides (LPS), lipoteichoic acid (LTA), oleic acid and others that in turn may lead to or enhanced abnormal immune responses through Toll-like receptor (TLR) activation and transcription factors such as NF-kB, AP-1 and IRF. In healthy subjects, various cytokines such as TNF, IL-4 and IL-10 are expressed and infiltration of neutrophils and Tregs and increase in mast cell numbers in the skin are observed upon UV exposure. However, in PLE, there is a reduced production of these cytokines and decreased infiltration of neutrophils and reduced numbers of mast cells in the skin. Moreover, Langerhans cell resistance to UV-R is seen in the skin of PLE patients compared to that of healthy controls. Taken together, all these events may be linked to the abrogation of UV-R-Induced suppression of the adaptive immune responses in healthy subjects but a failure of suppression in PLE patients. Consequently, an influx of CD4+ T cells and CD8+ T cells is observed in the skin of PLE patients leading to inflammation and manifestation of the typical skin rash upon UV exposure. Image reproduced from Patra and Wolf [206] with permissions (See attachments) from John Wiley and Sons.

2.3 Hypothesis and Aims

AMPs are more than just microbicidal, they possess immunomodulating properties. Apart from participating in innate immune responses, AMPs are also involved in activating and mediating adaptive immune responses [33-35,182-185]. The much abundant skin's physiologically beneficial microbiome vastly depends upon AMPs to be kept and maintained in homeostasis in order to release and allow the immune system to mount an immune response, when needed, and protecting against invading pathogens[206].

The hypothesis of this study was that (1) dysregulations in AMP expression may alter the microbial landscape on skin leading to abnormal immune responses. Another possibility could also be due to (2) already altered microbial landscape or production of microbial antigens due to UV-R, eventually leading to AMP expression. UV-R on the other hand is known to enhance the expression of AMPs [27], further studies are much warranted to understand the complex relationship between UV-R, AMPs and skin microbial communities, which could unravel the pathogenesis behind PLE[206].

The aim of this study was to evaluate the expression of various AMPs (HBD-2,3, S100A7, RNase7 and LL37 in PLE lesions and compare it to psoriasis, atopic dermatitis and healthy skin[206,161].

2.4 Material and Methods:

2.4.1 Samples:

Formalin-fixed paraffin-embedded (FFPE) skin biopsy samples of PLE of 12 patients (8 women and 4 men; median age: 60 years [range, 16-75]), lesional skin of 6 patients with AD (1 woman and 5 men; median age: 43 [range, 6-63]) and 6 patients with psoriasis (6 women; median age: 50 years [range, 31-74]) as well as samples from healthy, normal looking skin of 13 individuals (6 women and 7 men; median age: 72 years [range, 47-88]) were available for the study. The healthy tissue samples were from tumor adjacent skin, obtained during surgical excision of lesions such as nevi and non-melanoma skin cancers. The study was approved by the Ethics Committee of Medical University of Graz, Graz, Austria (18-068 ex 06/07 and 25-293 ex 12/13) and was performed in accordance with the guidelines of the Declaration of Helsinki Principles. All participants included in this investigation provided written informed consent[161].

	Face/head	Trunk	Extremities	sample size (n)
PLE	0	1	11	12
AD	0	3	3	6
PSO	1	1	4	6
HS	8	2	3	13

PLE: Polymorphic light eruption; AD: atopic dermatitis; PSO: psoriasis; HS: healthy skin

2.4.2 Immunohistochemical staining

FFPE tissue sections (3.5 µm) were deparaffinized and rehydrated for immunohistochemical staining. Slides with tissues sections were incubated for heat-induced antigen retrieval in Dako Target Retrieval Solution Citrate pH 6.0 (Dako S2369) or Dako Target Retrieval Solution pH 9,0 (Dako S2367) for 30 minutes in a steamer. The staining was then performed manually at 4°C antibody incubation using the Dako REAL™ Detection System, Peroxidase/AEC, using monoclonal antibodies directed against: HBD2 (1:400; Abcam,

#ab63982), HBD3 (1:100; LSbio, #LS-B86), psoriasin (1:300; Thermo Scientific, #MA1-91555), RNase7 (1:50; Abcam, #ab154143) and LL37 (1:50; Abcam, #63982). Images of stainings were acquired with a DP71 digital camera (Olympus, Vienna, Austria), attached to an Olympus BX51 microscope [161].

2.4.3 Quantitative analysis of AMP expression

Visual analysis was performed by counting positively stained cells in 5 randomly selected microscopic fields at a magnification of 40x using an ocular grid with area coverage of 0.25mm^2. For psoriasin, number of positively stained cells were counted in the epidermis. For HBD-2, positive cells and negative cells (HBD-2 unstained) were counted in the dermis, and the **percentage of positive cells** = $\left(\frac{number\ of\ positive\ cells}{number\ of\ positive + negative\ cells} * 100 \right)$ was determined. For LL-37 the number of positive blood vessels in the dermis was determined**.** Scoring of microscopic slides was performed in a blinded manner. Results of visual counts were averaged per patient and used for statistical analysis. For RNase7 and HBD-3, we quantified expression using ImmunoRatio plugin [198] in ImageJ software with the images acquired with an Olympus DP71 digital camera. The percentage of the DAB-stained nuclear area over the total nuclear area in epidermis and dermis was calculated and the percentages were subjected to statistical analysis [161].

2.4.4 Statistical analysis

Statistical analysis was performed using GraphPad Prism 6. For immunohistochemistry score comparison, unpaired non-parametric, Kruskal-Wallis test was used; each p-value was adjusted to account for multiple comparisons. A p-value smaller than 0.05 has been set as statistically significant [161].

2.5 Results:

2.5.1 Increased psoriasin expression in PLE

Psoriasin was most highly expressed by keratinocytes in PLE and psoriasis; it was expressed in the nucleus and cytoplasm (of the) stratum granulosum and stratum spinosum, whereas the basal layers and stratum corneum showed no expression in PLE, but little expression in psoriasis. In contrast, AD showed very little expression of psoriasin (only in stratum granulosum of the epidermis). In healthy skin, expression of psoriasin was found in stratum granulosum but was less intense and patchy compared to PLE or psoriasis. Overall, the expression of psoriasin in PLE was statistically significant compared to healthy skin[161].

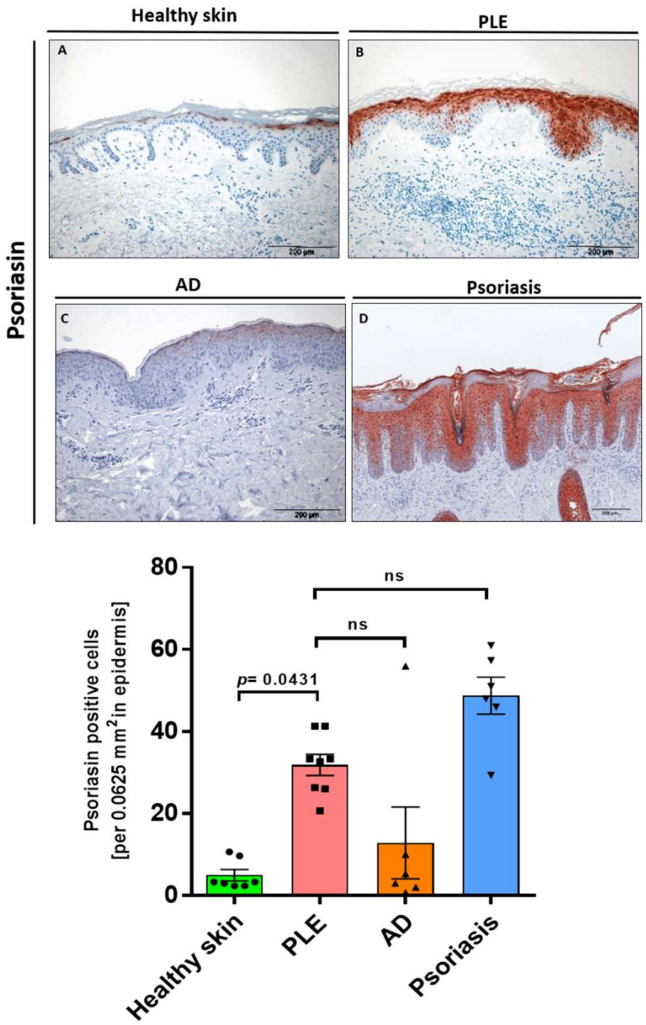

Figure 43: Increased psoriasin expression in PLE. *Immunohistochemical staining revealed keratinocytes on the upper epidermis and stratum corneum expressing psoriasin AMP. Data presented as mean ± SEM.*

2.5.2 RNase7 is increased in PLE and predominantly expressed in stratum corneum

RNase7 was expressed in PLE, mainly in keratinocytes of the stratum granulosum and stratum corneum and less intensively in the basal layers of the epidermis. Healthy skin and AD showed very low expression of RNase7 in stratum corneum and stratum granulosum. Psoriasis showed a high level of expression of RNase7 in stratum corneum, but subtle expression in other layers of the epidermis. Altogether the expression of RNase7 in PLE was significantly higher than in healthy skin or lesional skin of AD and psoriasis [161].

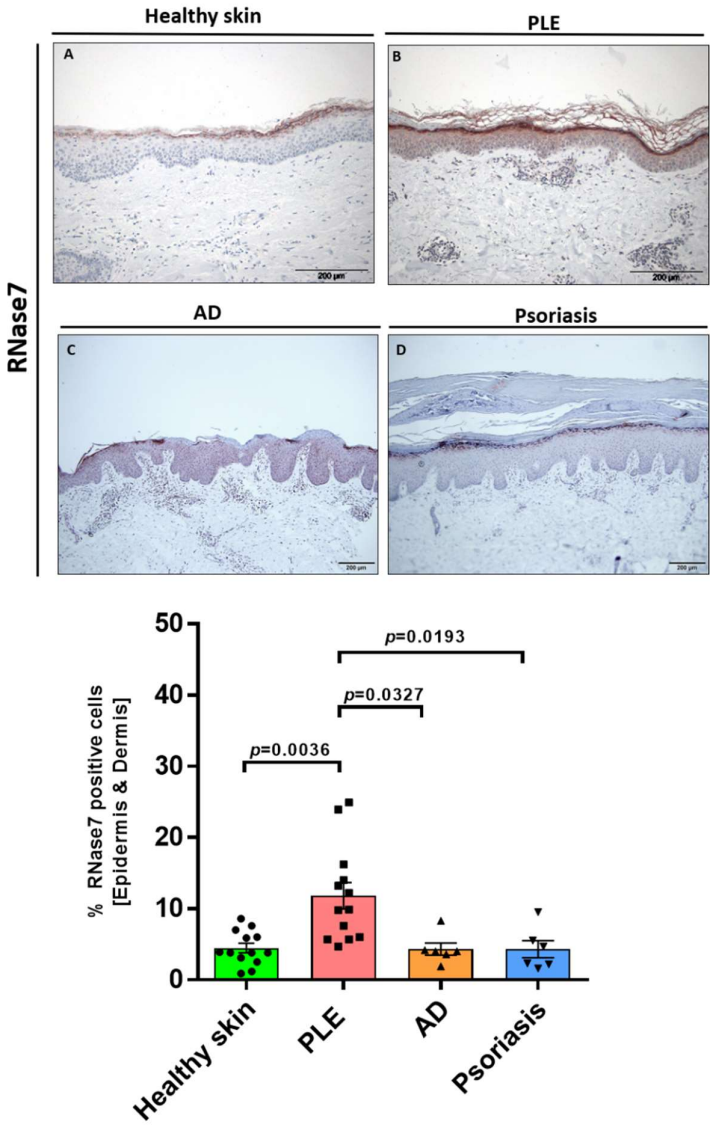

Figure 44: Increased RNase7 expression in PLE. *Immunohistochemical staining revealed keratinocytes, especially on the upper epidermis and stratum corneum expressing RNase7 AMP in PLE compared to HS, AD and Pso. Data presented as mean ± SEM.*

2.5.3 Increased HBD-2 expression in cellular infiltrate in PLE

HBD-2 was expressed in infiltrating cells in the dermis in PLE, AD and psoriasis whereas healthy skin showed no expression or very low expression of it. PLE showed significantly higher numbers of HBD-2 positive cells in the dermis compared to healthy skin [161].

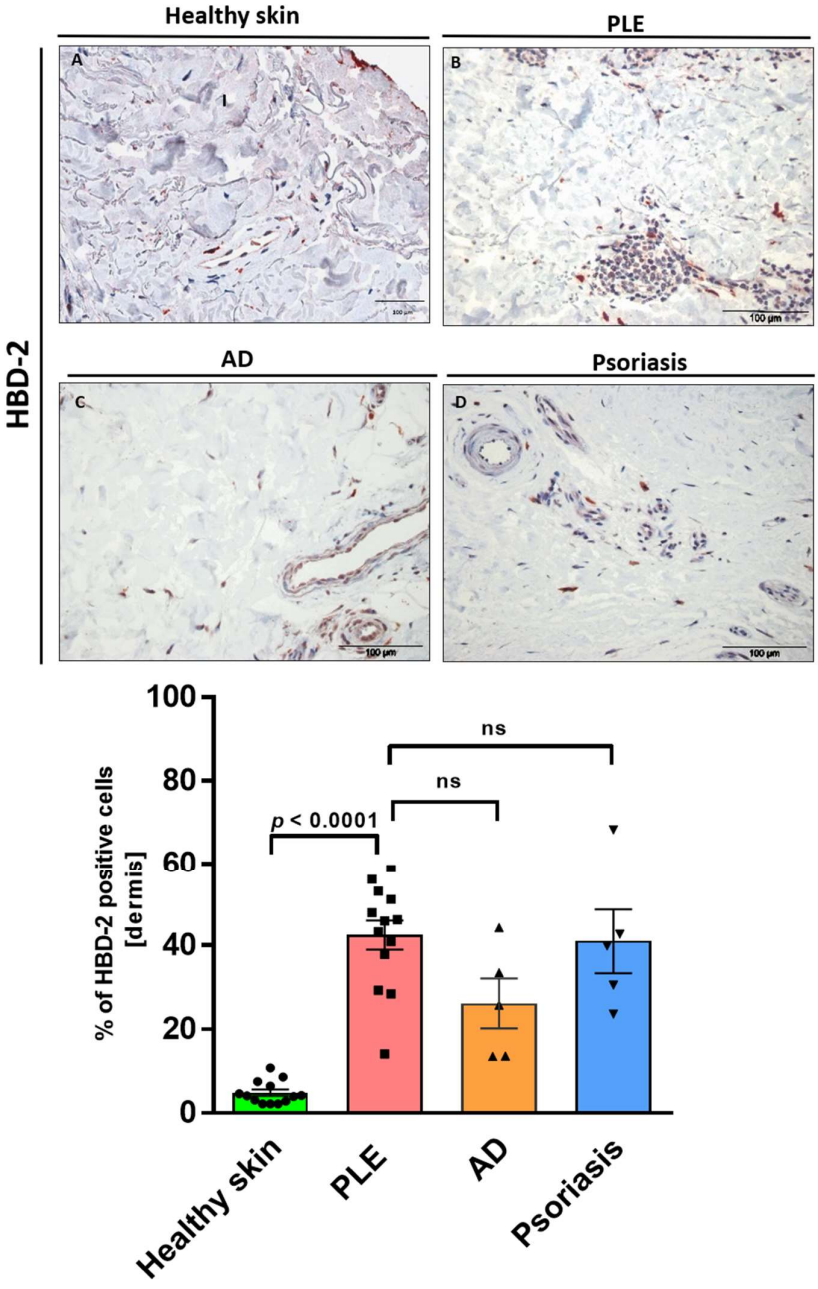

Figure 45: Increased HBD-2 expression in the dermal infiltrate PLE. *Immunohistochemical staining revealed infiltrated cells expressing significant amount of HBD-2 AMP in PLE compared to HS, AD and Pso. Data presented as mean ± SEM.*

2.5.4 PLE lesions have decreased expression of HBD-3

HBD-3 expression was only modestly expressed in the stratum granulosum but not at all in the other layers of the epidermis in PLE. In contrast, healthy skin, AD and psoriasis showed higher expression of HBD-3 in epidermal layers as well as infiltrating cells in the dermis. Statistical significance was reached when PLE was compared to AD [161].

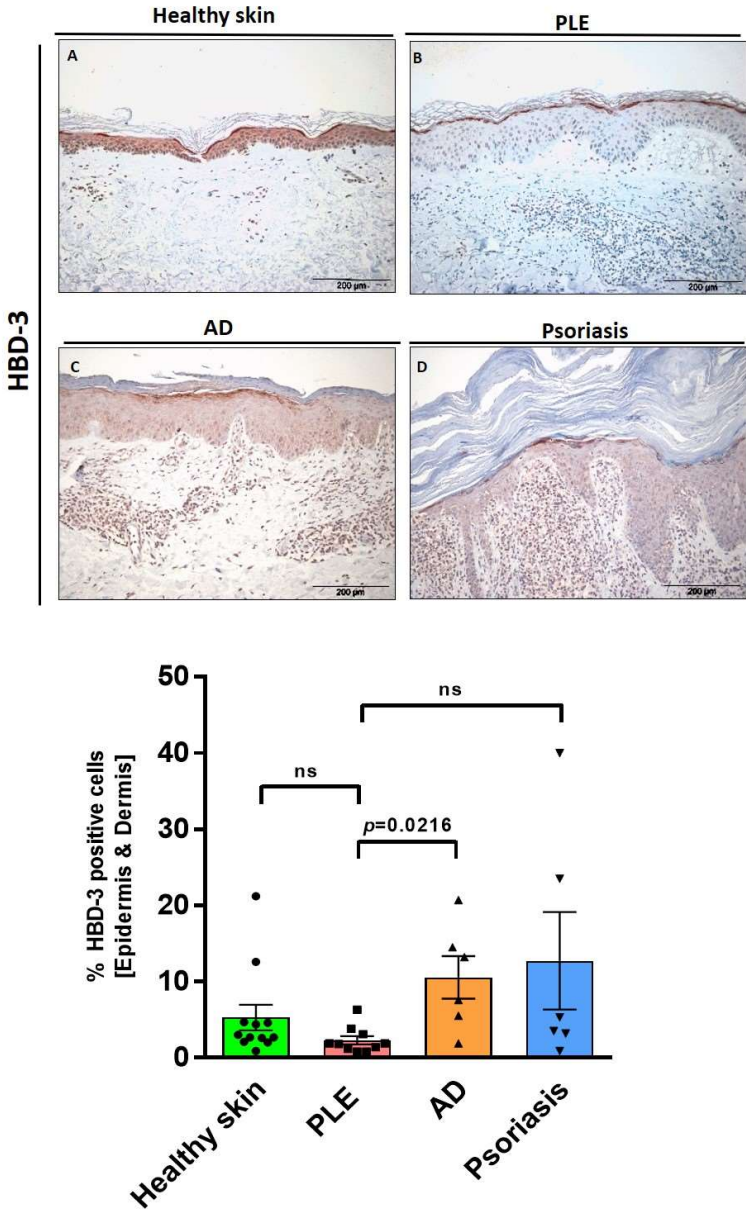

Figure 46: Decreased HBD-3 expression in PLE. *Immunohistochemical staining revealed reduced HBD-3 AMP expression in PLE compared to HS, AD and Pso. Data presented as mean ± SEM.*

2.5.5 LL-37 is significantly increased in and around blood vessels in PLE and psoriasis

LL-37 was profoundly expressed in and around blood vessels and glands in PLE and psoriasis. Healthy skin or AD showed no expression or very low expression of LL37. Overall, the increased expression of LL-37 in PLE and psoriasis was significant compared to healthy skin or AD [161].

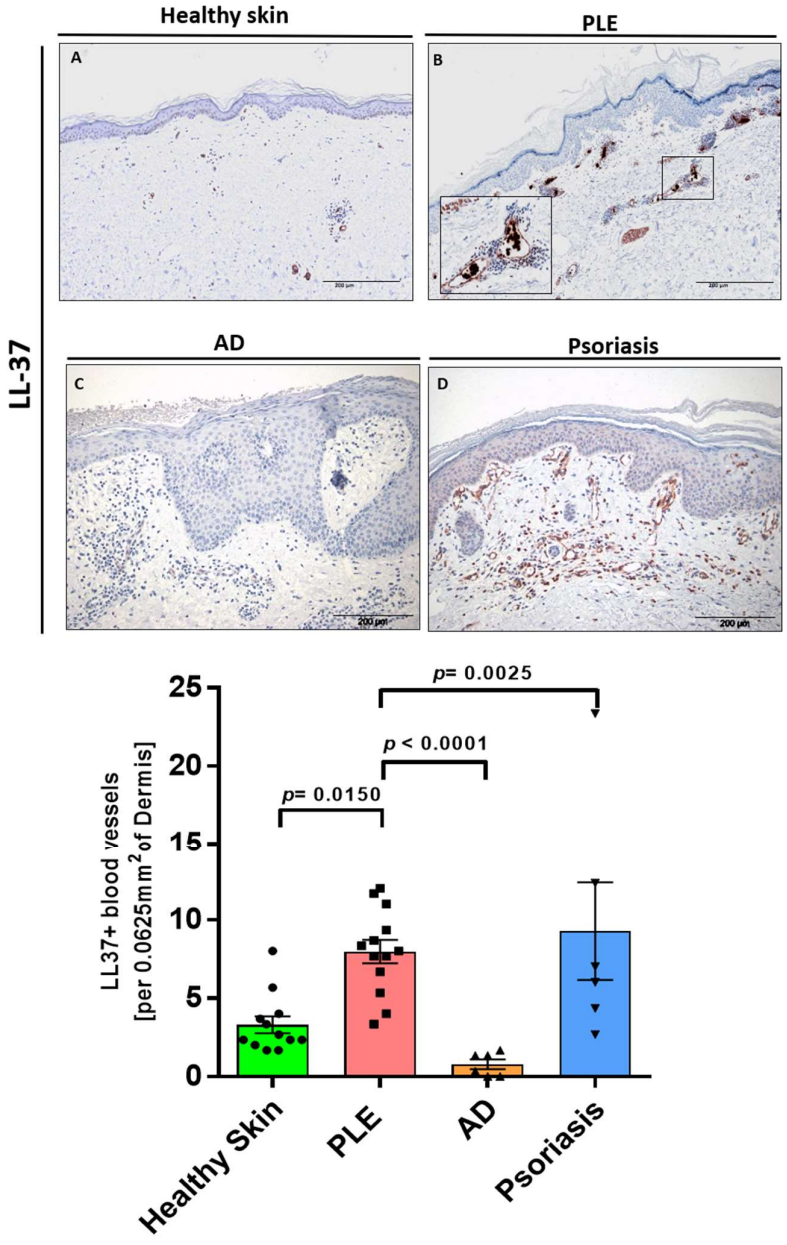

Figure 47: Increased LL-37 expression in PLE. *Immunohistochemical staining reveal increased expression of LL-37 in PLE and Pso, around blood vessels, glands and granulocytes compared to HS, AD and Pso. Data presented as mean ± SEM.*

2.5.6 Expression levels of AMPs are independent of age

To determine, if age played a role in differential expression of various AMPs in PLE, age-matched scoring analysis for various AMPs was performed. Statistical correlation analysis revealed the expression of AMPs were independent of age, except for psoriasin in PLE (r=0.7012, p= 0.0095). Moreover, there was no overall statistical correlation between sex and expression of any of the AMPs of this study [161].

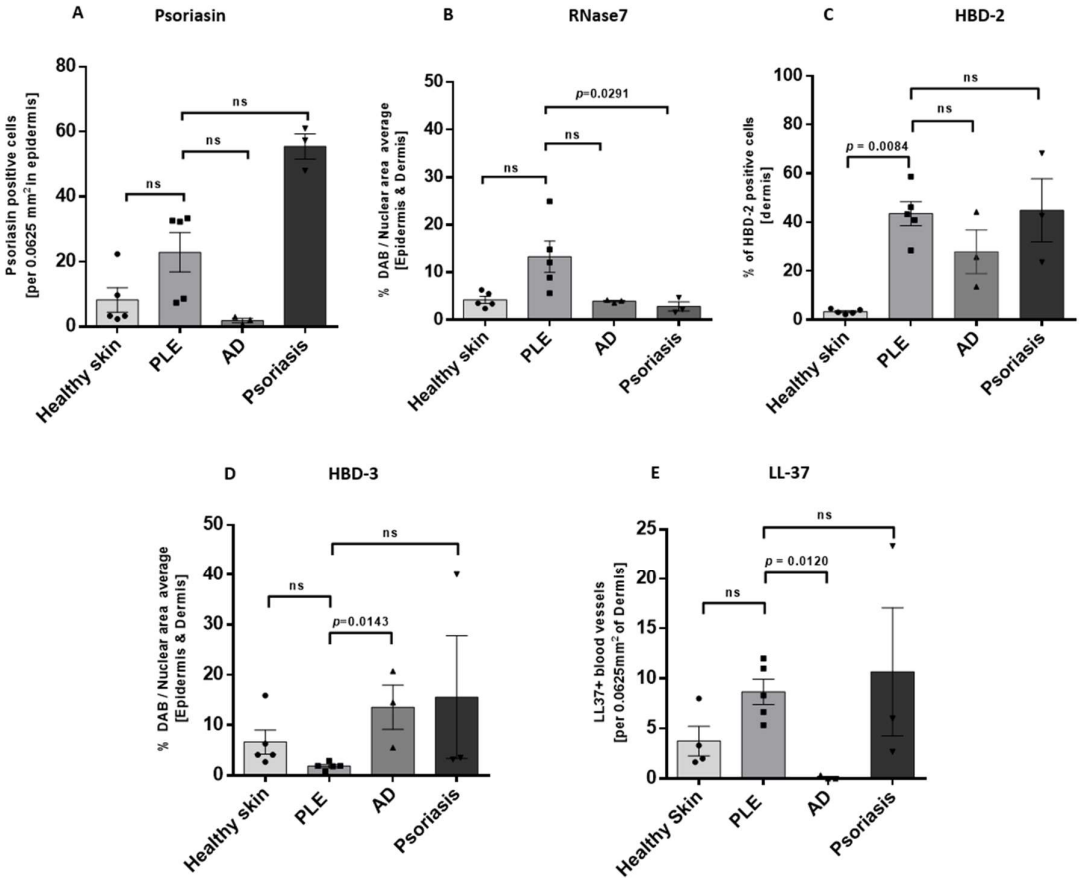

	Psoriasin	RNase7	HBD-2	HBD-3	LL-37
PLE	r= 0.7012, p= 0.0095	r= 0.2393, p= 0.4280	r= -0.1648, p= 0.5911	r= -0.2073, p= 0.5523	r= -0.0577, p= 0.8450
AD	r= 0.0285, p> 0.99	r= 0.6377, p= 0.2000	r= -0.6000, p= 0.3500	r= 0.4857, p= 0.3556	r= -0.3531, p= 0.4333
PSO	r= -0.0285, p> 0.99	r= 0.2571, p= 0.6583	r= -0.3000, p= 0.6833	r= 0.0857, p= 0.9194	r= 0.0857, p= 0.9194
HS	r= 0.5518, p= 0.0660	r= -0.3513, p= 0.2263	r= 0.3714, p= 0.2107	r= 0.6632, p= 0.0217	r= -0.2297, p= 0.4425

Figure 48: AMP expression is independent of age and sex. *Bar graphs represent scores from age-matched samples (40-65 years) in various disease conditions. Table shows r value and p value for co-relations analysis*

2.5.7 PLE lesions share similar AMPs expression profile similar to psoriasis, except for RNase7 and HBD-3

To determine the overall expression pattern of all the AMPs studied, heatmap was plotted by using the quantitative scores of individual AMPs using the online heat mapper tool (http://www.heatmapper.ca/) [123]. Genes are clustered by average linkage and distance measurement was done using the Euclidean method. The plot revealed a distinct expression patterns of HBD-2, - 3, RNase7, Psoriasin and LL-37 for different diseases and healthy skin.

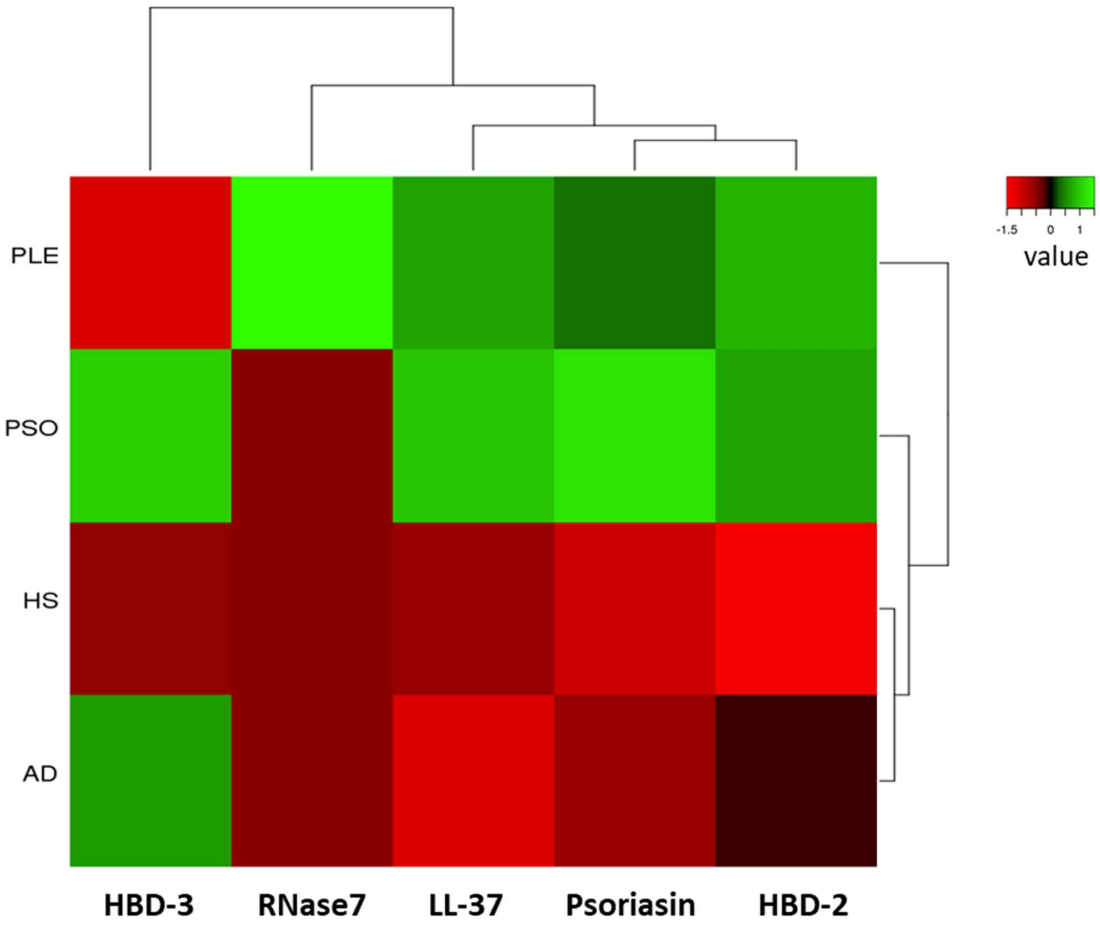

Figure 49: Heatmap showing expression patterns of AMPs in various diseases.

2.5.8 AMPs interact with other molecules within the skin

Online tool GeneMANIA [125] (https://genemania.org/) was used to predict the interactions and functional association of the AMPs investigated in this study (PLE lesions). We found several target genes interacting physically, colocalized or co-expressed together. Notably, these genes are involved in cytokine activity, inflammatory response, positive regulation of defense response and response to molecules of bacterial origin. Thus, the AMPs expressed in PLE lesions could be involved in signaling and contribute to disease pathogenesis.

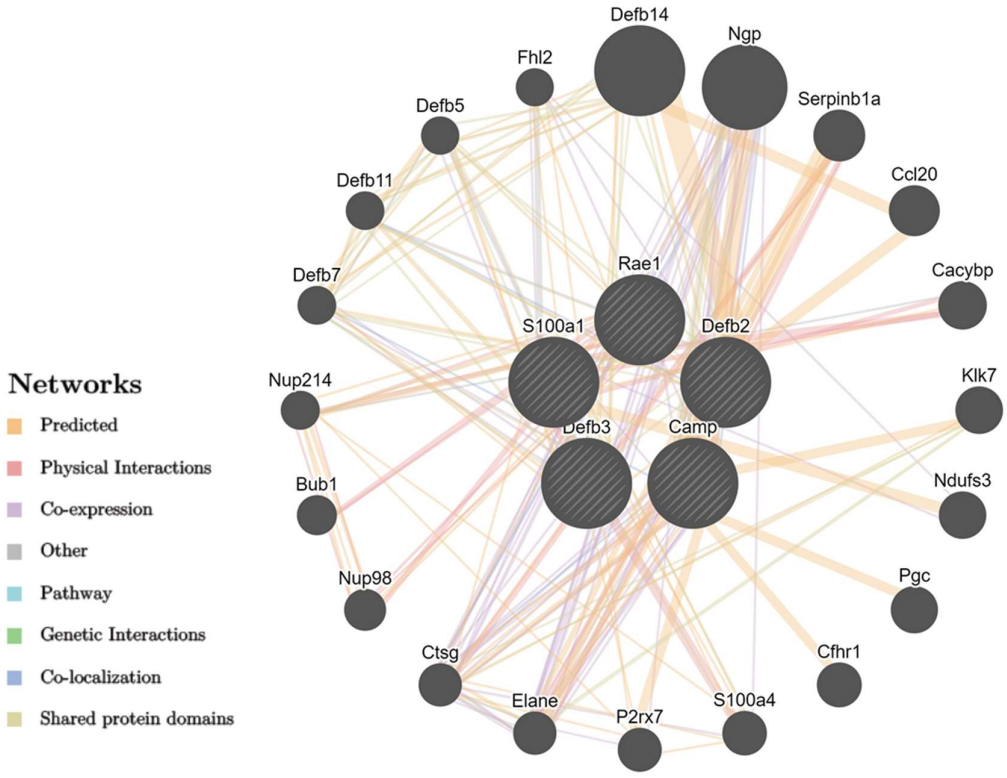

Figure 50: Effect of AMPs on gene interactions. *Gene interaction network of AMPs was established using geneMANIA. The genes involved in various functions are plotted.*

2.6 Discussion:

AMPs have been extensively studied for over 40 years of their role in innate immune system. Initial studies mostly focused on understanding the mechanisms behind microbial killing and to identify the structural features of various AMPs and their family members (for e.g., HBDs and S100 proteins). However recent works have demonstrated its multifunctional roles in mediating adaptive immune responses. AMPs have been constantly implicated in various inflammatory skin diseases such as lupus and psoriasis. Improving immune signaling via AMPs can indeed bolster immune response to infections, but at the same time, can also provide novel therapeutic options for treating autoimmune diseases.

The second part of the work in this thesis reveals a unique expression patterns of AMPs, psoriasin, RNase7, HBD-2, -3, and LL-37 in PLE lesions compared to AD, psoriatic and healthy skin [161]. AMPs are the key molecules that are produced in the skin during infection and/or inflammation. It has been shown that UV-R can induce the production of AMPs both *in vitro* and *in vivo* [31,186,195,199,200]. First identified by Moore during 60's, S100 protein family consists of 25 small acidic calcium binding protein members (10-12 kDa) [201]. The level and activity of S100 protein expression is modulated by binding of calcium followed by binding to specific target [202,203]. S100 proteins are involved in variety of cellular processes which includes calcium homeostasis, energy metabolism, cellular proliferation and differentiation, and apoptosis [203]. Psoriasin (S100A7) is reported to be expressed in inflamed skin and can exert a chemotactic influence on inflammatory cells [204]. Psoriasin shows high antibacterial activity against *E. coli* , but is less active against other type of bacteria [205]. Previous reports with immunohistochemical staining's showed that psoriasin was expressed in both normal and psoriatic skin [206]. In this study, psoriasin was observed to be highly expressed in PLE lesions and psoriatic skin. However, reduced or no expression was seen in healthy skin or in patients with AD, these observations are consistent with previous published reports [206-209]. Inflammatory cytokines such as IL-1α, IL-1β, IL-36, IL-17, TNF-α, and calcium, flagellin and UV exposure are known to induce the expression of psoriasin [205,210-212]. Pro-inflammatory cytokines IL-1β (can also act synergistically with IL-23 and IL17A) and IL-36 is reported to be increased in PLE patients [213], this enhanced expression could further induce the production of psoriasin in the skin [203,168]. Psoriasin shows strong antimicrobial potency against bacteria [205,214], one potential hypothesis could be drawn from increased expression of psoriasis is the potential involvement of microbes or microbial components

(photo-neo-antigen) in pathogenesis of PLE [161,215]. Psoriasin may have a determinant role in exacerbating the inflammatory reaction in PLE lesions. Psoriasin may also serve as a potential target for therapy, with minor undesired side effects due to its relatively narrow spectrum of biological effects [203]. For example, calcipotriol (Vitamin D analog) which is used to treat psoriasis, is known to decrease psoriasin expression. Interestingly, PLE patients treated with calcipotriol have decreased PLE symptoms [216] and this could be due to reduced psoriasin expression after the treatment. That said, various topical creams and gels containing psoriasin are now commercially available to treat psoriasis and other itchy skin conditions.

Ribonuclease A superfamily comprises of multiple peptides found in mammals. These peptides belonging to RNase A superfamily are secretory peptides which include hydrophobic signal peptide and matured peptide. These matured peptides are usually in the range of 12-16 kDa and contain 6-8 cysteine residues that help in forming disulfide bonds to maintain their tertiary structure [217]. The peptides in RNase A superfamily (canonical ribonucleases) include pancreatic RNase (RNase 1), eosinophil-derived neurotoxin (EDN/RNase 2), eosinophil cationic protein (ECP/RNase 3), RNase 4-8. There are newly identified noncanonical ribonucleases named RNase 9-13 in humans [218]. RNase7 is produced mostly by keratinocytes in large quantities and is bactericidal against a broad spectrum of gram-negative and gram-positive bacteria [219,220]. Notably, besides antibacterial activity, it has been recently shown that RNase7 shows immunomodulatory functions on T_H2 cells and cytokine production [161,221]. In this study, PLE lesions have increased expression of RNase7, mostly on stratum corneum and stratum granulosum, where most of the resident microbial population reside. Lesional skin of AD and psoriasis showed reduced or no expression of RNase7. Patients with AD showed substantially reduced expression of RNase7, this could also support the fact that AD patients have increased rate of microbial infection. In contrast to AD, psoriasis is characterized by lower infection rate through the epidermal barrier is disrupted. This lower infection rate in the psoriatic skin may be due to increased expression of various AMPs that fight off the invading microbes [217]. RNase7 is known to be constitutively expressed in healthy skin which maintains a constant state of immune homeostatic with the resident microbes [222-224]. This consistent expression of RNase7 is also observed in the study. Furthermore, microbes or microbial products, which are also hypothesized as triggers of PLE, could aggravate the expression of RNase7. In the skin, the outermost differentiated epidermal layers are known to constitutively produce RNase7 in

large quantities, which indicates that RNase7 expression is higher where microbial assaults are most likely to occur [217]. Apart from microbes, cytokines such as IL-17A and IFN-γ [225] are known to induce the expression of RNase7 in the skin. That said, a previous report shows elevated levels of IL-17 in serum of PLE patients [213]. This increase in IL-17 can indeed induce the expression of RNase7 in the lesions. UV-R can also induce RNase7 expression both *in vivo* and *in vitro* [31]. The hypothesis that reduced expression of AMPs, especially RNase7 in AD may be associated with increased bacterial growth is under debate. That said, an abnormal expression of RNase7 in PLE could imply a predisposition of microbial involvement in the pathogenesis of PLE. Even though RNase7 exhibits strong antimicrobial properties, additional studies are warranted to unravel its association to the adaptive immune arm. At this point, the path to a therapeutic application for RNase7 is poorly defined and requires better clarification of its underlying functions in regulating the immune responses [217].

Defensins (α-, β- and θ) are short cationic peptides with 6-8 cysteine residues. β-defensins are comprised of 38-42 amino acids [226]. β -defensins are natural occurring peptides capable of modulating immune responses, clear pathogens either without boosting inflammation or by promoting inflammation[226]. Human β-defensin 2 was first isolated from skin of psoriasis patient [227]. Inducers of HBD-2 include LPS, TNF-α, IL-1β, IL-1 α, bacterial infections [228] and 1,25-dihydroxyvitamin D_3 [229]. Although HBD-2 is an inducible AMP, it is also detected in normal human skin, with site-specific difference in relation to its anatomical position [230], also implied to site-specific microbiome of the skin. In this work, expression of HBD-2 was substantially increased in cellular infiltrate in PLE lesions, compared to healthy skin. IL-1β which is known to be expressed in PLE lesions [231] could potentially induce the expression of HBD-2 [213,232]. In an *ex vivo* experiment, the proinflammatory mediator TNF-α and IL-17 stimulated the expression of HBD-2 but not UV-R [233]. The presence of LPS and other microbial products or elements in PLE remains to be discovered. Commensal microbes such as *S. epidermidis* are known to induce HBD-2 and -3, thereby enhancing protection against pathogenic organisms. Despite being expressed in low quantities in healthy skin, HBD-2 is expressed substantially upon infection or during inflammatory condition such as psoriasis [230]. β-defensins can bind to microbes or their components which can attenuate pro-inflammatory response by releasing various cytokines and also parallelly enhance antigen-specific antibody responses [226]. HBD-2 and -3 have strong ability to break the tolerance to human DNA thereby forming complexes with self-nucleic acids and trigger an innate

immune response [234] . UV-B can modify nucleic acids which could then become potential photo-antigens [157,162,215], and hence stimulating an immune reaction as seen in PLE[161]. Depending on the cells that produce defensins, they show multiple functions such overlap with chemokines, thus causing recruitment of immune cells such as monocytes, macrophages, T -cells etc. HBD-3 is expressed by the same cells that can produce HBD-2 in the skin. In the present study the expression of HBD-3 in PLE lesions was observed to be considerably lower than in AD, psoriatic and healthy skin. The potent inducers for upregulating HBD-3 are similar to those of HBD-2. Among other β-defensins, HBD-3 is the only AMP which is regulated by insulin-like growth factors such as (IGF-1) and transforming growth factor (TGF-α) and microbial stimuli from keratinocytes. However, the lower or reduced expression of HBD-3 in PLE lesions in this study and a previous report [195] could suggest a differential microbial landscape in PLE patients that fails to induce HBD-3 [161] or a lower expression of HBD-3 can imply an increased microbial load.

Apart from defensins and S100 proteins, LL-37 is the only cathelicidin peptide that is detected in humans and produced in abundance in chronic inflammatory disease such as psoriasis. LL-37 is known to play a major role in the inflammatory cascade driving psoriatic disease [235-238]. LL-37 is produced by cells that are likely to encounter microbes or microbial products, such as keratinocytes, neutrophils, DCs, mast-cells, T-cells, and monocytes/macrophages. LL-37 acts directly on microbes by disrupting the microbial membrane, additionally, it can also interact with cytoplasmic targets and results in membrane disruption[239]. In this study and in a previous report [240], significant expression of LL-37 around blood vessels and glands in the dermis of the PLE lesions was observed. The observations from this study of increased LL-37 expression in lesional skin of psoriasis and decreased expression in AD are consistent with previous findings [241,242]. LL-37 is induced by UV-B [200], 1,25-dihydroxy vitamin D_3 [229], components of bacterial infections and stress, cytokines such as IFNγ, TNF-α, IL-6 and activated TLRs [243]. Low systemic levels of vitamin D have also been reported in PLE and other photodermatoses [244], hence LL-37 similar as Tregs could be induced in PLE by other, non-vitamin D-dependent factors [245]. Previous research indicates that LL-37 is a vital mediator in activating pDCs by forming aggregates with self-nucleic acids [236-238]. However, in PLE patients a complete absence of pDCs has been reported [246], suggesting that the high expression of LL-37 might be involved in other inflammatory processes. In psoriasis patients, LL-37 has been recognized as an autoantigen that stimulates circulating T-cells and contributes to the autoimmunity in these patients [247].

Since a similar autoimmune environment exists in PLE patients with an increased expression of LL-37, it is likely that there are increased LL-37 specific T cells. On the other hand, LL-37 shows broad antimicrobial activity to various microbes and the high expression of this peptide could be directly involved in the antimicrobial activity in PLE patients [161]. Novel molecular targets of LL-37 are in development and such molecules might be used to treat PLE. The major limitations of this study were the limited number of samples and the imperfect matching in age and sex of the patient groups. However, age- and sex-matched analysis showed that the expression of AMPs (except for psoriasin that was age-related in PLE) was neither age- nor sex-dependent in the sample sets of the study. Indeed, age-matched sample (Fig 48) analysis revealed a similar picture than the overall analysis [161].

In conclusion, this works demonstrates that various AMPs in PLE are differentially expressed at the protein level. Based on these results, it is tempting to speculate that a unique expression profile of AMPs in PLE strongly indicates the involvement of microbes or microbial elements in the pathogenesis of PLE and these elements could also be the yet unknown “photo-neo-antigens” thought to cause the disease after exposure to UV.

3 General Discussion:

Skin microbiome plays a major role in the development and maintaining tissue homeostasis and regulating the host immune responses. Despite the constant environmental assaults, such as the impact of UV-R, skin microbiome and the host must consistently maintain tissue homeostasis for the normal healthy physiological state. Failure in doing so could result in immunologically mediated skin diseases, including photodermatoses such as PLE. This thesis works demonstrates that UV exposure indeed modulates the skin resident microbes and the immune response and shows that skin microbiome plays a prominent role in UV-induced immune suppression **(chapter 1)**. These results may ultimately provide the key to understanding the pathogenesis of PLE, by investigating the key molecules i.e., AMPs, which are crucial in maintaining the homeostasis between the microbes and immune system **(chapter 2)**.

The first part **(chapter 1)** of this work shows the skin's response to UV-R, with increased epidermal thickness, layers and cellular infiltrate in the presence of skin microbiome. Further characterizing the immune cells after exposure to UV-R within skin and lymph node revealed a major influx (inflammatory monocytes, neutrophils) and outflux (dendritic cells) of immune cells. The data from this thesis work shows that UV-R affects the microbial landscape within the skin and leads to barrier dysfunction (TEWL), which could allow microbes or microbial antigens to enter the skin and thus cause a local pro-inflammatory environment. Furthermore, studies with germ-free and disinfected mice with the model of UV-induced immune suppression reveal that the skin microbiome affords immune protection by orchestrating local cellular and innate immune responses to UV. Transcriptomic analysis of UV-irradiate GF and SPF mice show that a single UV dose induced several pro-inflammatory genes such as IL1β**,** IL6, and IL18rap; increases microabscesses and neutrophilic infiltration in SPF mouse skin (likely due to presence of microbiome) versus induction of anti-inflammatory genes such as IL10, IL10ra, IL20rb, and IL7r; and increased numbers of macrophages and IL10+ cells in GF skin. Collectively, these findings suggest that the skin microbiome diminishes the immunosuppressive response to UV, by modulating cellular and immune function. Although there exists enormous knowledge in the field of photobiology in regard to effects of UV on cellular response, the contribution and effects of skin microbiome have been largely overlooked. These results **(chapter 1)** are critical to understand the effects of UV on the skin and its microbiome. Advances in sequencing

technologies and use of photoreactive dyes such as propidium monoazide (PMA), provides us with strong ability to detect microbial communities to a strain level and also differentiate between live and dead microbes (PMA), which is also used in this thesis work **(chapter 1)** to understand the effect of UV on skin microbiome. Collectively these applications and results are particularly promising in understanding UV-induced skin diseases such as PLE. The second part **(chapter 2)** of this thesis builds upon the hypothesis that UV-induced microbes or microbial elements could be involved in the pathogenesis of a common photodermatosis such as PLE. Abnormalities in AMP expression have been linked to many pathological skin conditions including psoriasis and atopic dermatitis among others. Recently, it has been also reported that certain skin commensals can indeed produce or induce AMP production and that any dysbiosis in skin microbiome (due to UV, **chapter 1**) is directly linked to changes in AMP expression. This work shows a unique profile of various AMPs such as S100A7 (psoriasin), RNase7, HBD-2, -3 and LL-37 in PLE and compared to other diseases such as atopic dermatitis and psoriasis and also healthy skin. The findings of this study reveal the unique expression pattern of AMPs, including LL-37 (as a potential driver) in PLE lesions that thus provide a further understanding of the pathogenesis of the disease and could help to unravel a complex network between AMPs, skin microbiome and the immune system. However, the potential case of dysbiosis in the skin microbiome in PLE patients is yet to be investigated, but the altered expression of various AMPs among different skin conditions in this study strongly implies that either microbial elements or microbes themselves may be involved in the pathogenesis of PLE. Indeed, these microbial elements could be the source of the yet undetected antigens formed in PLE patients after exposure to UV-R [152,215]. Additionally, PLE patients have long known to have resistance to UV-induced immune suppression, which leads to enhanced autoimmunity and formations of lesions. The results from **chapter 1** shows the involvement of skin microbiome in limiting UV-induced immune suppression, suggests that skin microbiome plays a major role in this process, and could be one of the major reasons of resistance observed in PLE patients. The exact role of skin microbiome in PLE remains elusive and is a promising area where microbiome-based treatments can be developed, if a dysbiosis in microbial communities exists in PLE. For instance, a deeper understating of UV-induced microbial metabolites in the skin may be of benefit in modulating the skin immune response or skin microbiome transplantation from a healthy donor to diseased skin might improve the disease. That said a recent work has shown successful in-human microbial transplantation in AD patients improved symptoms [248].

Collectively the data from my thesis bring in novel insights into the effects of UV exposure on the skin and the role of the resident skin microbiome. In accordance with the findings from this thesis **(chapter 1)**, a recent work has shown that UV exposure alters fecal microbiome in mice [249], thus UV exposure can indeed modulate skin microbiome and also systemically affect fecal microbiome. The microbial inhabitants of the skin are of great interest, due to their role in maintaining homeostasis, and therefore involved in health and diseases. Interestingly, various diseases are associated with abnormalities in production of AMPs **(chapter 2)**. For e.g., psoriasis patients upregulate S100 and LL37 and AD patients have reduced HBD expression. The former hypothesis is based on observations that patients with psoriasis rarely contract skin infections due to their aggravated AMP expression, whereas AD patients suffer from severe skin infection due to their reduced AMP expression.

The dynamics of the interactions between skin microbiome and the host immune system, mostly AMPs, is currently one of the most studied areas, and the data from my thesis extends this knowledge of the contribution of the skin microbiome to UV-induce immune suppression. Furthermore, the observations of microbial community modifications by UV can be used to generate hypotheses about putative disease-causing microbes, linked to progression of UV-induced skin cancers (actinic keratosis to squamous cell carcinoma), as shown very recently [250]. The organisms of interest can then be isolated and cultured to functionally study their role in animal disease models. Having said that, there are hurdles in performing such studies; one of the major challenges is to raise and bred germ-free animals and perform intricate UV-related experiments. Another task is to develop an *in vivo* model for PLE; so far there is no such model available. However, the microbiome of the PLE lesions is yet to be studied. If any core microbial population is identified, that is distinct from healthy skin, one could design experiments to study the effects of these microbes in the pathogenesis of PLE and develop therapeutic approaches to specifically targeting these microbes. The data from this thesis work shows that skin microbiome of certain quality and quantity shows a protective role against immune suppression **(chapter 1)**, possibly contributing to the resistance of UV-induced immune suppression via expression of AMPs **(chapter 2)** in pathogenesis of PLE.

4 References:

1 Lee CH, Wu SB, Hong CH *et al.* Molecular Mechanisms of UV-Induced Apoptosis and Its Effects on Skin Residential Cells: The Implication in UV-Based Phototherapy. *Int J Mol Sci* 2013; **14**: 6414-35.

2 Webb AR. Changes in Stratospheric Ozone Concentrations and Solar UV Levels. *Radiation Protection Dosimetry* 1997; **72**: 207-16.

3 Roy S. Impact of UV Radiation on Genome Stability and Human Health. *Adv Exp Med Biol* 2017; **996**: 207-19.

4 Tabazadeh A, Santee ML, Danilin MY *et al.* Quantifying denitrification and its effect on ozone recovery. *Science* 2000; **288**: 1407-11.

5 Kamenisch Y, Ivanova I, Drexler K *et al.* UVA, Metabolism and Melanoma: UVA makes Melanoma hungry for metastasis. *Exp Dermatol* 2018.

6 Hoffmann K, Kaspar K, Altmeyer P *et al.* UV transmission measurements of small skin specimens with special quartz cuvettes. *Dermatology* 2000; **201**: 307-11.

7 Khan AQ, Travers JB, Kemp MG. Roles of UVA radiation and DNA damage responses in melanoma pathogenesis. *Environ Mol Mutagen* 2018; **59**: 438-60.

8 Peak MJ, Peak JG. Single-strand breaks induced in Bacillus subtilis DNA by ultraviolet light: action spectrum and properties. *Photochem Photobiol* 1982; **35**: 675-80.

9 Peak MJ, Peak JG, Moehring MP *et al.* Ultraviolet action spectra for DNA dimer induction, lethality, and mutagenesis in Escherichia coli with emphasis on the UVB region. *Photochem Photobiol* 1984; **40**: 613-20.

10 Rozema J, Bjorn LO, Bornman JF *et al.* The role of UV-B radiation in aquatic and terrestrial ecosystems--an experimental and functional analysis of the evolution of UV-absorbing compounds. *J Photochem Photobiol B* 2002; **66**: 2-12.

11 Quaite FE, Sutherland BM, Sutherland JC. Quantitation of pyrimidine dimers in DNA from UVB-irradiated alfalfa (Medicago sativa L.) seedlings. *Appl Theor Electrophor* 1992; **2**: 171-5.

12 Sinha RP, Hader DP. UV-induced DNA damage and repair: a review. *Photochem Photobiol Sci* 2002; **1**: 225-36.

13 Xie Z, Wang Y, Liu Y *et al.* Ultraviolet-B exposure induces photo-oxidative damage and subsequent repair strategies in a desert cyanobacterium Microcoleus vaginatus Gom. *European Journal of Soil Biology* 2009; **45**: 377-82.

14 Valero A, Begum M, Leong SL *et al.* Effect of germicidal UVC light on fungi isolated from grapes and raisins. *Lett Appl Microbiol* 2007; **45**: 238-43.

15 Anderson RR, Parrish JA. The optics of human skin. *J Invest Dermatol* 1981; **77**: 13-9.

16 Patra V, Laoubi L, Nicolas JF *et al.* A Perspective on the Interplay of Ultraviolet-Radiation, Skin Microbiome and Skin Resident Memory TCRalphabeta+ Cells. *Front Med (Lausanne)* 2018; **5**: 166.

17 Fisher MS, Kripke ML. Systemic alteration induced in mice by ultraviolet light irradiation and its relationship to ultraviolet carcinogenesis. *Proc Natl Acad Sci U S A* 1977; **74**: 1688-92.

18 Elmets CA, Cala CM, Xu H. Photoimmunology. *Dermatol Clin* 2014; **32**: 277-90, vii.

19 Kripke ML, Lofgreen JS, Beard J *et al.* In vivo immune responses of mice during carcinogenesis by ultraviolet irradiation. *J Natl Cancer Inst* 1977; **59**: 1227-30.

20 Elmets CA, Bergstresser PR, Tigelaar RE *et al.* Analysis of the mechanism of unresponsiveness produced by haptens painted on skin exposed to low dose ultraviolet radiation. *J Exp Med* 1983; **158**: 781-94.

21 Kelly DA, Young AR, McGregor JM *et al.* Sensitivity to Sunburn Is Associated with Susceptibility to Ultraviolet Radiation–Induced Suppression of Cutaneous Cell–Mediated Immunity. *The Journal of Experimental Medicine* 2000; **191**: 561-6.

22 Cooper KD, Oberhelman L, Hamilton TA *et al.* UV exposure reduces immunization rates and promotes tolerance to epicutaneous antigens in humans: relationship to dose, CD1a-DR+

epidermal macrophage induction, and Langerhans cell depletion. *Proc Natl Acad Sci U S A* 1992; **89**: 8497-501.

23 Wolf P, Hoffmann C, Quehenberger F *et al.* Immune protection factors of chemical sunscreens measured in the local contact hypersensitivity model in humans. *J Invest Dermatol* 2003; **121**: 1080-7.

24 Applegate LA, Ley RD, Alcalay J *et al.* Identification of the molecular target for the suppression of contact hypersensitivity by ultraviolet radiation. *J Exp Med* 1989; **170**: 1117-31.

25 Wolf P, Nghiem DX, Walterscheid JP *et al.* Platelet-activating factor is crucial in psoralen and ultraviolet A-induced immune suppression, inflammation, and apoptosis. *Am J Pathol* 2006; **169**: 795-805.

26 De Fabo EC, Noonan FP. Mechanism of immune suppression by ultraviolet irradiation in vivo. I. Evidence for the existence of a unique photoreceptor in skin and its role in photoimmunology. *J Exp Med* 1983; **158**: 84-98.

27 Patra V, Bashir M, Somlapura M *et al.* Isomerization of urocanic acid by ultraviolet radiation and its role in modulation of skin microbiome, antimicrobial peptides, and immune function. *Journal of Investigative Dermatology* 2017; **137**: S261-S.

28 Cestari TF, Kripke ML, Baptista PL *et al.* Ultraviolet radiation decreases the granulomatous response to lepromin in humans. *J Invest Dermatol* 1995; **105**: 8-13.

29 Jeevan A, Evans R, Brown EL *et al.* Effect of local ultraviolet irradiation on infections of mice with Candida albicans, Mycobacterium bovis BCG, and Schistosoma mansoni. *J Invest Dermatol* 1992; **99**: 59-64.

30 Brown EL, Ullrich SE, Pride M *et al.* The effect of UV irradiation on infection of mice with Borrelia burgdorferi. *Photochem Photobiol* 2001; **73**: 537-44.

31 Glaser R, Navid F, Schuller W *et al.* UV-B radiation induces the expression of antimicrobial peptides in human keratinocytes in vitro and in vivo. *J Allergy Clin Immunol* 2009; **123**: 1117-23.

32 Brandwein M, Bentwich Z, Steinberg D. Endogenous Antimicrobial Peptide Expression in Response to Bacterial Epidermal Colonization. *Front Immunol* 2017; **8**: 1637.

33 Navid F, Boniotto M, Walker C *et al.* Induction of regulatory T cells by a murine beta-defensin. *J Immunol* 2012; **188**: 735-43.

34 Niyonsaba F, Ushio H, Nakano N *et al.* Antimicrobial peptides human beta-defensins stimulate epidermal keratinocyte migration, proliferation and production of proinflammatory cytokines and chemokines. *J Invest Dermatol* 2007; **127**: 594-604.

35 Biragyn A, Ruffini PA, Leifer CA *et al.* Toll-like receptor 4-dependent activation of dendritic cells by beta-defensin 2. *Science* 2002; **298**: 1025-9.

36 Patra V, Mayer G, Gruber-Wackernagel A *et al.* Unique profile of antimicrobial peptide expression in polymorphic light eruption lesions compared to healthy skin, atopic dermatitis, and psoriasis. *Photodermatol Photoimmunol Photomed* 2017.

37 Cooper KD, Fox P, Neises G *et al.* Effects of ultraviolet radiation on human epidermal cell alloantigen presentation: initial depression of Langerhans cell-dependent function is followed by the appearance of T6- Dr+ cells that enhance epidermal alloantigen presentation. *The Journal of Immunology* 1985; **134**: 129-37.

38 Cooper KD, Duraiswamy N, Hammerberg C *et al.* Neutrophils, Differentiated Macrophages, and Monocyte/Macrophage Antigen Presenting Cells Infiltrate Murine Epidermis After UV Injury. *Journal of Investigative Dermatology* 1993; **101**: 155-63.

39 Cooper KD, Neises GR, Katz SI. Antigen-Presenting OKM5+ Melanophages Appear in Human Epidermis After Ultraviolet Radiation. *Journal of Investigative Dermatology* 1986; **86**: 363-70.

40 Toews GB, Bergstresser PR, Streilein JW. Epidermal Langerhans cell density determines whether contact hypersensitivity or unresponsiveness follows skin painting with DNFB. *The Journal of Immunology* 1980; **124**: 445-53.

41 Noonan FP, Bucana C, Sauder DN *et al.* Mechanism of systemic immune suppression by UV irradiation in vivo. II. The UV effects on number and morphology of epidermal Langerhans cells and the UV-induced suppression of contact hypersensitivity have different wavelength dependencies. *The Journal of Immunology* 1984; **132**: 2408-16.
42 Achachi A, Vocanson M, Bastien P *et al.* UV Radiation Induces the Epidermal Recruitment of Dendritic Cells that Compensate for the Depletion of Langerhans Cells in Human Skin. *J Invest Dermatol* 2015; **135**: 2058-67.
43 Liu X, Huang H, Gao H *et al.* Regulatory B cells induced by ultraviolet B through toll-like receptor 4 signalling contribute to the suppression of contact hypersensitivity responses in mice. *Contact Dermatitis* 2018; **78**: 117-30.
44 Schwarz A, Noordegraaf M, Maeda A *et al.* Langerhans cells are required for UVR-induced immunosuppression. *J Invest Dermatol* 2010; **130**: 1419-27.
45 Hart PH, Grimbaldeston MA, Finlay-Jones JJ. Sunlight, immunosuppression and skin cancer: role of histamine and mast cells. *Clin Exp Pharmacol Physiol* 2001; **28**: 1-8.
46 Setlow RB, Carrier WL. Pyrimidine dimers in ultraviolet-irradiated DNA's. *Journal of Molecular Biology* 1966; **17**: 237-54.
47 Batista LF, Kaina B, Meneghini R *et al.* How DNA lesions are turned into powerful killing structures: insights from UV-induced apoptosis. *Mutat Res* 2009; **681**: 197-208.
48 Pfeifer GP. Formation and processing of UV photoproducts: effects of DNA sequence and chromatin environment. *Photochem Photobiol* 1997; **65**: 270-83.
49 Pierceall WE, Kripke ML, Ananthaswamy HN. N-ras mutation in ultraviolet radiation-induced murine skin cancers. *Cancer Res* 1992; **52**: 3946-51.
50 Jiveskog S, Ragnarsson-Olding B, Platz A *et al.* N-ras mutations are common in melanomas from sun-exposed skin of humans but rare in mucosal membranes or unexposed skin. *J Invest Dermatol* 1998; **111**: 757-61.
51 Menon EL, Perera R, Kuhn RJ *et al.* Reactive oxygen species formation by UV-A irradiation of urocanic acid and the role of trace metals in this chemistry. *Photochem Photobiol* 2003; **78**: 567-75.
52 Kaneko K, Walker SL, Lai-Cheong J *et al.* cis-Urocanic acid enhances prostaglandin E2 release and apoptotic cell death via reactive oxygen species in human keratinocytes. *J Invest Dermatol* 2011; **131**: 1262-71.
53 Sreevidya CS, Fukunaga A, Khaskhely NM *et al.* Agents that reverse UV-Induced immune suppression and photocarcinogenesis affect DNA repair. *J Invest Dermatol* 2010; **130**: 1428-37.
54 Kammeyer A, Eggelte TA, Overmars H *et al.* Oxidative breakdown and conversion of urocanic acid isomers by hydroxyl radical generating systems. *Biochim Biophys Acta* 2001; **1526**: 277-85.
55 Kammeyer A, Peters CP, Meijer SL *et al.* Anti-inflammatory effects of urocanic Acid derivatives in models ex vivo and in vivo of inflammatory bowel disease. *ISRN Inflamm* 2012; **2012**: 898153.
56 Kolgen W, Both H, van Weelden H *et al.* Epidermal langerhans cell depletion after artificial ultraviolet B irradiation of human skin in vivo: apoptosis versus migration. *J Invest Dermatol* 2002; **118**: 812-7.
57 Nishigori C, Yarosh D, O'Connor A *et al.* HindIII liposomes suppress delayed-type hypersensitivity responses in vivo and induce epidermal IL-10 in vitro. *J Immunol* 1998; **161**: 2684-91.
58 Loser K, Mehling A, Loeser S *et al.* Epidermal RANKL controls regulatory T-cell numbers via activation of dendritic cells. *Nat Med* 2006; **12**: 1372-9.
59 Dudda JC, Denfeld RW, Simon JC *et al.* UVB-irradiated dendritic cells fail to tolerize murine CD8 naive or effector T cells. *J Invest Dermatol* 2004; **122**: 945-52.

60 Pradhan S, Kim HK, Thrash CJ *et al.* A critical role for the proapoptotic protein bid in ultraviolet-induced immune suppression and cutaneous apoptosis. *J Immunol* 2008; **181**: 3077-88.
61 Patra V, Byrne SN, Wolf P. The Skin Microbiome: Is It Affected by UV-induced Immune Suppression? *Front Microbiol* 2016; **7**: 1235.
62 Medzhitov R. Toll-like receptors and innate immunity. *Nat Rev Immunol* 2001; **1**: 135-45.
63 Tabeta K, Georgel P, Janssen E *et al.* Toll-like receptors 9 and 3 as essential components of innate immune defense against mouse cytomegalovirus infection. *Proc Natl Acad Sci U S A* 2004; **101**: 3516-21.
64 Ewald SE, Lee BL, Lau L *et al.* The ectodomain of Toll-like receptor 9 is cleaved to generate a functional receptor. *Nature* 2008; **456**: 658-62.
65 Pacini L, Ceraolo MG, Venuti A *et al.* UV Radiation Activates Toll-Like Receptor 9 Expression in Primary Human Keratinocytes, an Event Inhibited by Human Papillomavirus 38 E6 and E7 Oncoproteins. *J Virol* 2017; **91**.
66 Park HS, Jin SP, Lee Y *et al.* Toll-like receptor 2 mediates a cutaneous reaction induced by repetitive ultraviolet B irradiation in C57/BL6 mice in vivo. *Exp Dermatol* 2014; **23**: 591-5.
67 Borkowski AW, Gallo RL. UVB radiation illuminates the role of TLR3 in the epidermis. *J Invest Dermatol* 2014; **134**: 2315-20.
68 Borkowski AW, Kuo IH, Bernard JJ *et al.* Toll-like receptor 3 activation is required for normal skin barrier repair following UV damage. *J Invest Dermatol* 2015; **135**: 569-78.
69 Bernard JJ, Cowing-Zitron C, Nakatsuji T *et al.* Ultraviolet radiation damages self noncoding RNA and is detected by TLR3. *Nat Med* 2012; **18**: 1286-90.
70 Zhang JM, An J. Cytokines, inflammation, and pain. *Int Anesthesiol Clin* 2007; **45**: 27-37.
71 Bruhs A, Schwarz T. Ultraviolet Radiation-Induced Immunosuppression: Induction of Regulatory T Cells. *Methods Mol Biol* 2017; **1559**: 63-73.
72 Schwarz T. Regulatory T cells induced by ultraviolet radiation. *Int Arch Allergy Immunol* 2005; **137**: 187-93.
73 Steinman RM, Banchereau J. Taking dendritic cells into medicine. *Nature* 2007; **449**: 419-26.
74 Seite S, Zucchi H, Moyal D *et al.* Alterations in human epidermal Langerhans cells by ultraviolet radiation: quantitative and morphological study. *Br J Dermatol* 2003; **148**: 291-9.
75 Velez TE, Bryce PJ, Hulse KE. Mast Cell Interactions and Crosstalk in Regulating Allergic Inflammation. *Curr Allergy Asthma Rep* 2018; **18**: 30.
76 Hart PH, Grimbaldeston MA, Finlay-Jones JJ. Mast cells in UV-B-induced immunosuppression. *J Photochem Photobiol B* 2000; **55**: 81-7.
77 Wille JJ, Kydonieus AF, Murphy GF. cis-urocanic acid induces mast cell degranulation and release of preformed TNF-alpha: A possible mechanism linking UVB and cis-urocanic acid to immunosuppression of contact hypersensitivity. *Skin Pharmacol Appl Skin Physiol* 1999; **12**: 18-27.
78 Lee PL, van Weelden H, Bruijnzeel PL. Neutrophil infiltration in normal human skin after exposure to different ultraviolet radiation sources. *Photochem Photobiol* 2008; **84**: 1528-34.
79 Hawk JL, Murphy GM, Holden CA. The presence of neutrophils in human cutaneous ultraviolet-B inflammation. *Br J Dermatol* 1988; **118**: 27-30.
80 Rijken F, Kiekens RC, van den Worm E *et al.* Pathophysiology of photoaging of human skin: focus on neutrophils. *Photochem Photobiol Sci* 2006; **5**: 184-9.
81 Rijken F, Bruijnzeel PL. The pathogenesis of photoaging: the role of neutrophils and neutrophil-derived enzymes. *J Investig Dermatol Symp Proc* 2009; **14**: 67-72.
82 Shi C, Pamer EG. Monocyte recruitment during infection and inflammation. *Nat Rev Immunol* 2011; **11**: 762-74.

83 Mahdavian Delavary B, van der Veer WM, van Egmond M *et al.* Macrophages in skin injury and repair. *Immunobiology* 2011; **216**: 753-62.
84 Enomoto A, Yoshihisa Y, Yamakoshi T *et al.* UV-B radiation induces macrophage migration inhibitory factor-mediated melanogenesis through activation of protease-activated receptor-2 and stem cell factor in keratinocytes. *Am J Pathol* 2011; **178**: 679-87.
85 Kripke ML. Antigenicity of murine skin tumors induced by ultraviolet light. *J Natl Cancer Inst* 1974; **53**: 1333-6.
86 Schwarz A, Maeda A, Wild MK *et al.* Ultraviolet radiation-induced regulatory T cells not only inhibit the induction but can suppress the effector phase of contact hypersensitivity. *J Immunol* 2004; **172**: 1036-43.
87 Schwarz T. The dark and the sunny sides of UVR-induced immunosuppression: photoimmunology revisited. *J Invest Dermatol* 2010; **130**: 49-54.
88 Cela EM, Gonzalez CD, Friedrich A *et al.* Daily very low UV dose exposure enhances adaptive immunity, compared with a single high-dose exposure. Consequences for the control of a skin infection. *Immunology* 2018; **154**: 510-21.
89 Torres A. Fitzpatrick's dermatology in general medicine, 5th ed. *Archives of Dermatology* 2001; **137**: 517-8.
90 Hauser C, Katz SI. Activation and expansion of hapten- and protein-specific T helper cells from nonsensitized mice. *Proc Natl Acad Sci U S A* 1988; **85**: 5625-8.
91 Aiba S, Katz SI. Phenotypic and functional characteristics of in vivo-activated Langerhans cells. *J Immunol* 1990; **145**: 2791-6.
92 Enk AH, Katz SI. Contact sensitivity as a model for T-cell activation in skin. *J Invest Dermatol* 1995; **105**: 80S-3S.
93 Nelson PJ, Krensky AM. Chemokines, chemokine receptors, and allograft rejection. *Immunity* 2001; **14**: 377-86.
94 Vocanson M, Hennino A, Rozieres A *et al.* Effector and regulatory mechanisms in allergic contact dermatitis. *Allergy* 2009; **64**: 1699-714.
95 Robert C, Kupper TS. Inflammatory skin diseases, T cells, and immune surveillance. *N Engl J Med* 1999; **341**: 1817-28.
96 Picker LJ, Michie SA, Rott LS *et al.* A unique phenotype of skin-associated lymphocytes in humans. Preferential expression of the HECA-452 epitope by benign and malignant T cells at cutaneous sites. *Am J Pathol* 1990; **136**: 1053-68.
97 Grabbe S, Schwarz T. Immunoregulatory mechanisms involved in elicitation of allergic contact hypersensitivity. *Immunol Today* 1998; **19**: 37-44.
98 Miyauchi H, Horio T. Ultraviolet B-Induced Local Immunosuppression of Contact Hypersensitivity Is Modulated by Ultraviolet Irradiation and Hapten Application. *Journal of Investigative Dermatology* 1995; **104**: 364-9.
99 Gallo RL. Human Skin Is the Largest Epithelial Surface for Interaction with Microbes. *J Invest Dermatol* 2017; **137**: 1213-4.
100 Hannigan GD, Grice EA. Microbial ecology of the skin in the era of metagenomics and molecular microbiology. *Cold Spring Harb Perspect Med* 2013; **3**: a015362.
101 Nakatsuji T, Chiang HI, Jiang SB *et al.* The microbiome extends to subepidermal compartments of normal skin. *Nat Commun* 2013; **4**: 1431.
102 Byrd AL, Belkaid Y, Segre JA. The human skin microbiome. *Nat Rev Microbiol* 2018; **16**: 143-55.
103 Grice EA, Kong HH, Renaud G *et al.* A diversity profile of the human skin microbiota. *Genome Res* 2008; **18**: 1043-50.
104 Gao Z, Tseng CH, Pei Z *et al.* Molecular analysis of human forearm superficial skin bacterial biota. *Proc Natl Acad Sci U S A* 2007; **104**: 2927-32.
105 Costello EK, Lauber CL, Hamady M *et al.* Bacterial community variation in human body habitats across space and time. *Science* 2009; **326**: 1694-7.

106 Findley K, Oh J, Yang J *et al.* Topographic diversity of fungal and bacterial communities in human skin. *Nature* 2013; **498**: 367-70.
107 Probst AJ, Auerbach AK, Moissl-Eichinger C. Archaea on human skin. *PLoS One* 2013; **8**: e65388.
108 Moissl-Eichinger C, Probst AJ, Birarda G *et al.* Human age and skin physiology shape diversity and abundance of Archaea on skin. *Sci Rep* 2017; **7**: 4039.
109 Koskinen K, Pausan MR, Perras AK *et al.* First Insights into the Diverse Human Archaeome: Specific Detection of Archaea in the Gastrointestinal Tract, Lung, and Nose and on Skin. *MBio* 2017; **8**.
110 Chen AC, McMillan NA, Antonsson A. Human papillomavirus type spectrum in normal skin of individuals with or without a history of frequent sun exposure. *J Gen Virol* 2008; **89**: 2891-7.
111 Antonsson A, Erfurt C, Hazard K *et al.* Prevalence and type spectrum of human papillomaviruses in healthy skin samples collected in three continents. *J Gen Virol* 2003; **84**: 1881-6.
112 Foulongne V, Sauvage V, Hebert C *et al.* Human skin microbiota: high diversity of DNA viruses identified on the human skin by high throughput sequencing. *PLoS One* 2012; **7**: e38499.
113 SanMiguel A, Grice EA. Interactions between host factors and the skin microbiome. *Cell Mol Life Sci* 2015; **72**: 1499-515.
114 Lai Y, Di Nardo A, Nakatsuji T *et al.* Commensal bacteria regulate Toll-like receptor 3-dependent inflammation after skin injury. *Nat Med* 2009; **15**: 1377-82.
115 Vatanen T, Kostic AD, d'Hennezel E *et al.* Variation in Microbiome LPS Immunogenicity Contributes to Autoimmunity in Humans. *Cell* 2016; **165**: 842-53.
116 Gallo RL, Hooper LV. Epithelial antimicrobial defence of the skin and intestine. *Nat Rev Immunol* 2012; **12**: 503-16.
117 Meisel JS, Sfyroera G, Bartow-McKenney C *et al.* Commensal microbiota modulate gene expression in the skin. *Microbiome* 2018; **6**: 20.
118 Canesso MC, Vieira AT, Castro TB *et al.* Skin wound healing is accelerated and scarless in the absence of commensal microbiota. *J Immunol* 2014; **193**: 5171-80.
119 Gao Z, Tseng CH, Strober BE *et al.* Substantial alterations of the cutaneous bacterial biota in psoriatic lesions. *PLoS One* 2008; **3**: e2719.
120 Klymiuk I, Bambach I, Patra V *et al.* 16S Based Microbiome Analysis from Healthy Subjects' Skin Swabs Stored for Different Storage Periods Reveal Phylum to Genus Level Changes. *Front Microbiol* 2016; **7**: 2012.
121 Eden E, Navon R, Steinfeld I *et al.* GOrilla: a tool for discovery and visualization of enriched GO terms in ranked gene lists. *BMC Bioinformatics* 2009; **10**: 48.
122 Supek F, Bosnjak M, Skunca N *et al.* REVIGO summarizes and visualizes long lists of gene ontology terms. *PLoS One* 2011; **6**: e21800.
123 Babicki S, Arndt D, Marcu A *et al.* Heatmapper: web-enabled heat mapping for all. *Nucleic Acids Res* 2016; **44**: W147-53.
124 Kramer A, Green J, Pollard J, Jr. *et al.* Causal analysis approaches in Ingenuity Pathway Analysis. *Bioinformatics* 2014; **30**: 523-30.
125 Warde-Farley D, Donaldson SL, Comes O *et al.* The GeneMANIA prediction server: biological network integration for gene prioritization and predicting gene function. *Nucleic Acids Res* 2010; **38**: W214-20.
126 Biniek K, Levi K, Dauskardt RH. Solar UV radiation reduces the barrier function of human skin. *Proc Natl Acad Sci U S A* 2012; **109**: 17111-6.
127 Kambayashi H, Odake Y, Takada K *et al.* Involvement of changes in stratum corneum keratin in wrinkle formation by chronic ultraviolet irradiation in hairless mice. *Exp Dermatol* 2003; **12 Suppl 2**: 22-7.

128 MacLeod AS, Rudolph R, Corriden R *et al.* Skin-resident T cells sense ultraviolet radiation-induced injury and contribute to DNA repair. *J Immunol* 2014; **192**: 5695-702.
129 Nakatsuji T, Chen TH, Butcher AM *et al.* A commensal strain of Staphylococcus epidermidis protects against skin neoplasia. *Sci Adv* 2018; **4**: eaao4502.
130 Oppenheim JJ, Biragyn A, Kwak LW *et al.* Roles of antimicrobial peptides such as defensins in innate and adaptive immunity. *Ann Rheum Dis* 2003; **62 Suppl 2**: ii17-21.
131 Kolter J, Feuerstein R, Spoeri E *et al.* Streptococci Engage TLR13 on Myeloid Cells in a Site-Specific Fashion. *J Immunol* 2016; **196**: 2733-41.
132 Wolf P, Byrne SN, Limon-Flores AY *et al.* Serotonin signalling is crucial in the induction of PUVA-induced systemic suppression of delayed-type hypersensitivity but not local apoptosis or inflammation of the skin. *Exp Dermatol* 2016; **25**: 537-43.
133 Maeda A, Beissert S, Schwarz T *et al.* Phenotypic and functional characterization of ultraviolet radiation-induced regulatory T cells. *J Immunol* 2008; **180**: 3065-71.
134 Naik S, Bouladoux N, Wilhelm C *et al.* Compartmentalized control of skin immunity by resident commensals. *Science* 2012; **337**: 1115-9.
135 Enk CD, Sredni D, Blauvelt A *et al.* Induction of IL-10 gene expression in human keratinocytes by UVB exposure in vivo and in vitro. *J Immunol* 1995; **154**: 4851-6.
136 Kang K, Hammerberg C, Meunier L *et al.* CD11b+ macrophages that infiltrate human epidermis after in vivo ultraviolet exposure potently produce IL-10 and represent the major secretory source of epidermal IL-10 protein. *J Immunol* 1994; **153**: 5256-64.
137 de Waal Malefyt R, Abrams J, Bennett B *et al.* Interleukin 10(IL-10) inhibits cytokine synthesis by human monocytes: an autoregulatory role of IL-10 produced by monocytes. *J Exp Med* 1991; **174**: 1209-20.
138 Watanabe H, Gaide O, Petrilli V *et al.* Activation of the IL-1beta-processing inflammasome is involved in contact hypersensitivity. *J Invest Dermatol* 2007; **127**: 1956-63.
139 Myles IA, Fontecilla NM, Valdez PA *et al.* Signaling via the IL-20 receptor inhibits cutaneous production of IL-1beta and IL-17A to promote infection with methicillin-resistant Staphylococcus aureus. *Nat Immunol* 2013; **14**: 804-11.
140 Feldmeyer L, Keller M, Niklaus G *et al.* The inflammasome mediates UVB-induced activation and secretion of interleukin-1beta by keratinocytes. *Curr Biol* 2007; **17**: 1140-5.
141 Esaki H, Ewald DA, Ungar B *et al*. Identification of novel immune and barrier genes in atopic dermatitis by means of laser capture microdissection. *J Allergy Clin Immunol* 2015; **135**: 153-63.
142 Willis CR, Seamons A, Maxwell J *et al.* Interleukin-7 receptor blockade suppresses adaptive and innate inflammatory responses in experimental colitis. *J Inflamm (Lond)* 2012; **9**: 39.
143 Ryser S, Schuppli M, Gauthier B *et al.* UVB-induced skin inflammation and cutaneous tissue injury is dependent on the MHC class I-like protein, CD1d. *J Invest Dermatol* 2014; **134**: 192-202.
144 Dawes JM, Calvo M, Perkins JR *et al.* CXCL5 mediates UVB irradiation-induced pain. *Sci Transl Med* 2011; **3**: 90ra60.
145 D'Ambrosio D, Panina-Bordignon P, Sinigaglia F. Chemokine receptors in inflammation: an overview. *J Immunol Methods* 2003; **273**: 3-13.
146 Sather BD, Treuting P, Perdue N *et al.* Altering the distribution of Foxp3(+) regulatory T cells results in tissue-specific inflammatory disease. *J Exp Med* 2007; **204**: 1335-47.
147 Sells RE, Hwang ST. Paradoxical increase in skin inflammation in the absence of CCR4. *J Invest Dermatol* 2010; **130**: 2697-9.
148 Lehtimaki S, Tillander S, Puustinen A *et al.* Absence of CCR4 exacerbates skin inflammation in an oxazolone-induced contact hypersensitivity model. *J Invest Dermatol* 2010; **130**: 2743-51.
149 Naik S, Bouladoux N, Linehan JL *et al.* Commensal-dendritic-cell interaction specifies a unique protective skin immune signature. *Nature* 2015; **520**: 104-8.

150 O'Neill CA, Monteleone G, McLaughlin JT *et al.* The gut-skin axis in health and disease: A paradigm with therapeutic implications. *Bioessays* 2016; **38**: 1167-76.
151 Parodi A, Paolino S, Greco A *et al.* Small intestinal bacterial overgrowth in rosacea: clinical effectiveness of its eradication. *Clin Gastroenterol Hepatol* 2008; **6**: 759-64.
152 Matson V, Fessler J, Bao R *et al.* The commensal microbiome is associated with anti-PD-1 efficacy in metastatic melanoma patients. *Science* 2018; **359**: 104-8.
153 Ericsson AC, Gagliardi J, Bouhan D *et al.* The influence of caging, bedding, and diet on the composition of the microbiota in different regions of the mouse gut. *Sci Rep* 2018; **8**: 4065.
154 Kim D, Hofstaedter CE, Zhao C *et al.* Optimizing methods and dodging pitfalls in microbiome research. *Microbiome* 2017; **5**: 52.
155 Studies in abnormal human sensitivity to light. IV. Photoallergic concept of prurigo aestivalis. *Journal of Allergy and Clinical Immunology* 1943; **14**: 347.
156 Gruber-Wackernagel A, Byrne SN, Wolf P. Pathogenic mechanisms of polymorphic light eruption. *Front Biosci (Elite Ed)* 2009; **1**: 341-54.
157 Wolf P, Byrne SN, Gruber-Wackernagel A. New insights into the mechanisms of polymorphic light eruption: resistance to ultraviolet radiation-induced immune suppression as an aetiological factor. *Exp Dermatol* 2009; **18**: 350- 6.
158 Pao C, Norris PG, Corbett M *et al.* Polymorphic light eruption: prevalence in Australia and England. *Br J Dermatol* 1994; **130**: 62-4.
159 Oakley AM, Ramsey ML. Polymorphic Light Eruption. In: *StatPearls*. Treasure Island (FL). 2018.
160 Rhodes LE, Bock M, Janssens AS *et al.* Polymorphic light eruption occurs in 18% of Europeans and does not show higher prevalence with increasing latitude: multicenter survey of 6,895 individuals residing from the Mediterranean to Scandinavia. *J Invest Dermatol* 2010; **130**: 626-8.
161 Patra V, Mayer G, Gruber-Wackernagel A *et al.* Unique profile of antimicrobial peptides expression in polymorphic light eruption lesions compared to healthy skin, atopic dermatitis, and psoriasis. *Photodermatology, Photoimmunology & Photomedicine*: n/a-n/a.
162 Gruber-Wackernagel A, Byrne SN, Wolf P. Polymorphous light eruption: clinic aspects and pathogenesis. *Dermatol Clin* 2014; **32**: 315-34, viii.
163 Verheyen AM, Lambert JR, Van Marck EA *et al.* Polymorphic light eruption--an immunopathological study of provoked lesions. *Clin Exp Dermatol* 1995; **20**: 297-303.
164 Guarrera M, Cardo P, Rebora AE *et al.* Polymorphous light eruption and benign summer light eruption in Italy. *Photodermatol Photoimmunol Photomed* 2011; **27**: 35-9.
165 Jansen CT. Heredity of chronic polymorphous light eruptions. *Arch Dermatol* 1978; **114**: 188-90.
166 Granstein RD, Sauder DN. Whole-body exposure to ultraviolet radiation results in increased serum interleukin-1 activity in humans. *Lymphokine Res* 1987; **6**: 187-93.
167 Urbanski A, Schwarz T, Neuner P *et al.* Ultraviolet light induces increased circulating interleukin-6 in humans. *J Invest Dermatol* 1990; **94**: 808-11.
168 Lembo S, Caiazzo G, Balato N *et al.* Polymorphic light eruption and IL-1 family members: any difference with allergic contact dermatitis? *Photochem Photobiol Sci* 2017; **16**: 1471-9.
169 Holzle E, Plewig G, Hofmann C *et al.* POLYMORPHOUS LIGHT ERUPTION-EXPERIMENTAL REPRODUCTION OF SKIN-LESIONS. *Journal of the American Academy of Dermatology* 1982; **7**: 111-25.
170 Hönigsmann H. Polymorphous light eruption. In: *Clinical photomedicine*: Marcel Dekker Inc, New York. 1993; 167-80.
171 Diffey BL, Farr PM. An evaluation of sunscreens in patients with broad action-spectrum photosensitivity. *Br J Dermatol* 1985; **112**: 83-6.
172 Wolf P, Soyer HP, Fink-Puches R *et al.* Recurrent post-herpetic erythema multiforme mimicking polymorphic light and juvenile spring eruption: report of two cases in young boys. *Br J Dermatol* 1994; **131**: 364-7.

173 Lever W, Schaumburg-Lever G. Noninfectious vesicular and bullous diseases. *Histopathology of the Skin* 1990: 622-34.
174 Norris PG, Morris J, McGibbon DM *et al.* Polymorphic light eruption: an immunopathological study of evolving lesions. *Br J Dermatol* 1989; **120**: 173-83.
175 Damian DL, Barnetson RS, Halliday GM. Low-dose UVA and UVB have different time courses for suppression of contact hypersensitivity to a recall antigen in humans. *J Invest Dermatol* 1999; **112**: 939-44.
176 Kelly DA, Walker SL, McGregor JM *et al.* A single exposure of solar simulated radiation suppresses contact hypersensitivity responses both locally and systemically in humans: quantitative studies with high-frequency ultrasound. *J Photochem Photobiol B* 1998; **44**: 130-42.
177 Ullrich SE. Modulation of Immunity by Ultraviolet Radiation: Key Effects on Antigen Presentation. *Journal of Investigative Dermatology* 1995; **105**: S30-S6.
178 Duthie, Kimber, Norval. The effects of ultraviolet radiation on the human immune system. *British Journal of Dermatology* 1999; **140**: 995-1009.
179 Meunier L, Bata-Csorgo Z, Cooper KD. In Human Dermis, Ultraviolet Radiation Induces Expansion of a CD36+ CD11b+ CD1- Macrophage Subset by Infiltration and Proliferation; CD1+ Langerhans-Like Dendritic Antigen-Presenting Cells are Concomitantly Depleted. *Journal of Investigative Dermatology* 1995; **105**: 782-8.
180 A. G-W, I. B, F.J. L *et al*. Randomized double-blinded placebo-controlled intra-individual trial on topical treatment with a 1,25-dihydroxyvitamin D3 analogue in polymorphic light eruption. *British Journal of Dermatology* 2011; **165**: 152-63.
181 T. G, S. T, P. K *et al.* T regulatory cells and related immunoregulatory factors in polymorphic light eruption following ultraviolet A1 challenge. *British Journal of Dermatology* 2013; **169**: 1288-94.
182 Chadebech P, Goidin D, Jacquet C *et al.* Use of human reconstructed epidermis to analyze the regulation of beta-defensin hBD-1, hBD-2, and hBD-3 expression in response to LPS. *Cell Biol Toxicol* 2003; **19**: 313-24.
183 Joly S, Organ CC, Johnson GK *et al.* Correlation between beta-defensin expression and induction profiles in gingival keratinocytes. *Mol Immunol* 2005; **42**: 1073-84.
184 Kolls JK, McCray PB, Jr., Chan YR. Cytokine-mediated regulation of antimicrobial proteins. *Nat Rev Immunol* 2008; **8**: 829-35.
185 Yang D, Chertov O, Bykovskaia SN *et al.* Beta-defensins: linking innate and adaptive immunity through dendritic and T cell CCR6. *Science* 1999; **286**: 525-8.
186 Hong SP, Kim MJ, Jung MY *et al.* Biopositive effects of low-dose UVB on epidermis: coordinate upregulation of antimicrobial peptides and permeability barrier reinforcement. *J Invest Dermatol* 2008; **128**: 2880-7.
187 Yang D, Biragyn A, Kwak LW *et al.* Mammalian defensins in immunity: more than just microbicidal. *Trends Immunol* 2002; **23**: 291-6.
188 Wang TT, Nestel FP, Bourdeau V *et al.* Cutting edge: 1,25-dihydroxyvitamin D3 is a direct inducer of antimicrobial peptide gene expression. *J Immunol* 2004; **173**: 2909-12.
189 Damian DL, Kim YJ, Dixon KM *et al.* Topical calcitriol protects from UV-induced genetic damage but suppresses cutaneous immunity in humans. *Exp Dermatol* 2010; **19**: e23-30.
190 Mason RS, Sequeira VB, Dixon KM *et al.* Photoprotection by 1alpha,25-dihydroxyvitamin D and analogs: further studies on mechanisms and implications for UV-damage. *J Steroid Biochem Mol Biol* 2010; **121**: 164-8.
191 Zhang L-j, Gallo RL. Antimicrobial peptides. *Current Biology* 2016; **26**: R14-R9.
192 Katz E, Demain AL. The peptide antibiotics of Bacillus: chemistry, biogenesis, and possible functions. *Bacteriol Rev* 1977; **41**: 449-74.
193 Jeong H, Sim YM, Kim HJ *et al.* Genome Sequence of the Vancomycin-Producing Amycolatopsis orientalis subsp. orientalis Strain KCTC 9412T. *Genome Announc* 2013; **1**.

194 Gallo RL, Bernard JJ. Innate immune sensors stimulate inflammatory and immunosuppressive responses to UVB radiation. *J Invest Dermatol* 2014; **134**: 1508-11.
195 Felton S, Navid F, Schwarz A *et al.* Ultraviolet radiation-induced upregulation of antimicrobial proteins in health and disease. *Photochem Photobiol Sci* 2013; **12**: 29-36.
196 Gruber-Wackernagel A, Bambach I, Legat FJ *et al.* Randomized double-blinded placebo-controlled intra-individual trial on topical treatment with a 1,25-dihydroxyvitamin D analogue in polymorphic light eruption. *Br J Dermatol* 2011; **165**: 152-63.
197 Gruber-Wackernagel A, Obermayer-Pietsch B, Byrne SN *et al.* Patients with polymorphic light eruption have decreased serum levels of 25-hydroxyvitamin-D(3) that increase upon 311 nm UVB photohardening. *Photochem Photobiol Sci* 2012; **11**: 1831-6.
198 Tuominen VJ, Ruotoistenmaki S, Viitanen A *et al.* ImmunoRatio: a publicly available web application for quantitative image analysis of estrogen receptor (ER), progesterone receptor (PR), and Ki-67. *Breast Cancer Res* 2010; **12**: R56.
199 Kennedy Crispin M, Fuentes-Duculan J, Gulati N *et al.* Gene profiling of narrowband UVB-induced skin injury defines cellular and molecular innate immune responses. *J Invest Dermatol* 2013; **133**: 692-701.
200 Mallbris L, Edstrom DW, Sundblad L *et al.* UVB upregulates the antimicrobial protein hCAP18 mRNA in human skin. *J Invest Dermatol* 2005; **125**: 1072-4.
201 Moore BW. A soluble protein characteristic of the nervous system. *Biochem Biophys Res Commun* 1965; **19**: 739-44.
202 Brodersen DE, Etzerodt M, Madsen P *et al.* EF-hands at atomic resolution: the structure of human psoriasin (S100A7) solved by MAD phasing. *Structure* 1998; **6**: 477-89.
203 D'Amico F, Skarmoutsou E, Granata M *et al.* S100A7: A rAMPing up AMP molecule in psoriasis. *Cytokine Growth Factor Rev* 2016; **32**: 97-104.
204 Jinquan T, Vorum H, Larsen CG *et al.* Psoriasin: a novel chemotactic protein. *J Invest Dermatol* 1996; **107**: 5-10.
205 Glaser R, Harder J, Lange H *et al.* Antimicrobial psoriasin (S100A7) protects human skin from Escherichia coli infection. *Nat Immunol* 2005; **6**: 57-64.
206 Broome AM, Ryan D, Eckert RL. S100 protein subcellular localization during epidermal differentiation and psoriasis. *J Histochem Cytochem* 2003; **51**: 675-85.
207 Anderson KS, Wong J, Polyak K *et al.* Detection of psoriasin/S100A7 in the sera of patients with psoriasis. *Br J Dermatol* 2009; **160**: 325-32.
208 D'Amico F, Trovato C, Skarmoutsou E *et al.* Effects of adalimumab, etanercept and ustekinumab on the expression of psoriasin (S100A7) in psoriatic skin. *J Dermatol Sci* 2015; **80**: 38-44.
209 Harder J, Dressel S, Wittersheim M *et al.* Enhanced expression and secretion of antimicrobial peptides in atopic dermatitis and after superficial skin injury. *J Invest Dermatol* 2010; **130**: 1355-64.
210 Nguyen TT, Niyonsaba F, Akiyama T *et al.* Effects of IL-36 cytokines on S100A7/psoriasin and cathelicidin LL-37 expression and production by primary human keratinocytes. *Journal of Dermatological Science* 2013; **69**: e78-e9.
211 Abtin A, Eckhart L, Mildner M *et al.* Flagellin is the principal inducer of the antimicrobial peptide S100A7c (psoriasin) in human epidermal keratinocytes exposed to Escherichia coli. *FASEB J* 2008; **22**: 2168-76.
212 Niyonsaba F, Hattori F, Maeyama K *et al.* Induction of a microbicidal protein psoriasin (S100A7), and its stimulatory effects on normal human keratinocytes. *J Dermatol Sci* 2008; **52**: 216-9.
213 Wolf P, Gruber-Wackernagel A, Rinner B *et al.* Phototherapeutic hardening modulates systemic cytokine levels in patients with polymorphic light eruption. *Photochem Photobiol Sci* 2013; **12**: 166-73.
214 Li X, de Leeuw E, Lu W. Total chemical synthesis of human psoriasin by native chemical ligation. *Biochemistry* 2005; **44**: 14688-94.

215 Patra V, Wolf P. Microbial elements as the initial triggers in the pathogenesis of polymorphic light eruption? *Exp Dermatol* 2016.
216 Gruber-Wackernagel A, Bambach I, Legat FJ *et al.* Randomized double-blinded placebo-controlled intra-individual trial on topical treatment with a 1,25-dihydroxyvitamin D(3) analogue in polymorphic light eruption. *Br J Dermatol* 2011; **165**: 152-63.
217 Becknell B, Spencer JD. A Review of Ribonuclease 7's Structure, Regulation, and Contributions to Host Defense. *Int J Mol Sci* 2016; **17**: 423.
218 Cho S, Beintema JJ, Zhang J. The ribonuclease A superfamily of mammals and birds: identifying new members and tracing evolutionary histories. *Genomics* 2005; **85**: 208-20.
219 Harder J, Schroder JM. RNase 7, a novel innate immune defense antimicrobial protein of healthy human skin. *J Biol Chem* 2002; **277**: 46779-84.
220 Koten B, Simanski M, Glaser R *et al.* RNase 7 contributes to the cutaneous defense against Enterococcus faecium. *PLoS One* 2009; **4**: e6424.
221 Kopfnagel V, Wagenknecht S, Brand L *et al.* RNase 7 downregulates TH2 cytokine production by activated human T-cells. *Allergy* 2017.
222 Cho JS, Xuan C, Miller LS. Lucky number seven: RNase 7 can prevent Staphylococcus aureus skin colonization. *J Invest Dermatol* 2010; **130**: 2703-6.
223 Zanger P, Holzer J, Schleucher R *et al.* Constitutive expression of the antimicrobial peptide RNase 7 is associated with Staphylococcus aureus infection of the skin. *J Infect Dis* 2009; **200**: 1907-15.
224 Simanski M, Dressel S, Glaser R *et al.* RNase 7 protects healthy skin from Staphylococcus aureus colonization. *J Invest Dermatol* 2010; **130**: 2836-8.
225 Simanski M, Rademacher F, Schroder L *et al.* IL-17A and IFN-gamma synergistically induce RNase 7 expression via STAT3 in primary keratinocytes. *PLoS One* 2013; **8**: e59531.
226 Kalenik BM, Gora-Sochacka A, Sirko A. Beta-defensins - Underestimated peptides in influenza combat. *Virus Res* 2018; **247**: 10-4.
227 Harder J, Bartels J, Christophers E *et al.* A peptide antibiotic from human skin. *Nature* 1997; **387**: 861.
228 Liu AY, Destoumieux D, Wong AV *et al.* Human beta-defensin-2 production in keratinocytes is regulated by interleukin-1, bacteria, and the state of differentiation. *J Invest Dermatol* 2002; **118**: 275-81.
229 Gonzalez-Curiel I, Trujillo V, Montoya-Rosales A *et al.* 1,25-dihydroxyvitamin D3 induces LL-37 and HBD-2 production in keratinocytes from diabetic foot ulcers promoting wound healing: an in vitro model. *PLoS One* 2014; **9**: e111355.
230 Chieosilapatham P, Ogawa H, Niyonsaba F. Current insights into the role of human beta-defensins in atopic dermatitis. *Clin Exp Immunol* 2017; **190**: 155-66.
231 Janssens AS, Pavel S, Tensen CP *et al.* Reduced IL-1Ra/IL-1 ratio in ultraviolet B-exposed skin of patients with polymorphic light eruption. *Exp Dermatol* 2009; **18**: 212-7.
232 Schornagel IJ, Sigurdsson V, Nijhuis EH *et al.* Decreased neutrophil skin infiltration after UVB exposure in patients with polymorphous light eruption. *J Invest Dermatol* 2004; **123**: 202-6.
233 Balato A, Schiattarella M, Lembo S *et al.* Interleukin-1 family members are enhanced in psoriasis and suppressed by vitamin D and retinoic acid. *Arch Dermatol Res* 2013; **305**: 255-62.
234 Lande R, Chamilos G, Ganguly D *et al.* Cationic antimicrobial peptides in psoriatic skin cooperate to break innate tolerance to self-DNA. *Eur J Immunol* 2015; **45**: 203-13.
235 Zanetti M. Cathelicidins, multifunctional peptides of the innate immunity. *J Leukoc Biol* 2004; **75**: 39-48.
236 Lande R, Gregorio J, Facchinetti V *et al.* Plasmacytoid dendritic cells sense self-DNA coupled with antimicrobial peptide. *Nature* 2007; **449**: 564-9.
237 Chamilos G, Gregorio J, Meller S *et al.* Cytosolic sensing of extracellular self-DNA transported into monocytes by the antimicrobial peptide LL37. *Blood* 2012; **120**: 3699-707.

238 Ganguly D, Chamilos G, Lande R *et al.* Self-RNA-antimicrobial peptide complexes activate human dendritic cells through TLR7 and TLR8. *J Exp Med* 2009; **206**: 1983-94.
239 Verjans ET, Zels S, Luyten W *et al.* Molecular mechanisms of LL-37-induced receptor activation: An overview. *Peptides* 2016; **85**: 16-26.
240 Wolf P, Weger W, Patra V *et al.* Desired response to phototherapy vs photoaggravation in psoriasis: what makes the difference? *Exp Dermatol* 2016; **25**: 937-44.
241 Veran JL, Fornecker D, Bloch JG *et al.* [Chronic atrophic polychondritis associated with psoriasis and ulcero-hemorrhagic rectocolitis]. *Rev Rhum Mal Osteoartic* 1990; **57**: 442-3.
242 Kanda N, Hau CS, Tada Y *et al.* Decreased serum LL-37 and vitamin D3 levels in atopic dermatitis: relationship between IL-31 and oncostatin M. *Allergy* 2012; **67**: 804-12.
243 Vandamme D, Landuyt B, Luyten W *et al.* A comprehensive summary of LL-37, the factotum human cathelicidin peptide. *Cell Immunol* 2012; **280**: 22-35.
244 Rhodes LE, Webb AR, Berry JL *et al.* Sunlight exposure behaviour and vitamin D status in photosensitive patients: longitudinal comparative study with healthy individuals at U.K. latitude. *Br J Dermatol* 2014; **171**: 1478-86.
245 Schweintzger NA, Gruber-Wackernagel A, Shirsath N *et al.* Influence of the season on vitamin D levels and regulatory T cells in patients with polymorphic light eruption. *Photochem Photobiol Sci* 2016; **15**: 440-6.
246 Wackernagel A, Massone C, Hoefler G *et al.* Plasmacytoid dendritic cells are absent in skin lesions of polymorphic light eruption. *Photodermatol Photoimmunol Photomed* 2007; **23**: 24-8.
247 Lande R, Botti E, Jandus C *et al.* The antimicrobial peptide LL37 is a T-cell autoantigen in psoriasis. *Nat Commun* 2014; **5**: 5621.
248 Myles IA, Earland NJ, Anderson ED *et al.* First-in-human topical microbiome transplantation with Roseomonas mucosa for atopic dermatitis. *JCI Insight* 2018; **3**.
249 Ghaly S, Kaakoush NO, Lloyd F *et al.* Ultraviolet Irradiation of Skin Alters the Faecal Microbiome Independently of Vitamin D in Mice. *Nutrients* 2018; **10**.
250 Wood DLA, Lachner N, Tan JM *et al.* A Natural History of Actinic Keratosis and Cutaneous Squamous Cell Carcinoma Microbiomes. *MBio* 2018; **9**.

License agreements

JOHN WILEY AND SONS LICENSE TERMS AND CONDITIONS

Jul 18, 2018

This Agreement between Medical University of Graz -- Vijay Kumar Patra ("You") and John Wiley and Sons ("John Wiley and Sons") consists of your license details and the terms and conditions provided by John Wiley and Sons and Copyright Clearance Center.

License Number	4391990387988
License date	Jul 18, 2018
Licensed Content Publisher	John Wiley and Sons
Licensed Content Publication	Allergy
Licensed Content Title	Effector and regulatory mechanisms in allergic contact dermatitis
Licensed Content Author	M. Vocanson, A. Hennino, A. Rozières, et al
Licensed Content Date	Nov 5, 2009
Licensed Content Volume	64
Licensed Content Issue	12
Licensed Content Pages	16
Type of use	Dissertation/Thesis
Requestor type	University/Academic
Format	Print and electronic
Portion	Figure/table
Number of figures/tables	1
Original Wiley figure/table number(s)	Figure 1
Will you be translating?	No
Title of your thesis / dissertation	Insight into the role of skin microbiome in UV-induced immune modulation and its potential link to pathogenesis of polymorphic light eruption.
Expected completion date	Sep 2018
Expected size (number of pages)	150
Requestor Location	Medical University of Graz stiftingstalstrasse 24 Graz, 8010 Austria Attn: Vijay Kumar Patra
Publisher Tax ID	EU826007151
Total	0.00 EUR
Terms and Conditions	

TERMS AND CONDITIONS

This copyrighted material is owned by or exclusively licensed to John Wiley & Sons, Inc. or one of its group companies (each a"Wiley Company") or handled on behalf of a society with which a Wiley Company has exclusive publishing rights in relation to a particular work

JOHN WILEY AND SONS LICENSE TERMS AND CONDITIONS

Jul 18, 2018

This Agreement between Medical University of Graz -- Vijay Kumar Patra ("You") and John Wiley and Sons ("John Wiley and Sons") consists of your license details and the terms and conditions provided by John Wiley and Sons and Copyright Clearance Center.

License Number	4391990184569
License date	Jul 18, 2018
Licensed Content Publisher	John Wiley and Sons
Licensed Content Publication	Experimental Dermatology
Licensed Content Title	Microbial elements as the initial triggers in the pathogenesis of polymorphic light eruption?
Licensed Content Author	VijayKumar Patra, Peter Wolf
Licensed Content Date	Nov 29, 2016
Licensed Content Volume	25
Licensed Content Issue	12
Licensed Content Pages	3
Type of use	Dissertation/Thesis
Requestor type	Author of this Wiley article
Format	Print and electronic
Portion	Full article
Will you be translating?	No
Title of your thesis / dissertation	Insight into the role of skin microbiome in UV-induced immune modulation and its potential link to pathogenesis of polymorphic light eruption.
Expected completion date	Sep 2018
Expected size (number of pages)	150
Requestor Location	Medical University of Graz stiftingstalstrasse 24 Graz, 8010 Austria Attn: Vijay Kumar Patra
Publisher Tax ID	EU826007151
Total	0.00 EUR
Terms and Conditions	

TERMS AND CONDITIONS

This copyrighted material is owned by or exclusively licensed to John Wiley & Sons, Inc. or one of its group companies (each a"Wiley Company") or handled on behalf of a society with which a Wiley Company has exclusive publishing rights in relation to a particular work (collectively "WILEY"). By clicking "accept" in connection with completing this licensing transaction, you agree that the following terms and conditions apply to this transaction

SPRINGER NATURE LICENSE TERMS AND CONDITIONS

Jul 18, 2018

This Agreement between Medical University of Graz -- Vijay Kumar Patra ("You") and Springer Nature ("Springer Nature") consists of your license details and the terms and conditions provided by Springer Nature and Copyright Clearance Center.

License Number	4391990316121
License date	Jul 18, 2018
Licensed Content Publisher	Springer Nature
Licensed Content Publication	Nature Reviews Microbiology
Licensed Content Title	The human skin microbiome
Licensed Content Author	Allyson L. Byrd, Yasmine Belkaid, Julia A. Segre
Licensed Content Date	Jan 15, 2018
Licensed Content Volume	16
Licensed Content Issue	3
Type of Use	Thesis/Dissertation
Requestor type	academic/university or research institute
Format	print and electronic
Portion	figures/tables/illustrations
Number of figures/tables/illustrations	1
High-res required	no
Will you be translating?	no
Circulation/distribution	<501
Author of this Springer Nature content	no
Title	Insight into the role of skin microbiome in UV-induced immune modulation and its potential link to pathogenesis of polymorphic light eruption.
Instructor name	n/a
Institution name	n/a
Expected presentation date	Sep 2018
Portions	Figure 2
Requestor Location	Medical University of Graz stiftingstalstrasse 24 Graz, 8010 Austria Attn: Vijay Kumar Patra
Billing Type	Invoice
Billing Address	Medical University of Graz stiftingstalstrasse 24

JOHN WILEY AND SONS LICENSE TERMS AND CONDITIONS

Jul 18, 2018

This Agreement between Medical University of Graz -- Vijay Kumar Patra ("You") and John Wiley and Sons ("John Wiley and Sons") consists of your license details and the terms and conditions provided by John Wiley and Sons and Copyright Clearance Center.

License Number	4391990100962
License date	Jul 18, 2018
Licensed Content Publisher	John Wiley and Sons
Licensed Content Publication	Photodermatology, Photoimmunology & Photomedicine
Licensed Content Title	Unique profile of antimicrobial peptide expression in polymorphic light eruption lesions compared to healthy skin, atopic dermatitis, and psoriasis
Licensed Content Author	VijayKumar Patra, Gerlinde Mayer, Alexandra Gruber-Wackernagel, et al
Licensed Content Date	Oct 16, 2017
Licensed Content Volume	34
Licensed Content Issue	2
Licensed Content Pages	8
Type of use	Dissertation/Thesis
Requestor type	Author of this Wiley article
Format	Print and electronic
Portion	Full article
Will you be translating?	No
Title of your thesis / dissertation	Insight into the role of skin microbiome in UV-induced immune modulation and its potential link to pathogenesis of polymorphic light eruption.
Expected completion date	Sep 2018
Expected size (number of pages)	150
Requestor Location	Medical University of Graz stiftingstalstrasse 24 Graz, 8010 Austria Attn: Vijay Kumar Patra
Publisher Tax ID	EU826007151
Total	0.00 EUR
Terms and Conditions	

TERMS AND CONDITIONS

This copyrighted material is owned by or exclusively licensed to John Wiley & Sons, Inc. or one of its group companies (each a"Wiley Company") or handled on behalf of a society with which a Wiley Company has exclusive publishing rights in relation to a particular work

WOLTERS KLUWER HEALTH, INC. LICENSE TERMS AND CONDITIONS

Aug 28, 2018

This Agreement between Medical University of Graz -- Vijay Kumar Patra ("You") and Wolters Kluwer Health, Inc. ("Wolters Kluwer Health, Inc.") consists of your license details and the terms and conditions provided by Wolters Kluwer Health, Inc. and Copyright Clearance Center.

License Number	4417600114605
License date	Aug 28, 2018
Licensed Content Publisher	Wolters Kluwer Health, Inc.
Licensed Content Publication	International Anesthesiology Clinics
Licensed Content Title	Cytokines, Inflammation, and Pain
Licensed Content Author	Jun-Ming Zhang and Jianxiong An
Licensed Content Date	Apr 1, 2007
Licensed Content Volume	45
Licensed Content Issue	2
Type of Use	Dissertation/Thesis
Requestor type	Individual
STM publisher name	
Portion	Figures/table/illustration
Number of figures/tables/illustrations	1
Figures/tables/illustrations used	1
Author of this Wolters Kluwer article	No
Title of your thesis / dissertation	Insight into the role of skin microbiome in UV-induced immune modulation and its potential link to pathogenesis of polymorphic light eruption.
Expected completion date	Sep 2018
Estimated size(pages)	150
Requestor Location	Medical University of Graz stiftingstalstrasse 24 Graz, 8010 Austria Attn: Vijay Kumar Patra
Publisher Tax ID	EU826013006
Billing Type	Invoice
Billing Address	Medical University of Graz stiftingstalstrasse 24